TAMPERE UNIVERSITY OF TECHNOLOGY

JANNE PULKKINEN

TIME DOMAIN MEASUREMENT METHOD FOR ELECTROMAGNETIC INTERFERENCE

Licentiate thesis

Examiners: professor Jouko Halttunen
and Dr.Tech Jukka Ruoskanen
Examiners and topic approved by the
Faculty Council of the Faculty of
Engineering Sciences on 6 March 2013

TIIVISTELMÄ

TAMPEREEN TEKNILLINEN YLIOPISTO

PULKKINEN, JANNE: Time domain measurement method for electromagnetic interference

Lisensiaatintutkimus, 80 sivua, 19 liitesivua
Toukokuu 2013
Teknisten tieteiden tiedekunta
Systeemitekniikan laitos
Tarkastajat: Professori Jouko Halttunen ja TkT Jukka Ruoskanen
Avainsanat: Sähkömagneettinen yhteensopivuus, sähkömagneettiset häiriöt, aikatason mittausmenetelmä, Fourier-muunnos, ikkunafunktiot

Tutkimuksen tarkoituksena oli selvittää, voidaanko taajuustasossa suoritettavat standardin MIL-STD-461F testimenetelmän CE102 mukaiset johtuvien sähkömagneettisten häiriöiden mittaukset korvata aikatason mittausmenetelmällä. Aikatason mittausmenetelmässä mittaukset suoritetaan mittausvastaanottimen tai spektrianalysaattorin sijaan digitaalioskilloskoopilla, ja tämän jälkeen taajuustason esitys muodostetaan matemaattisesti perustuen diskreettiin Fourier-muunnokseen ja muuhun signaalinkäsittelyyn, jolla otetaan huomioon aikatason mittausmenetelmän ja -laitteiston erityispiirteet. Lisäksi tutkimuksessa arvioitiin aikatason mittausmenetelmän etuja ja haittoja verrattuna taajuustason mittausmenetelmään sekä aikatason mittausmenetelmään liittyviä mittausepävarmuustekijöitä.

Tutkimus jakautuu kolmeen pääosaan. Ensimmäisen osan muodostavat kirjallisuusselvitys aikatason mittausmenetelmistä sekä tutkimuksessa esimerkkitapauksena käsitellyn MIL-STD-461F -standardin testimenetelmän CE102 esittely. Toisen ja tutkimuksen kannalta keskeisimmän osan muodostaa aikatason mittausjärjestelmän rakentaminen ja sillä suoritetut mittaukset sekä mittausjärjestelmän kehittäminen. Tutkimuksen kolmannessa osassa arvioidaan aikatason mittausmenetelmän ja rakennetun mittausjärjestelmän käyttökelpoisuutta perustuen mittaustulosten tilastolliseen analyysiin sekä vertaileviin mittauksiin standardinmukaisella mittauslaitteistolla.

Tutkimuksen lopputuloksena voidaan todeta, että aikatason mittausmenetelmä on varteenotettava ja laitteistokustannuksiltaan edullinen vaihtoehto taajuustason mittausmenetelmälle, mutta varsinkin johtuvien häiriöiden mittauksissa se on usein työläämpi ja enemmän aikaa vievä kuin taajuustason mittausmenetelmä. Lisäksi aikatason mittausjärjestelmän rakentaminen vaatii aikaa sekä syvällisiä tietoja mittaustekniikasta ja signaalinkäsittelystä.

Aikatason mittausmenetelmällä on kuitenkin monia hyviä puolia ja siihen liittyvää tutkimusta kannattaa ehdottomasti jatkaa. Mahdollisia jatkotutkimuskohteita ovat mm. erilaisten ikkunafunktioiden soveltaminen kapeakaistaisten häiriöiden mittauksissa ja transientti-ilmiöiden mittaukset.

ABSTRACT

TAMPERE UNIVERSITY OF TECHNOLOGY

PULKKINEN, JANNE: Time domain measurement method for electromagnetic interference

Licentiate Thesis, 80 pages, 19 Appendix pages
Month and year of thesis completion: May 2013
Examiners: Professor Jouko Halttunen and Dr. Tech Jukka Ruoskanen
Keywords: Electromagnetic compatibility (EMC), Electromagnetic interference (EMI), Time domain electromagnetic interference measurement method (TDEMI), Fourier transform, Window functions

The aim of this research was to study the feasibility of the time domain electromagnetic interference (TDEMI) measurement method in MIL-STD-461F compliance measurements. In the TDEMI measurement method, the measurement in time domain is performed with digital oscilloscope. After time domain measurement, comparable frequency domain amplitude spectrum is produced by Discrete Fourier Transform and by other signal processing with PC. The pros and cons of TDEMI measurement method compared to frequency domain measurement method are also evaluated in this research as well as statistical properties of TDEMI measurement results.

The research is divided in three major parts. The first part of the research is a literature review of the most essential publications related to TDEMI measurement methods and the introduction to the CE102 test method which was studied as an example. The second and the most important part of the research is the building up the TDEMI measurement system and EMI measurements with built system. Improvements for the TDEMI measurement system are also introduced in the second part. The third part is the evaluation of the built TDEMI measurement system. This is done by statistical analysis of measurement results and by comparative measurements with standard frequency domain measurement system.

The conclusion of the research is that the TDEMI measurement method is a feasible low-cost alternative for the frequency domain measurements in MIL-STD-461F CE102 measurements. In most of the practical cases the TDEMI measurement method is more time consuming than the CE102 frequency domain measurement, but if the interference signal contains infrequent phenomena, TDEMI measurement method may save time. The building up a TDEMI measurement system requires deep knowledge in measurement technology and in signal processing.

The TDEMI measurement method has also many benefits and it seems to be developable method. Possible further research areas are related to application of different window functions in the algorithm for narrowband interference and to measurements of transient interference signals with TDEMI measurement system.

PREFACE

This research has been carried out during the years 2012 and 2013, alongside my main duties in the Finnish Defence Forces. This has meant long days and even nights with the research work, but on the other hand, I have learned a lot and my knowledge in measurement technology and signal processing has increased significantly.

First of all, I would like to thank my supervisor, Professor Jouko Halttunen for his guidance and support. I am also very thankful to Dr. Tech Jukka Ruoskanen at Finnish Defence Forces Technical Research Centre for his valuable comments and suggestions to improve the thesis.

I would like to thank also Dr. Tech Heikki Jokinen at Tampere University of Technology for his support concerning the application of different window functions and Mr Esa Kilpinen at Army Materiel Command for the possibility to perform comparative measurements at Army Materiel Command's EMC laboratory.

Finally, I would like to thank my family for the support and understanding.

Tampere, May 2013

Janne Pulkkinen

CONTENTS

LIST OF ACRONYMS AND SYMBOLS

$A_{v\text{-}t}$	Impulse Area
AC	Alternating Current
A/D	Analog to Digital
α_{window}	6 dB bandwidth of the applied window function
$B_{6\ dB\ receiver}$	6 dB bandwidth of the measurement receiver
BNC	Bayonet Neill-Concelman (Connector Type)
BW	Bandwidth
CE	Conducted Emission
CISPR	Comité International Spécial des Perturbations Radioélectriques, Special International Committee on Radio Interference
COTS	Commercial Off-The-Shelf
DC	Direct Current
DFT	Discrete Fourier Transform
EMC	Electromagnetic Compatibility
EMI	Electromagnetic Interference
EUT	Equipment under Test
F_{C1}	Correction for Capacitor C_1 of LISN
F_{C2}	Frequency Response Correction for Frequency Band 10 kHz to 150 kHz
F_{C3}	Frequency Response Correction for Frequency Band 150 kHz to 10 MHz
f_{AL1} - f_{AL5}	Frequencies of Aliased Test Signals
$f_{aliased}$	Frequency of Aliased Signal
f_{input}	Frequency of Test Signal Used in Aliasing Demonstration
f_{prf}	Pulse Repetition Frequency
f_s	Sampling Frequency
f_{s1}	Sampling Frequency for Frequency Band 10 kHz to 150 kHz
f_{s2}	Sampling Frequency for Frequency Band 150 kHz to 10 MHz
FC(f)	Frequency Response Correction Curve
FEMIT	Fast Emission Measurement in Time Domain
FFT	Fast Fourier Transform

G	Gain
G_C	Coherent Gain
IEC	International Electrotechnical Commission
IEEE	Institute of Electrical and Electronics Engineers
IF	Intermediate Frequency
JTF	Joint Task Force
LISN	Line Impedance Stabilization Network
MRTDEMI	Multiresolution Domain Electromagnetic Interference
PC	Personal Computer
$PC(f_{prf})$	Pulse Response Correction Curve
PCB	Printed Circuit Board
q_j	Individual Measurement Result
$\overline{q}$	Arithmetic Mean of the Individual Measurement Results
RBW	Resolution Bandwidth
RMS	Root Mean Square
SPICE	Simulation Program with Integrated Circuit Emphasis
$s(q)$	Experimental Standard Deviation
$s(\overline{q})$	Experimental Standard Deviation of the Mean
T	Capture Time in Time Domain Measurements
T_{min}	Minimum Capture Time in Time Domain Measurements
T_r	Repetition Period
T_{tot}	Total Capture Time of Oscilloscope
T_{tot1}	Total Capture Time of Oscilloscope for Frequency Band 10 kHz to 150 kHz
T_{tot2}	Total Capture Time of Oscilloscope for Frequency Band 150 kHz to 10 MHz
T_1	Capture Time for Frequency Band 10 kHz to 150 kHz
T_2	Capture Time for Frequency Band 150 kHz to 10 MHz
t_{pulse}	Period of a Pulse
TDEMI	Time Domain Electromagnetic Interference
τ_{in}	Width of the Input Pulse
U	Expanded Uncertainty
$u(\overline{q})$	Standard Uncertainty

V_{in}	Input Voltage
V_{out}	Output Voltage
X_{as}	Amplitude Spectrum
X_c	Normalized Result of Discrete Fourier Transform
$X(k)$	Result of Discrete Fourier Transform of Vector x

1 INTRODUCTION

Most of the standardized radiated and conducted emission measurements are carried out in the frequency domain with an Electromagnetic Interference (EMI) measurement receiver or a sweeping spectrum analyzer. Frequency domain measurements can take quite a long time and be expensive especially when the testing is carried out in accredited Electromagnetic Compatibility (EMC) test laboratory. These facts have inspired researchers to develop faster low-cost time domain interference measurement methods which are based on time domain measurements with digital oscilloscopes or A/D converters. After time domain measurement, comparable frequency domain amplitude spectrum is produced by Fourier transform methods and other signal processing with PC. Above-mentioned time domain measurement method is often called Fast Emission Measurement in Time Domain (FEMIT) or Time Domain Electromagnetic Interference Measurement (TDEMI measurement). In this thesis the latter term TDEMI measurement method is used.

Figure 1.1 below shows an example of so-called traditional and standardized frequency domain EMI measurement system. This EMI measurement system and the measurement units are similar to U.S. military EMC standard MIL-STD-461 [1].

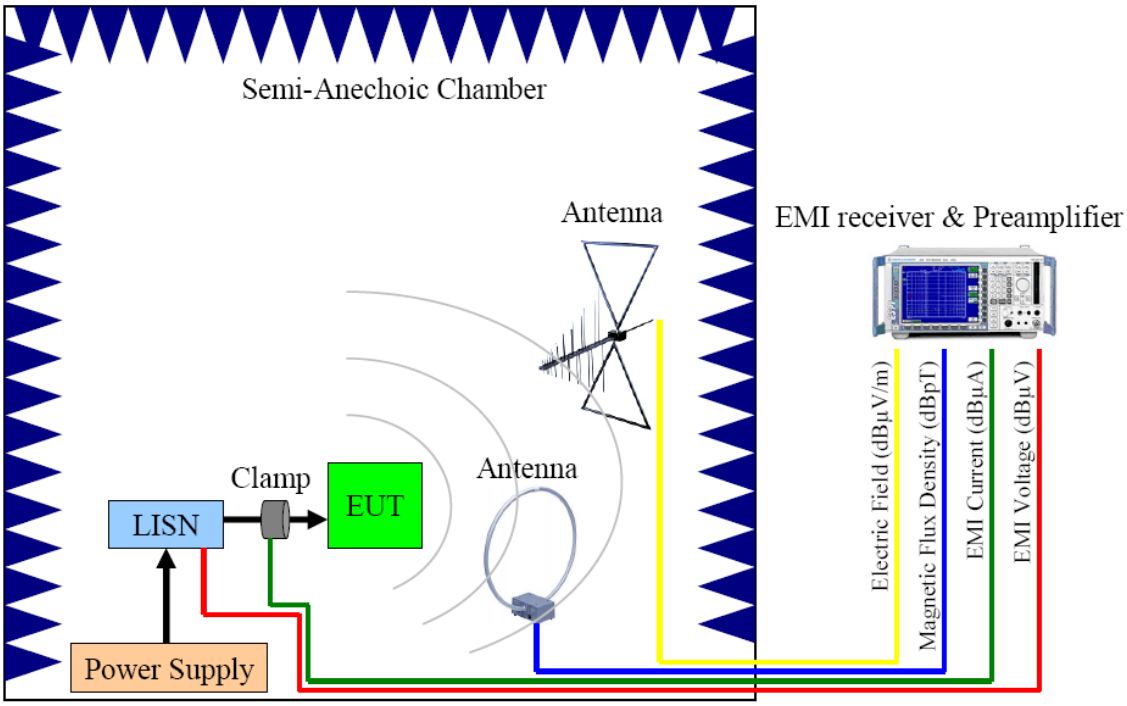

Figure 1.1 *Example of frequency domain EMI measurement system.*

In TDEMI measurement system the frequency domain part (EMI receiver or spectrum analyzer) is replaced by time domain measurement system consisting of anti-aliasing low pass filter, digitizing oscilloscope or A/D converter and PC with suitable software to produce Fourier transform based amplitude spectrum. In TDEMI

measurements the need for low noise preamplifier may be higher than in frequency domain measurements because of the lower sensitivity of the measurement device. In conducted emission measurements the preamplifier is typically not needed. An example of TDEMI measurement system is shown in figure 1.2.

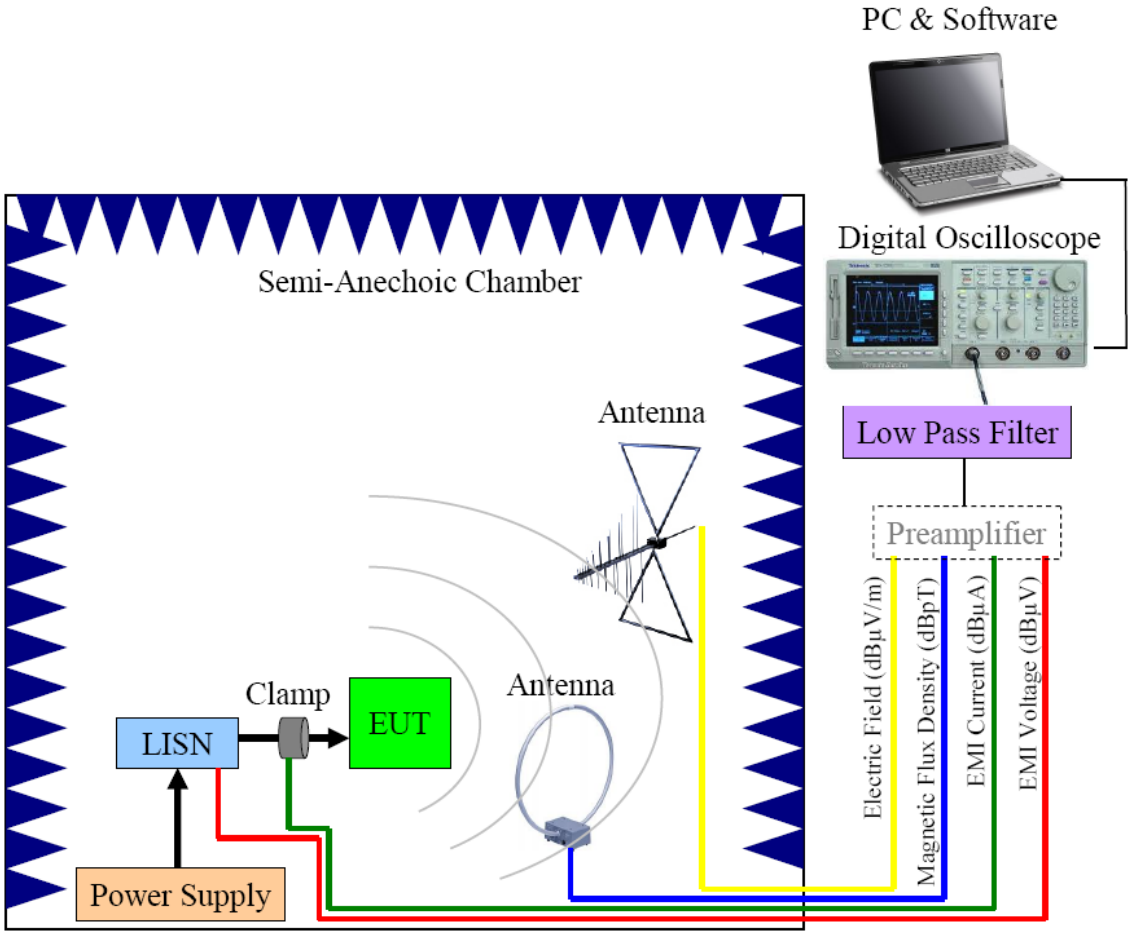

Figure 1.2 *Example of time domain EMI measurement system.*

As shown in figure 1.2, all of the frequency domain EMI measurements can be replaced by TDEMI measurements.

First publication related to TDEMI has been published over twenty years ago [2] and some other publications which also refer to the time domain methods in EMI measurements have been published in the nineties [3][4][5].

In 2001, Keller and Feser [6] from the University of Stuttgart presented a time domain EMI measurement system in EMC 2001 Conference in Zurich. The perspective in their conference paper is speeding up the radiated emission measurement process with a reliable test method. Their test method is based on the procedure shown in figure 1.3. This procedure is called basic algorithm in their later publications.

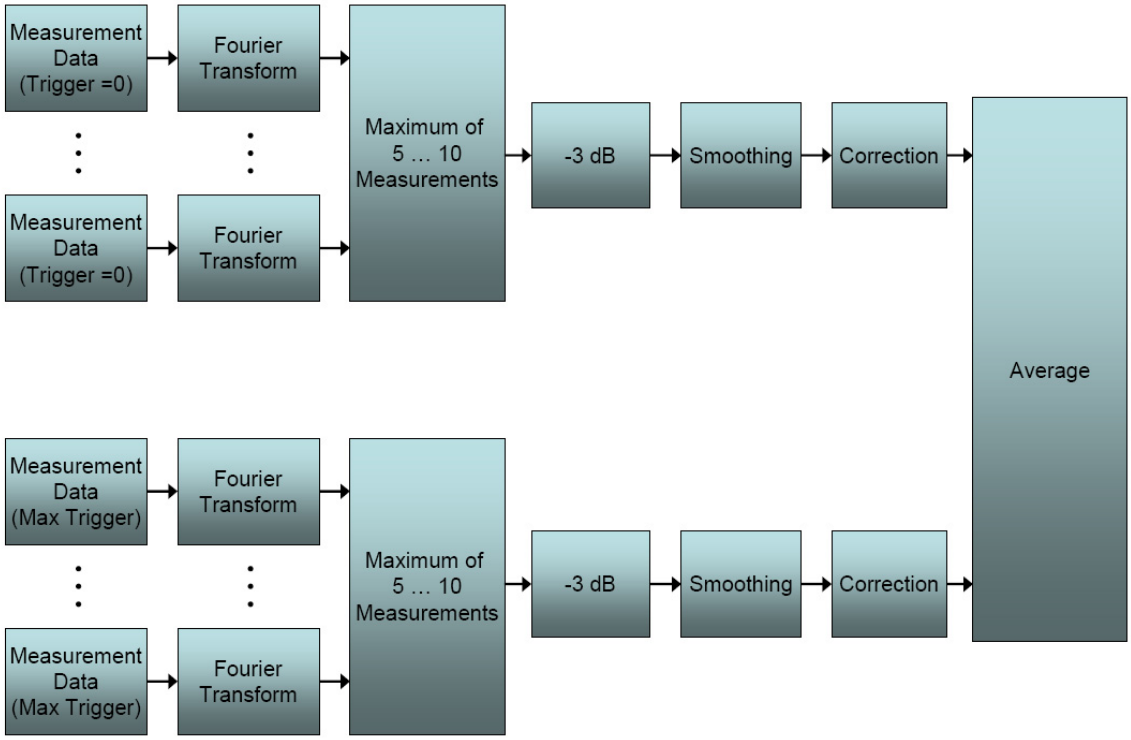

Figure 1.3 *Algorithm used in Keller's and Feser's paper Fast Emission Measurement in Time domain from 2001 [6].*

In the algorithm, the measurement data is first acquired by two sets of oscilloscope measurements. In the first set the trigger level is zero and in the second set the trigger level is as high as possible (= max trigger). After measurement data acquisition the Discrete Fourier Transform (DFT) is used to produce amplitude spectrum. Maximum of the produced amplitude spectrums is taken into account. As the DFT gives the peak values while EMI receiver and spectrum analyzer give RMS values, the maximum amplitude spectrums shall be corrected by reducing the results by 3 dB. Results are also smoothed with a 3-point window. Correction before averaging the maximum amplitude spectrums from two separate sets incorporates corrections for antenna, cables and preamplifier.

In addition to measurements with the algorithm presented above, their paper includes some discussion of measurement accuracy and limitations for the time domain EMI measurement system. Conclusion of their paper [6] is that the emission measurements in time domain can significantly reduce the time needed for measurements, and measurement results are within 2 to 3 dB margin when compared to frequency domain measurement results. Proposed applications for the TDEMI measurement system are:

- Quick preview of critical frequency ranges
- Repeated emission checks
- Measurement of short phenomena
- Searching of direction of the highest radiation.

Keller and Feser improved their TDEMI measurement system so that the measurement accuracy of narrowband and broadband interference signals is increased. Their paper [7] in EMC 2002 conference introduces separate algorithms for narrowband and broadband interference signals. For TDEMI measurement system, it is vital that the correct algorithm is used for narrowband and broadband interference. Figure 1.4 shows how the interference differentiation and classification is done.

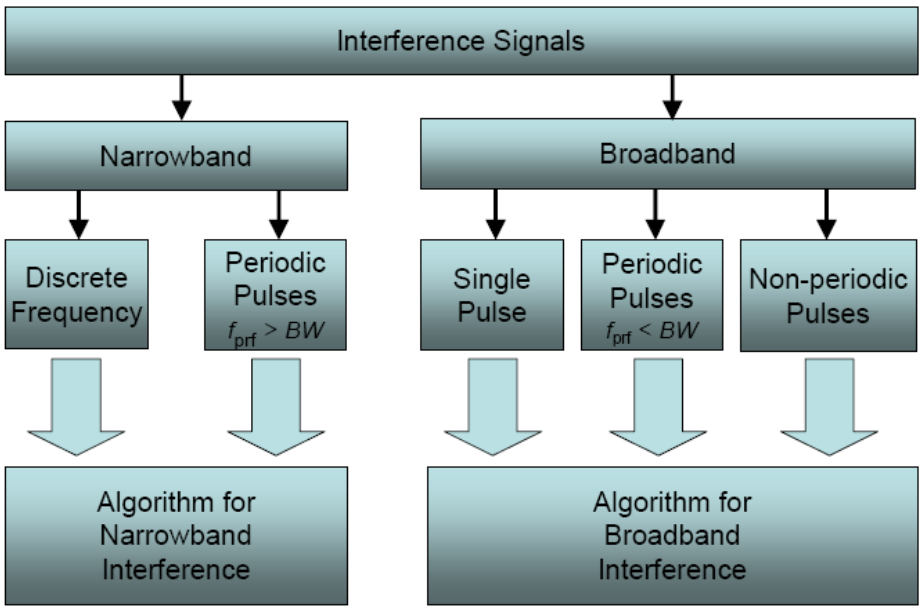

Figure 1.4 *Interference classifications [7].*

According to Keller and Feser the narrowband signals are sinusoidal oscillations of a discrete frequency or periodic pulses which have repetition frequency f_{prf} higher than the bandwidth (BW) of the measurement system. Figure 1.5 describes the basic concept of algorithm for narrowband interference signals.

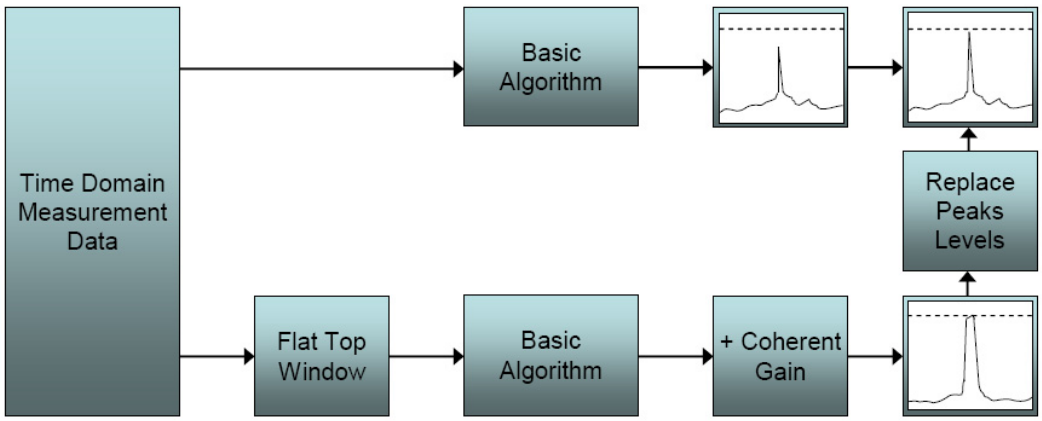

Figure 1.5 *Algorithm for correction of narrowband interference i.e. peaks [7].*

The main idea of the algorithm is to use window functions to reduce the so-called scallop loss and to correct the level of narrowband peaks. The scallop loss is the loss caused by spectral leakage which occurs when the peak of the narrowband signal is located between DFT steps. According to algorithm the amplitude spectrum is first produced with previously introduced basic algorithm (figure 1.3) and after that, the level of peaks is corrected according to results from signal processing with Flat Top window. More detailed introduction and demonstrations of this algorithm can be found in Chapter 5 of this thesis.

As shown in figure 1.4 the broadband interference signals are caused by single or non-periodic pulses and by pulses with a repetition frequency f_{prf} lower than the bandwidth BW. The algorithm for these kinds of broadband interference signals is described in figure 1.6.

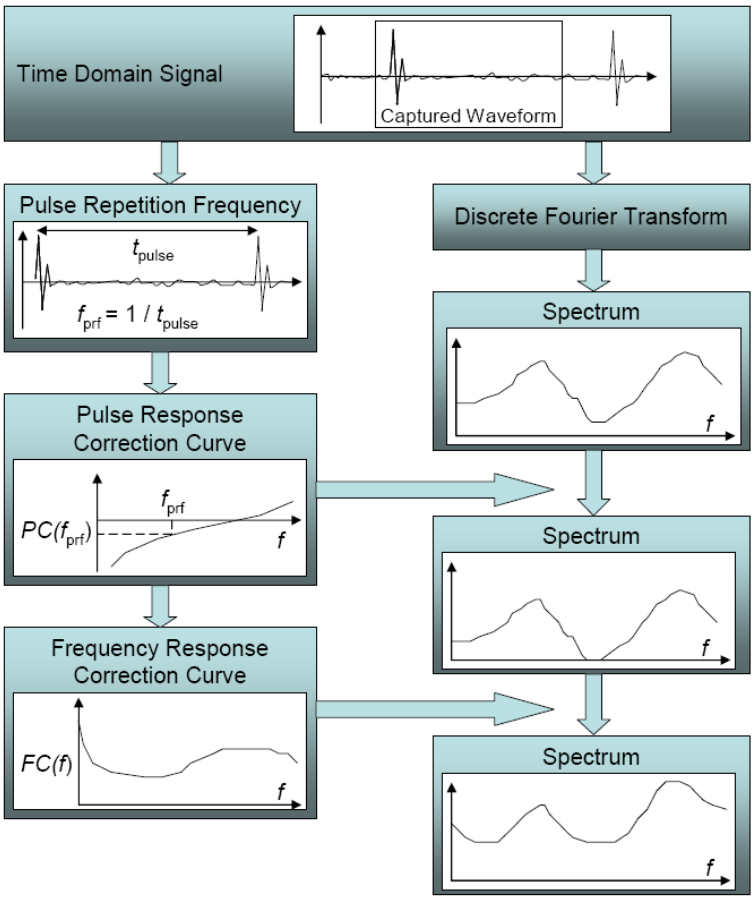

Figure 1.6 *Algorithm for correction of broadband interference [7].*

The algorithm for broadband signals is based on knowledge about the pulse response characteristics of an EMI receiver or a spectrum analyzer and the TDEMI measurement system. Above-mentioned pulse response characteristics are basis for the pulse response correction curve which is used to correct the amplitude of the spectrum. To get the correct value from pulse response correction curve, the pulse repetition frequency shall first be determined from the time domain signal. The last step in the

algorithm is the frequency response correction which incorporates corrections for antenna, cables and preamplifier etc. But how this algorithm is used for single and non-periodic pulses which have no clear pulse repetition frequency remains unclear in their paper [7]. As the algorithm for narrowband interference signals, also this algorithm for broadband interference signals is studied more in Chapter 5 of this thesis.

Keller and Feser have published several other papers concerning TDEMI measurement systems after the two papers [6][7]. From this thesis point of view the most significant paper [8] was published in 2007. This paper introduces improvements for the previously described algorithms. In this paper the fact that the interference signals are typically mixtures of several different signals containing narrowband and broadband components is taken into account. The solution is called superposition of the part spectra.

In addition to Keller and Feser, Krug and Russer from the Technical University of Munich have also made noticeable research work on time domain methods and they have published several publications together with other researchers. In their paper [9] from 2003 the previous studies related to time domain methods from different authors are summarized. The new point of view in this paper is the use of Welch and Bartlett periodograms instead of Fast Fourier Transform (FFT). TDEMI measurement system that is capable to emulate conventional quasi-peak detector is presented in [10] 2003 and signal processing related to time domain method is discussed in their conference papers [11][12] also from the year 2003. Especially the paper [12], which deals with the signal processing strategies for different kind of signals (stationary, quasi-stationary and non-stationary signals etc.) is very useful from this thesis point of view. Uncertainty of time domain measurements is also analyzed in their conference paper [13] which focuses to statistical evaluation of FEMIT methods.

Even though the main reason for developing the time domain measurement methods is very practical, most of the published papers have very theoretical approach to this issue. More practical point of view to time domain measurement methods can be found in conference paper by Pontt et al. [14]. This paper discusses the development of a simple and cost effective pre-compliance measurement system for conducted emissions in industrial environment.

Aforementioned TDEMI measurement systems are typically based on measurements with digital oscilloscopes i.e. with one A/D converter. This limits the dynamic range and frequency range of the TDEMI measurement system. Further studies are more related to measurement systems with several parallel A/D converters and FFT-based banks of receivers. These more sophisticated TDEMI measurements systems have improved dynamic range and broader frequency band up to 18 GHz. Improved dynamic ranges and broader measurement frequency bands make TDEMI measurement system suitable also for compliance measurements. In 2005, Braun et al. presented a Multiresolution Time Domain EMI Measurement System (MRTDEMI) that fulfils almost all CISPR 16-1 requirements [15] and can be used up to 1 GHz frequency. This MRTDEMI measurement system is based on a power splitter and three parallel A/D

converters. TDEMI measurement systems which can be applied beyond 1 GHz are introduced e.g. in [16][17].

Couple of dedicated working groups have been formed to study how the time domain measurements can be used in compliance measurements according to CISPR standards. Working groups have generated drafts for CISPR to allow the use of FFT-based measurement instruments and time domain techniques in standardized EMC measurements [18][19]. Latest versions of CISPR 16-1 and 16-2 standards recognize FFT-based measurement instruments and allow the use of FFT-based measurement instrument.

H. Westenberger from German measurement instrument manufacturer Rohde & Schwarz has also analyzed the use of time domain methods for CISPR 16 compliant EMI measurements in his conference paper [20] from 2009. The paper includes a short review of time domain measurement technique and an introduction of technical implementation based on enhanced EMI measurement receiver with real-time FFT spectrum analyzer. The paper [20] describes well the current situation of time domain measurement technique:

- Time domain technique has been seen as an effective method for several years
- Measurement time can be significantly reduced by using time domain technique
- Time domain technique gives realistic and reliable measurement results
- Time domain technique can be used in pre-compliance measurements but also in compliance measurements.

An extensive summary of the time domain EMC measurement methods and recent research work can be found in P. Russer's presentation [19] from 2011. This document gives very good overview on time domain EMC measurement methods together with great number references.

2 RESEARCH PROBLEM AND OBJECTIVES

As described in the Chapter 1, TDEMI measurement methods and FFT-based measurement instruments can be used in CISPR 16 based compliance measurements. Still it is not yet possible to use TDEMI measurement methods in compliance measurements required by U.S. military standard MIL-STD-461F [1].

The aim of this research is to study the feasibility of TDEMI measurement methods in MIL-STD-461F compliance measurements. The EMI measurement method studied as an example is the conducted emission measurement method CE102. Fundamental questions in this research are:

- Can frequency domain EMI measurement method be replaced by time domain EMI measurement method in MIL-STD-461F CE102 compliance measurements?
- What are pros and cons of TDEMI measurement methods when applied in MIL-STD-461F CE102 measurements?
- What is the optimal and proposed configuration for the TDEMI measurement system in MIL-STD-461F CE102 measurements? In this case configuration means in addition to physical parts also signal processing algorithms and methods.
- What is the measurement uncertainty of the TDEMI measurement system?

Experimental measurements with time TDEMI measurement methods are essential part of the research. This means that in the different phases of this research, studied methods and algorithms are evaluated by measurements. In some cases, simulations are used instead of measurements.

The first task in this research is to build a TDEMI measurement system based on the literature introduced in the Chapter 1 and to evaluate the built system. Second task is to study how the TDEMI measurement system could possibly be improved by different methods and signal processing. Third task is the validation of the proposed TDEMI measurement system. This task incorporates evaluation of measurement uncertainty and also comparison of TDEMI measurement system and standard frequency domain MIL-STD-461F CE102 measurement system.

Before actual research, the CE102 measurement method (requirement) which is used as a reference should be studied. This is done in Chapter 3.

3 REQUIREMENT CE102 OF MIL-STD-461F STANDARD

3.1 Purpose of CE102 requirement

CE102 requirement defines the measurement method and limits for conductive emissions on power leads within a frequency range of 10 kHz to 10 MHz. The purpose of this requirement is to ensure that the level of the conductive emissions on power leads is low enough for two reasons:

1) at lower frequencies, to ensure that the equipment does not corrupt the total power quality of larger installation. Power quality requirements for larger installations are described for example in documents MIL-STD-704 for aircraft, MIL-STD-1399 for ships, MIL-STD-1539 for space systems, and MIL-STD-1275 for military vehicles.

2) at higher frequencies, to ensure that the potential radiation from power leads does not cause significant radiated emissions. For this reason the CE102 measurement should be performed before radiated emission measurements e.g. RE102 measurements.

3.2 General requirements of MIL-STD-461F

Requirement CE102 consists of general requirements described in section 3.2 and detailed requirements described in section 3.3. Following general requirements, introduced in subsections 3.1.2.1 - 3.1.2.7 of this thesis, are essential for CE102 measurements. These general requirements are requirements for measurement system but also for EUT.

3.2.1 Switching transients

Manually actuated switching functions may produce transient emissions which exceed the emission limits. Switching operations of inductive components like relays, contactors and solenoids cause current and voltage spikes and surges. These kind of transient emissions caused by manual switching functions are excluded from the requirements of MIL-STD-461F, although requirements for these transients can be found for example in MIL-STD-1275 which has a connection to MIL-STD-461F as described previously.

Transient emissions caused by automatic switching functions and operations are in the scope of MIL-STD-461F.

3.2.2 Tolerances

MIL-STD-461F defines following general tolerances:

- Amplitude, measurement receiver ±2 dB
- Amplitude, measurement system ±3 dB
  (measurement receivers, transducers, cables etc.)
- Capacitance ±20 %
- Distance ±5 %
- Frequency ±2 %
- Resistance ±5 %
- Time (waveforms) ±5 %

In addition to above listed tolerances, the MIL-STD-461F defines the ±20 % tolerance for the LISN impedance. This issue is discussed in more details in subsection 3.2.5.

3.2.3 Shielded enclosures and ambient electromagnetic level

MIL-STD-461F recommends that the measurements should be performed inside shielded enclosures. This is a reasonable recommendation for radiated emission measurements but the conducted emission measurements may also be performed outside shielded enclosures.

When measurements are performed inside a shielded enclosure, the MIL-STD-461F requires that the measured ambient electromagnetic level shall be at least 6 dB below the specified limits with the EUT de-energized and all auxiliary equipment turned on. This requirement is rather easy to fulfil also without shielded enclosure during conducted emission measurements and therefore MIL-STD-461F allows performing measurements also outside shielded enclosures.

When conducted emission measurements are performed outside shielded enclosures, the ambient conducted interference on power leads should be measured with the leads disconnected from the EUT and connected to a resistive load which draws the same current as the EUT.

3.2.4 Ground plane

MIL-STD-461F requires that the EUT should be installed on a ground plane that simulates the actual installation. If the EUT's actual installation does not comprise a ground plane, the EUT shall be placed on a non-conductive table. In cases where the EUT's actual installation is not known, a metallic ground plane of 2.25 m^2 or larger shall be used. MIL-STD-461F defines also other requirements for metallic ground plane like

surface resistance etc. Detailed requirements can be found in subsection 4.3.5.1 of MIL-STD-461F.

3.2.5 Power source impedance

Line Impedance Stabilization Networks (LISNs) shall be used in EUT power supply inputs to

1. filter the possible interference from power supply network
2. stabilize the power line impedance
3. provide measurement point (signal output port).

The required circuit schematic for LISN circuit is shown in figure 3.1. It should be noted that this circuit schematic is not included in CISPR 16-1 standard which defines four different LISN circuit schematics that are widely used in testing of commercial products.

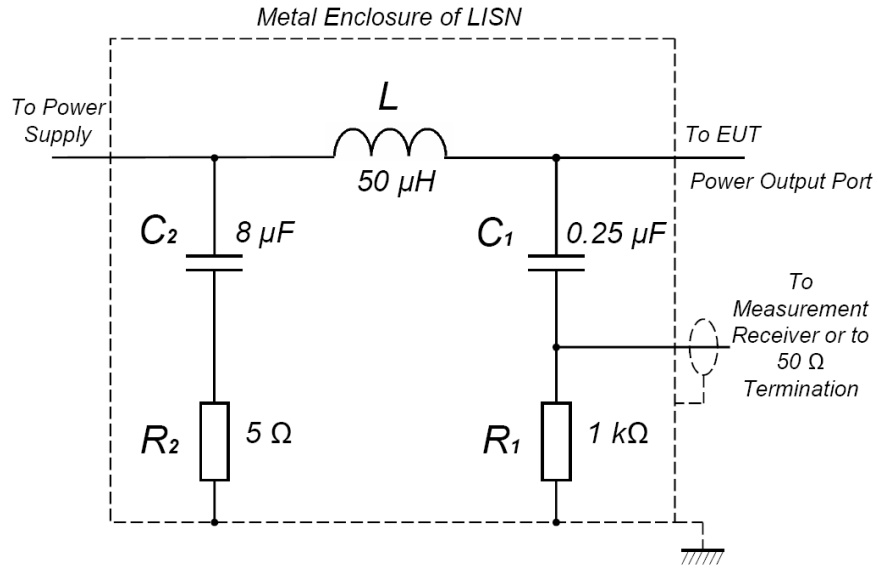

Figure 3.1 *MIL-STD-461F LISN circuit schematics.*

The impedance of LISN is the impedance between power output port and the metal enclosure of the LISN. MIL-STD-461F requirement for this impedance versus frequency is shown figure 3.2.

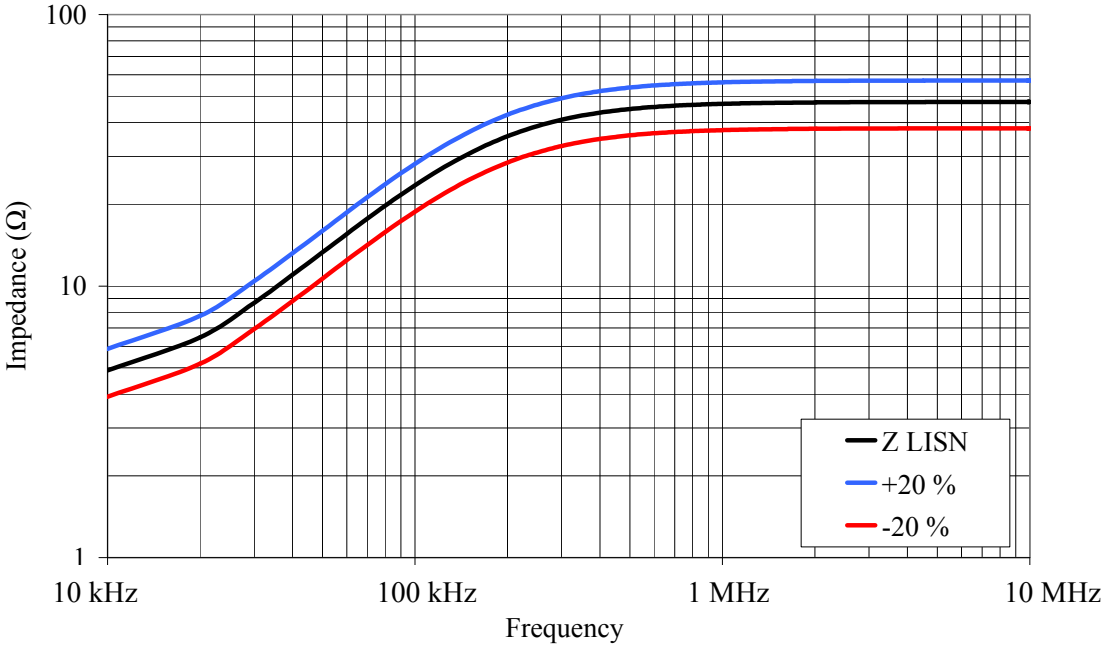

Figure 3.2 *MIL-STD-461F requirement for LISN impedance with allowed ±20 % tolerances.*

As the figure 3.2 shows, MIL-STD-461F gives ±20 % tolerances for the LISN impedance value. This can have an effect on measurement results i.e. conducted emission measurements with different LISNs, having different impedance, may cause divergence in measurement results even if the LISN impedances are inside tolerance.

3.2.6 EUT cables and bonding

The main principle concerning the EUT cables and cable arrangement during testing is that the cables and their arrangement shall be as in real installation. The same applies also to the bonding of EUT units together or to the ground plane. Bonding straps and cables shall be identical to those used in real installation. Detailed requirements for cabling arrangements are described in subsection 4.3.8 of MIL-STD-461F.

3.2.7 Bandwidth, detector and measurement time

Key parameters for measurements are resolution bandwidth (RBW), detector type and measurement time (sweep time). Table 3.1 shows the MIL-STD-461F requirements for these parameters in the CE102 frequency range (10 kHz to 10 MHz).

Table 3.1 *Resolution bandwidths and measurement times.*

Frequency	Resolution Bandwidth (6 dB)	Dwell Time	Measurement Time (analog measurement receiver)
10 kHz – 150 kHz	1 kHz	0.015 s	0.015 s / kHz
150 kHz – 10 MHz	10 kHz	0.015 s	1.5 s / MHz

Resolution bandwidths applied in MIL-STD-461F measurements are different than in CISPR based measurements. In the frequency range of 10 kHz to 10 MHz MIL-STD-461F uses 1 kHz and 10 kHz resolution bandwidths when CISPR based standards use 200 Hz and 9 kHz resolution bandwidths. MIL-STD-461F allows also using broader bandwidths but in these cases results can't be corrected using any factors.

Another difference between MIL-STD-461F and CISPR measurements is the type of the detector. MIL-STD-461F requires peak detector while CISPR requires quasi-peak and average detectors. In practise peak detector is also used in CISPR measurements because it reduces the measurement time significantly. Typical procedure is to pre-scan the frequency range with peak detector and to check if there are any emissions that exceed limits. If emissions are below limits when peak detector is used, it is clear that quasi-peak and average detectors can't produce any higher amplitude and measurements with quasi-peak or average detectors are not needed. If some of the peaks exceed the limit, these peaks are re-measured with quasi-peak and average detectors.

Measurement time and number of sweeps are very important parameters for emission measurements. MIL-STD-461F allows the use of single sweep or multiple fast sweep method (alternative scanning technique). If a single sweep method is used, the sweep time can be calculated by using equation 3.1.

$$\text{Sweep time 1} = 2 \cdot \frac{\text{Span}}{\text{Resolution Bandwidth}} \cdot \text{Dwell time} \tag{3.1}$$

Sweep times for CE102 measurements are:

$$\text{10 kHz – 150 kHz: Sweep time} = 2 \cdot \frac{150\ \text{kHz} - 10\ \text{kHz}}{1\ \text{kHz}} \cdot 0.015\ \text{s} = 4.2\ \text{s}$$

$$\text{150 kHz–10 MHz: Sweep time} = 2 \cdot \frac{10000\ \text{kHz} - 150\ \text{kHz}}{10\ \text{kHz}} \cdot 0.015\ \text{s} = 29.55\ \text{s}$$

Instead of single sweep several faster sweeps can be used. This is very convenient when interference i.e. peaks occur randomly or with a low repetition rate. The sweep time for one fast sweep can be calculated by using equation 3.2.

$$\text{Sweep time 2} = \frac{2 \cdot \frac{\text{Span}}{\text{Resolution Bandwidth}}}{\text{Resolution Bandwidth}} \tag{3.2}$$

The number of fast sweeps can then calculated by equation 3.3.

$$\text{Number of fast sweeps} = \frac{\text{Sweep time 1}}{\text{Sweep time 2}} \tag{3.3}$$

This number of sweeps with fast sweep time corresponds to the sweep time for single sweep method. As obvious, the maximum hold function shall be used with this multiple fast sweep method.

Regardless of the method the total measurement time shall be long enough to capture all kind of emissions, infrequent or frequent.

3.3 Detailed requirements

Detailed requirements define how the measurement system should be calibrated before measurements and how the measurements should be conducted. Also the limit levels are naturally very important.

3.3.1 CE102 Limit level

Figure 3.3 defines the maximum allowed emission voltage level i.e. limit line. Basic curve is the limit for 28 volt equipment and the limit level is greater (relaxed) for the equipment which use higher supply voltage as shown in figure 3.3.

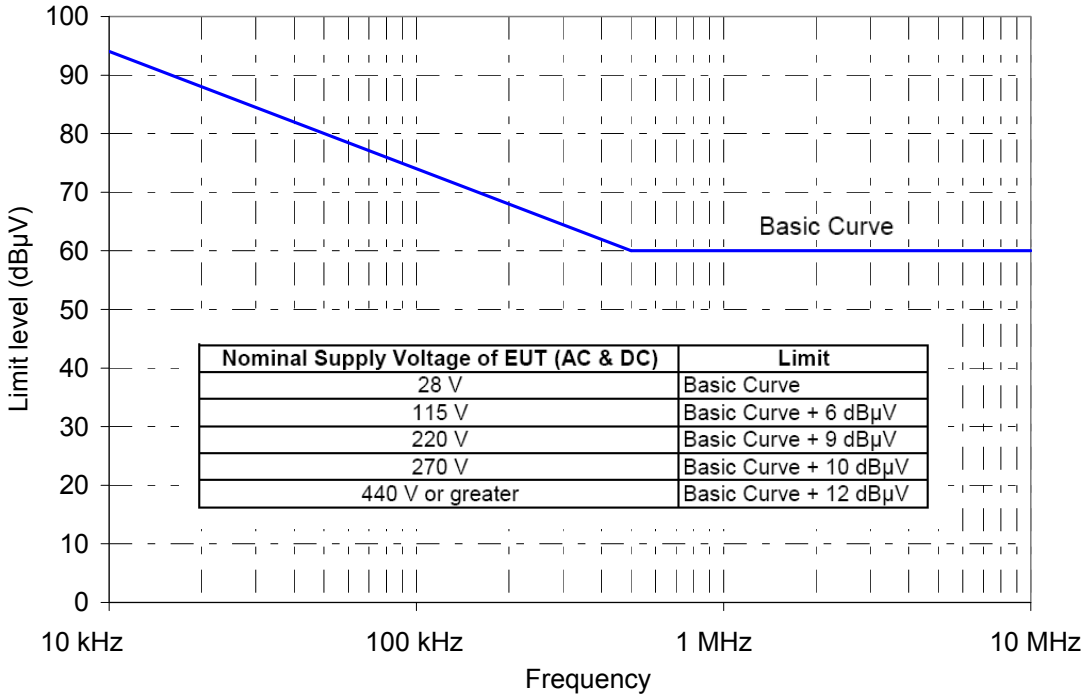

Nominal Supply Voltage of EUT (AC & DC)	Limit
28 V	Basic Curve
115 V	Basic Curve + 6 dBµV
220 V	Basic Curve + 9 dBµV
270 V	Basic Curve + 10 dBµV
440 V or greater	Basic Curve + 12 dBµV

Figure 3.3 *MIL-STD-461F limit levels for CE102 measurement.*

It is important to realize that the voltage levels described in figure 3.3 are typical for U.S. military standards and for U.S. equipment. The 28 V supply voltage is very typical for military equipment. This voltage level is related to 28 Vdc nominal voltage used in military vehicles and it corresponds to 24 Vdc nominal voltage which is used in civilian standards. The nominal voltage 28 Vdc used in U.S. military standards refers to charging voltage and the nominal voltage 24 Vdc used in civilian standards (IEC, EN,

ISO etc.) refers to nominal voltage of batteries. This means that the same voltage level has two different definitions. In practise the basic limit curve is used when dc equipment is tested including 12 Vdc equipment.

115 V nominal voltage is typical for aircraft's 400 Hz power system. This voltage is phase voltage (voltage between line and neutral) and the corresponding main voltage (between lines) is 200 V. Also the higher nominal voltages described in figure 3.3 are typical for U.S. power supply systems.

In Europe the typical nominal ac voltage is 400V/230V (50 Hz). This voltage level can't be found from the MIL-STD-461F. It is also unclear if the main voltage value or phase voltage value should be used for three phase equipment.

3.3.2 Calibration

Before conducting measurements the measurement system shall be calibrated. This shall be done by injecting 10 kHz, 100 kHz, 2 MHz and 10 MHz sinusoidal signals to the power output ports of LISNs. The level of these calibration signals shall be at least 6 dB below the limit line. Measurement receiver shall then indicate signal levels which are within ±3 dB range compared to the injected signal levels. Figure 3.4 shows the concept of calibration setup.

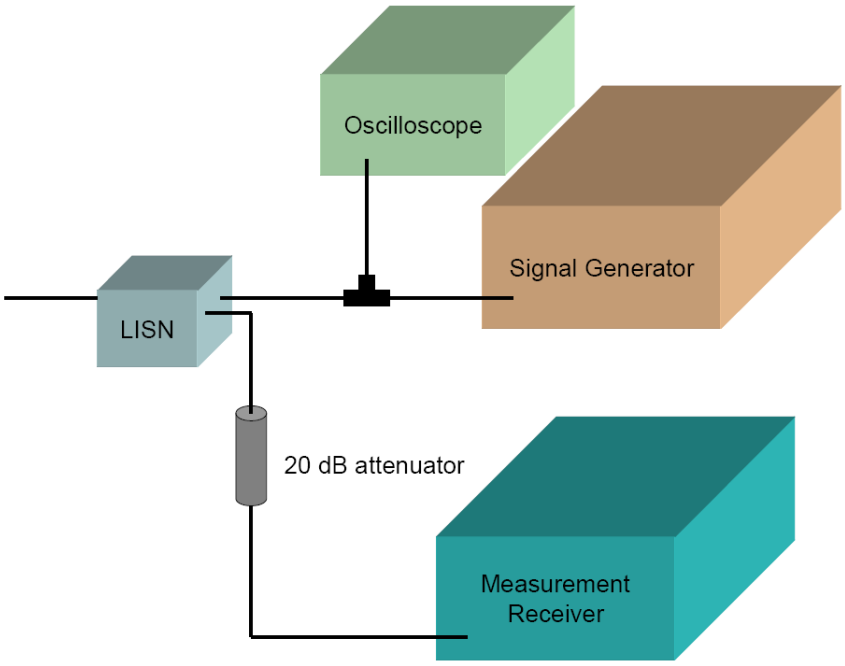

Figure 3.4 *CE102 measurement setup calibration.*

The 20 dB attenuator between LISN and the measurement receiver protects the receiver from overload. Overload is possible, especially when 115 Vac 400 Hz power is supplied through the LISN. The effect of 20 dB attenuator shall be compensated with an appropriate correction. Another correction is needed because of the voltage drop across

the 0.25 µF coupling capacitor in LISN (capacitor C_1 in figure 3.1). MIL-STD-461F gives the following equation 3.4 for the correction F_{C1}.

$$F_{C1} = 20 \cdot \log_{10} \frac{\sqrt{1\text{Hz}^2 + 5.6 \cdot 10^{-9} \cdot f^2}}{7.48 \cdot 10^{-5} \cdot f} \tag{3.4}$$

The value of the correction F_{C1} versus frequency f is plotted in figure 3.5.

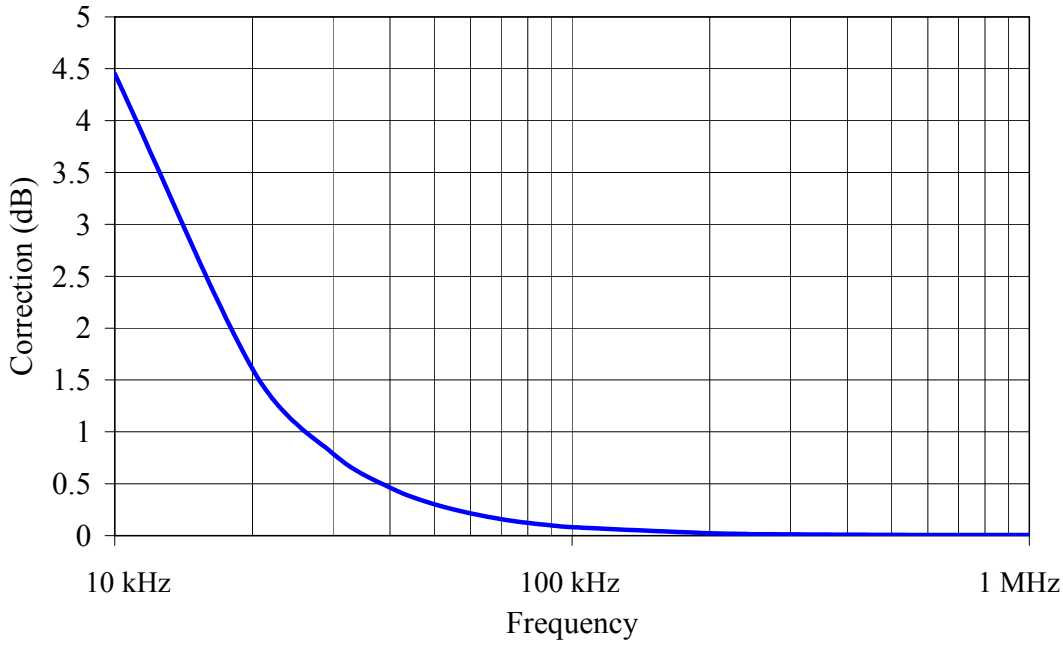

Figure 3.5 *Correction for 0.25 µF capacitor.*

As the figure 3.5 shows, the correction has a value of 4.45 dB at 10 kHz but the value decreases rapidly and it is close to 0 dB already at 100 kHz.

The oscilloscope in the calibration setup is needed to check the level of calibration signals at 10 kHz and 100 kHz frequencies. At these frequencies the LISN impedance is not around 50 Ω as it can be seen in figure 3.2. Therefore the signal level shall be checked with oscilloscope.

3.3.3 CE102 measurement

After calibrating the measurement system, the CE102 measurement shall be done to each power lead of EUT according to the general and detailed requirements defined by MIL-STD-461F. Figure 3.6 shows the basic measurement setup.

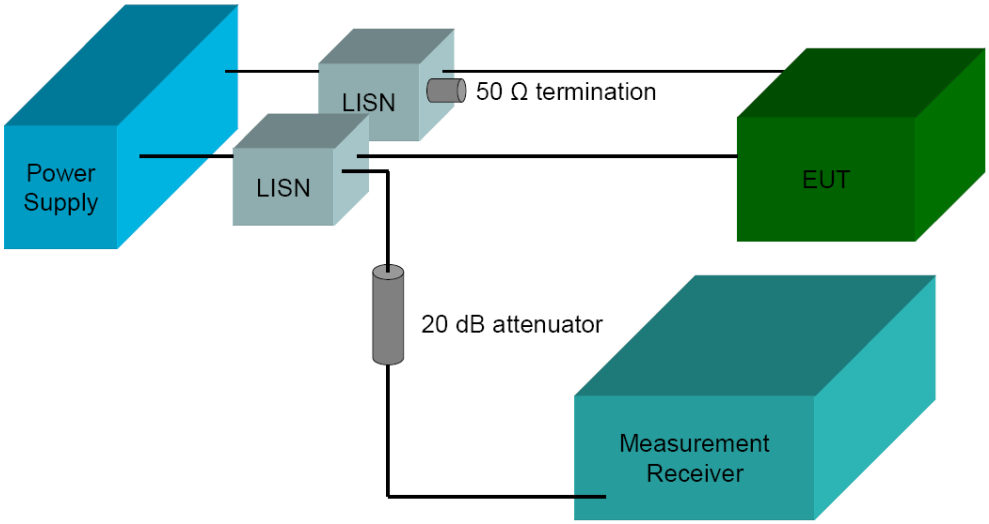

Figure 3.6 *CE102 measurement setup.*

The signal output port of the LISN shall be connected to measurement receiver through 20 dB attenuator and the signal output ports of other LISN(s) shall be terminated to 50 Ω termination.

3.4 The Reference EMI source

The essential part of this research work is the experimental measurements of typical EMI sources. For this purpose a device called the reference EMI source, including switch-mode DC/DC power supply and brushed DC motor, was built. Switch-mode power supplies and brushed DC motors represent very common EMI sources which cause problems for product manufacturers. The reference EMI source is used as an EUT in measurements.

Appendix 1 of this thesis shows the circuit diagram for the reference EMI source and Appendix 2 shows the assembly drawing for the reference EMI source. Picture of the reference EMI source is shown is figure 3.7.

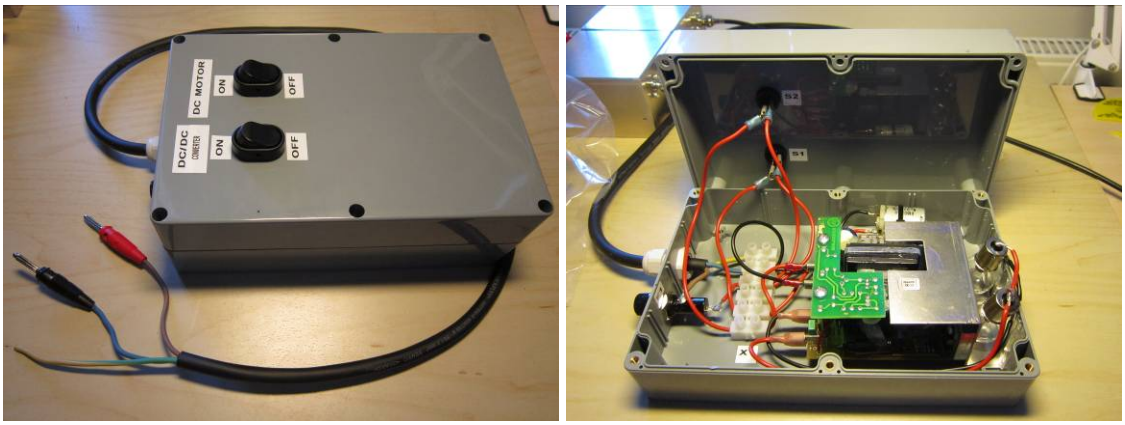

a) b)

Figure 3.7 a) *The reference EMI source from outside* ***b)*** *The reference EMI source from inside.*

The reference EMI source is built according to following requirements and principles:

- Nominal operating voltage is 12 Vdc for electrical safety reasons. This nominal voltage allows also to use one 12 V battery as an interference-free power source.
- Plastic enclosure is used. This represents the typical solution in COTS products.
- Power for reference EMI source is delivered via unshielded cable which has two wires; + 12 Vdc and return (GND).
- The conducted interference in power supply cable is mostly differential mode interference because of the plastic enclosure and two-wire system.
- Brushed DC motor and switch-mode DC/DC converter can be used concurrently or separately.
- Reference EMI source is equipped with a fuse or circuit breaker to avoid short-circuiting of battery.

4 BASIC ALGORITHM FOR THE TIME DOMAIN EMISSION MEASUREMENT

Sections 4.1 to 4.4 introduce the basic elements for the TDEMI measurement system. These basic elements are shown in figure 4.1 below. The first essential element is the correct acquisition of time domain measurement data which requires anti-aliasing filters and correct choice of capture times. These issues are discussed in sections 4.1 and 4.2. Section 4.3 introduces Discrete Fourier Transform (DFT) and Matlab functions which are used to produce amplitude spectrum by DFT. Section 4.4 describes how the corrections used in frequency response correction are determined.

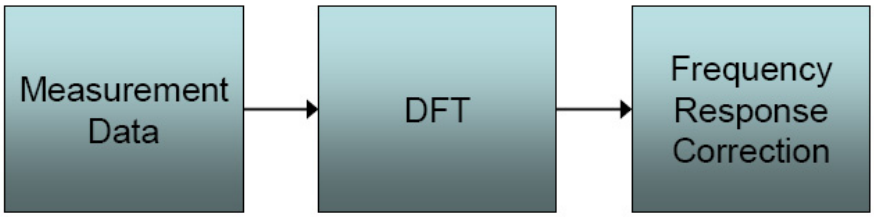

Figure 4.1 *Basic algorithm for time domain emission measurement system.*

First experimental measurements of TDEMI measurement system are described in Section 4.5. These measurements are based on the basic algorithm introduced by C. Keller and K. Feser [6].

4.1 Measurement data acquisition

Because of the two different resolution bandwidths used in CE102 measurement, the measurement data acquisition must be done in two separate parts i.e. for two frequency bands described in table 3. Parameters for data acquisition are the sampling frequency f_s and the capture time T. These parameters must fulfil the following requirements:

1. Sampling frequency f_s shall be 2 to 4 times the upper end of frequency band under investigation [7].
2. Capture time $T = \frac{1}{\Delta f}$, (4.1)

   where Δf is the frequency resolution which corresponds to the resolution bandwidth applied in frequency domain measurement.

On the frequency range from 10 kHz to 150 kHz the sampling frequency f_{s1} shall be at least 300 kHz according to the requirement 1. The oscilloscope used in this research

allows taking 2400 samples per total capture time T_{tot}. The total capture time T_{tot} is the maximum length of the captured waveform in oscilloscope mode and it depends on the chosen time/division setting. Total capture time (T_{tot1}) 6 ms which corresponds to 500 µs/div setting gives us 400 kHz sampling frequency f_{s1} as shown below.

$$f_{s1} = \frac{1}{\left(\frac{0.006\,\mathrm{s}}{2400}\right)} = 400\,\mathrm{kHz}$$

To fulfil the requirement 2, when Δf is 1 kHz, the capture time T_1 must be 1 ms.

$$T_1 = \frac{1}{1000\frac{1}{\mathrm{s}}} = 1\ \mathrm{ms}$$

This means that only part (1 ms) of the total captured waveform (6 ms) will be used. Figure 4.2 shows the total capture time T_{tot1} and capture time T_1 on oscilloscope screen.

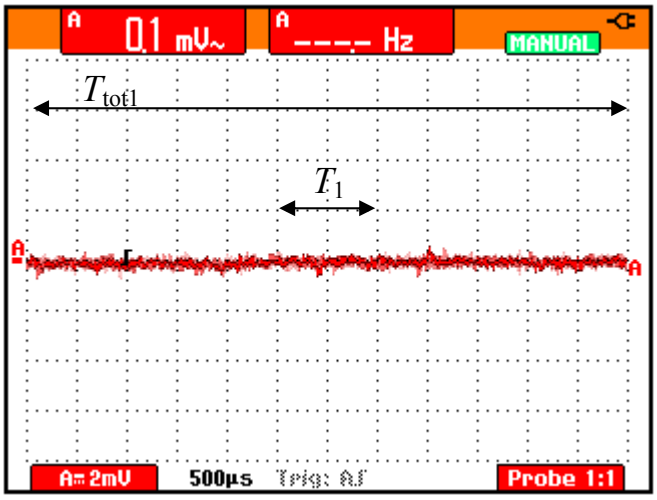

Figure 4.2 *Total capture time T_{tot1} and capture time T_1 on frequency range from 10 kHz to 150 kHz. T_1 can be chosen arbitrarily from the T_{tot1}.*

On the frequency range from 150 kHz to 10 MHz the sampling frequency f_{s2} shall be at least 20 MHz according to the requirement 1. Total capture time (T_{tot2}) 120 µs which corresponds to 10 µs/div setting, gives us 20 MHz sampling frequency f_{s2} as shown below.

$$f_{s2} = \frac{1}{\left(\frac{120 \cdot 10^{-6}\,\mathrm{s}}{2400}\right)} = 20\,\mathrm{MHz}$$

To fulfil the requirement 2, when Δf is 10 kHz, the capture time T_2 must be 100 µs.

$$T_2 = \frac{1}{10000\frac{1}{\mathrm{s}}} = 100\ \mu\mathrm{s}$$

In this case most of the captured waveform will be used as shown in figure 4.3.

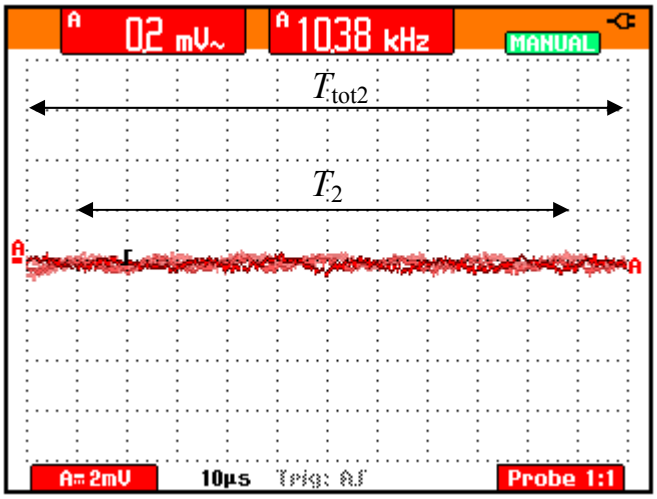

Figure 4.3 *Total capture time T_{tot2} and capture time T_2 on frequency range 150 kHz to 10 MHz. T_2 can be chosen arbitrarily from the T_{tot2}.*

MIL-STD-461F requirement for minimum frequency resolution is 1 % or two times the resolution bandwidth used in measurement. In this research work the frequency resolution is equal to the resolution bandwidth which clearly fulfils the frequency resolution requirement.

4.2 Anti-aliasing filters

According to the sampling theorem, input signals with frequencies below $f_s/2$ can be reliably detected. If the input signal has spectral components above $f_s/2$, these components will fold back to frequency range 0 to $f_s/2$ and sum with frequency components below $f_s/2$. This leads to incorrect frequency domain measurement results and the phenomenon is called aliasing. The level of aliasing (summing) depends on power and phase of the signal.

To avoid aliasing the input signal must be low pass filtered before sampling. In theory, the low pass filter should filter off all of the frequency components above $f_s/2$. In practise this is not possible and the low pass filter is a compromise and it possibly causes some errors to measurement results.

In this research, two low pass filters are used to avoid aliasing. Circuit diagrams and measured frequency responses (gain) of the low pass filters #1 and #2 are shown in figures 4.4 and 4.5. Measurements are done with 50 Ω input impedance (signal generator) and 50 Ω output impedance (spectrum analyzer). The frequency responses of the filters are also simulated with SPICE program called LTSPICE and the results are shown in figures 4.4 and 4.5.

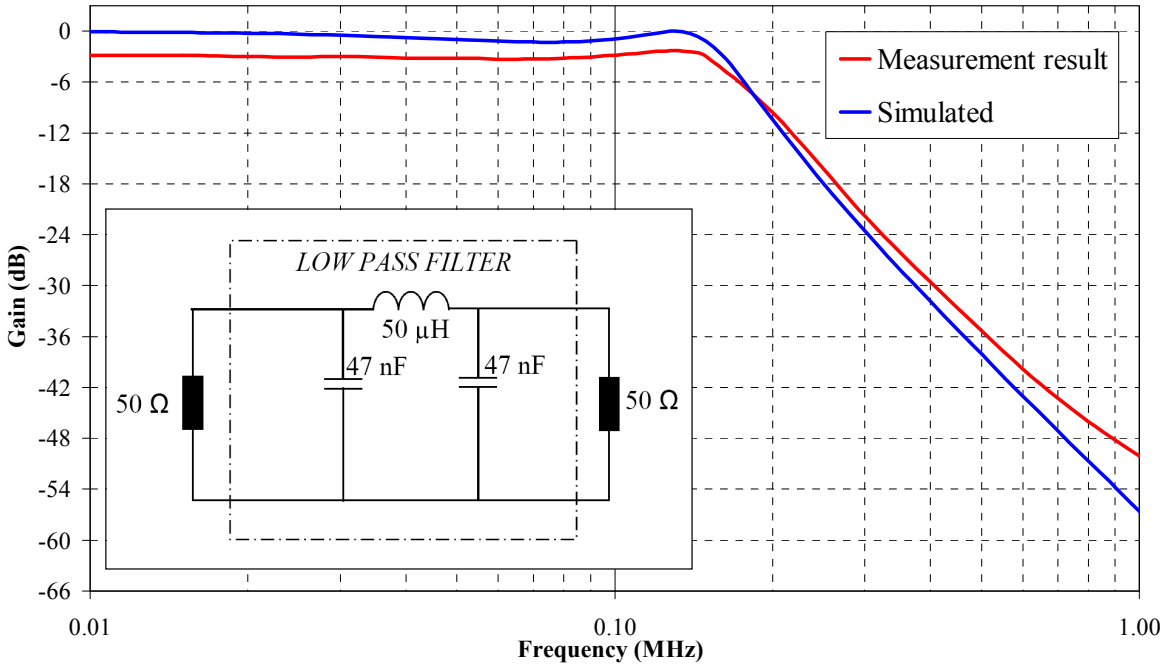

Figure 4.4 *Circuit, simulated and measured frequency responses of low pass filter #1.*

The implementation of the low pass filter #1 is a second order π-filter as shown in figure 4.4. The 3 dB cut-off frequency of this filter is around 170 kHz which fulfils the anti-aliasing requirement.

Figure 4.5 shows the simulated and measured frequency responses of the low pass filter #2 which is used on frequency range 150 kHz to 10 MHz.

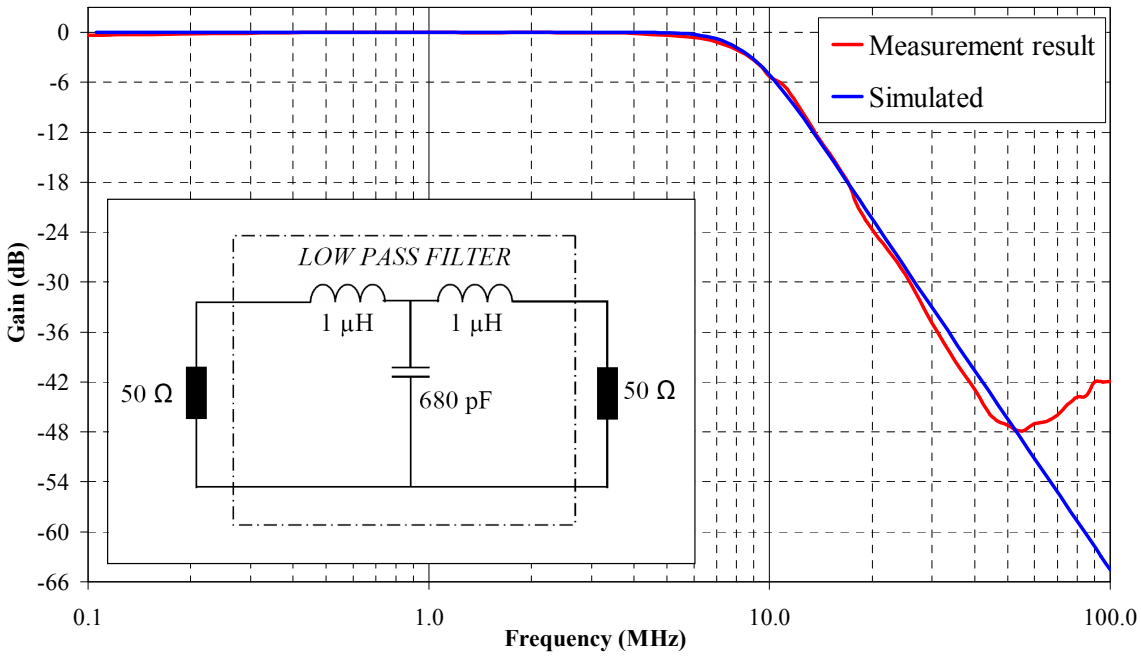

Figure 4.5 *Circuit, simulated and measured frequency responses of low pass filter #2.*

Low pass filter #2 is a second order T-filter. The 3 dB cut-off frequency of this filter is around 9 MHz, which may cause small error to measurement result.

Another possible reason for measurement errors is the phase shift caused by the anti-aliasing filter. This phase shift may cause the summing of the signals which are not summed in the real world, Figures 4.6 and 4.7 show the simulated gains and phases of the low pass filters.

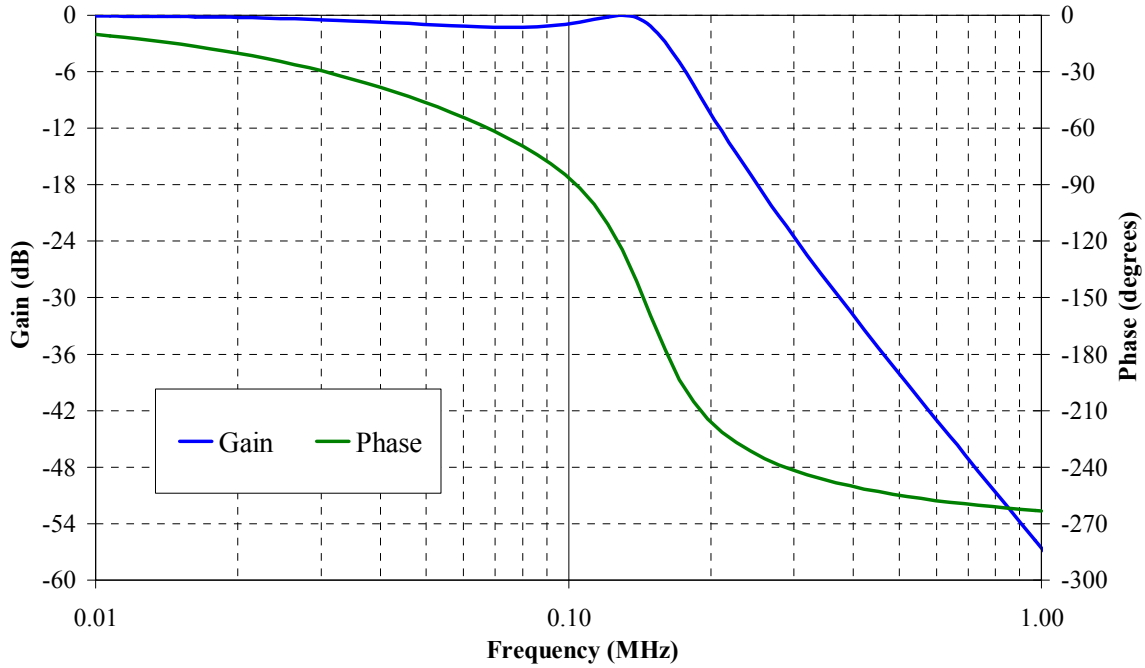

Figure 4.6 *Simulated gain and phase of low pass filter #1.*

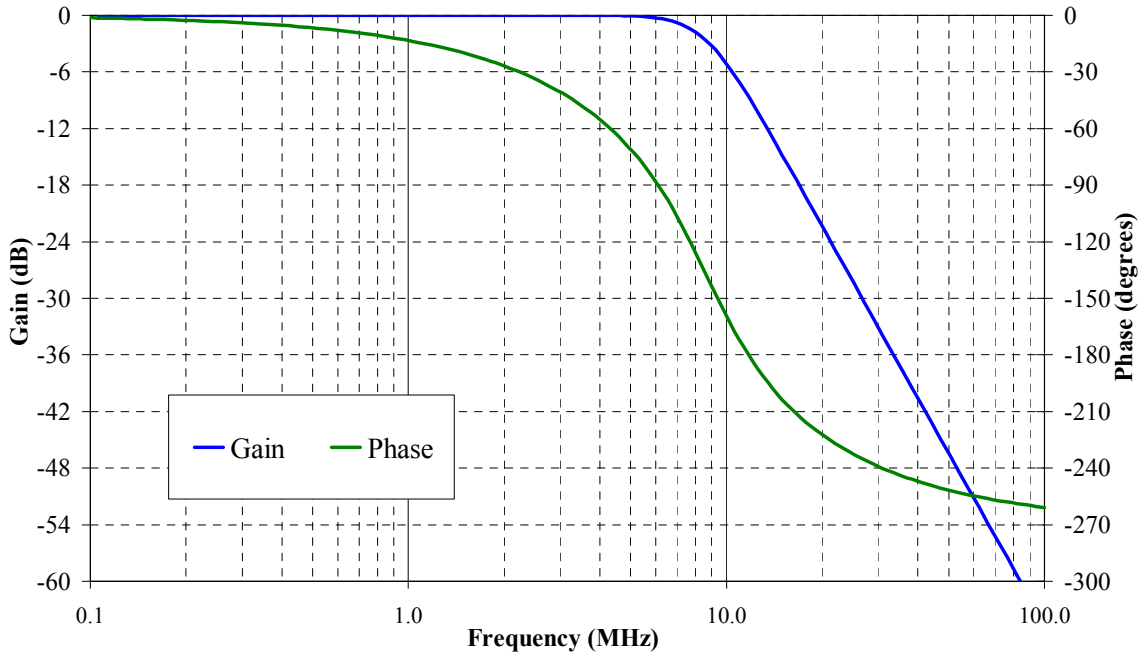

Figure 4.7 *Simulated gain and phase of low pass filter #2.*

Following demonstration illustrates the aliasing phenomenon and the effect of low pass filtering. The frequency range under investigation is the lower measurement frequency band of the CE102 measurement (10 kHz to 150 kHz). Sinusoidal test signals with 80 dBµV amplitude are produced by signal generator (50 Ω output) and measured

by oscilloscope with and without low pass filter #1. As the oscilloscope used in this research has only high impedance (1 MΩ) input, the measurement results do not directly correspond to the results of EMI receiver or spectrum analyzer equipped with 50 Ω input. Oscilloscope equipped with 1 MΩ input gives two times higher amplitude values than EMI receiver or spectrum analyzer in the low frequency measurements. In the low frequency measurements with short cables, the amplitude can be corrected by reducing the result with factor 0.5. If the measured signals contain higher frequency components, the solution described above is no longer acceptable. Higher frequency components and impedance mismatch causes so called standing waves which lead to incorrect amplitude values. The preferred solution is to terminate the oscilloscope's high impedance input with a 50 Ω feed-through termination or with a BNC T-junction and 50 Ω BNC termination as shown in figure 4.7. Both termination alternatives are feasible below 100 MHz and can be used to ensure that correct amplitude values are measured.

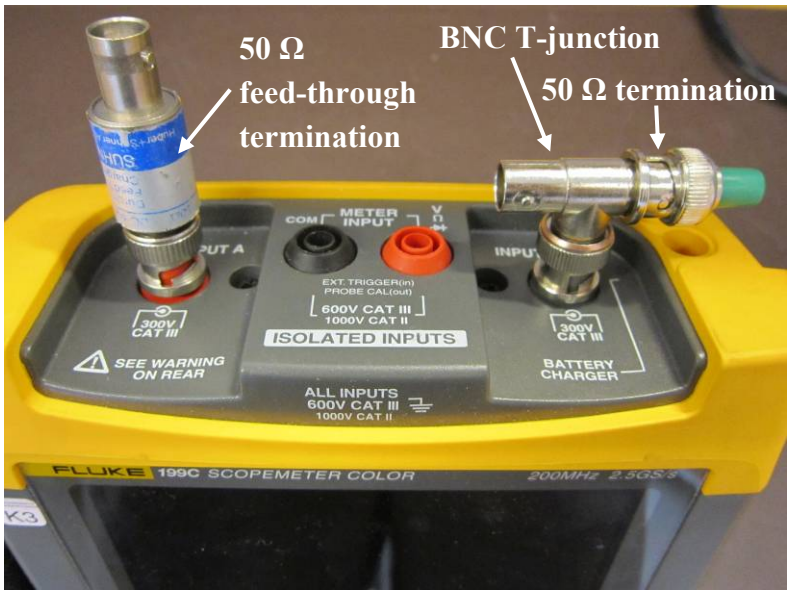

Figure 4.7 *50 Ω feed-through termination and 50 Ω T- termination in the oscilloscope's high impedance inputs.*

The Fourier transform and frequency domain measurement results are produced with MATLAB program. The sampling frequency f_s is 200 kHz and frequencies of the five sinusoidal test signals are listed in the first column of table 4.1.

According to anti-aliasing theory the signals above $f_s/2$ will fold back to frequency band below $f_s/2$ as the equation 4.2 below describes

$$f_{\text{aliased}} = \left| f_{\text{input}} - n \cdot f_s \right| , \tag{4.2}$$

where f_{input} is the frequency of input signal and n is integer.
(n is 0 when $f_{\text{input}} \leq f_s/2$ and $n > 0$ when $f_{\text{input}} > f_s/2$)

Equation 4.2 leads to aliased frequencies which are listed in the second column of table 4.1. The measured amplitudes of the aliased signals without and with low pass filter are also listed in the table 4.1. The reason for 3 dBµV difference between the

amplitude reading of signal generator (80 dBµV) and the amplitude values listed in third column is that the signal generator reading is a RMS value and the Fourier transform returns the peak value of the signal.

Table 4.1 *Test signals and measurement results of aliasing demonstration.*

f_{input} (kHz)	$f_{aliased} = f_{AL}$ (kHz)	Amplitude without filter (dBµV)	Amplitude with filter (dBµV)	Difference in amplitudes (dB)
260	$f_{AL1} = 140$	83.0	67.0	16.0
290	$f_{AL2} = 110$	83.0	63.6	19.4
320	$f_{AL3} = 80$	83.0	58.2	24.8
450	$f_{AL4} = 50$	83.0	37.2	45.8
425	$f_{AL5} = 25$	83.0	48.4	34.6

A graphical presentation of measurement results is shown in figure 4.8. The left hand side measurement result (a) is from the measurement without low pass filter #1 and the right hand side measurement result (b) is from measurement with low pass filter #1.

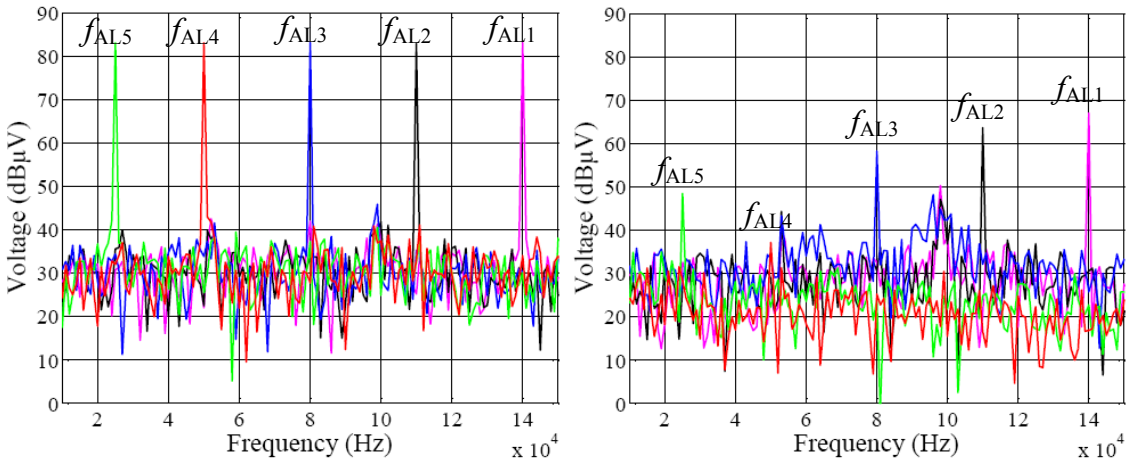

Figure 4.8 *Aliased test signals a) without low pass filter #1 and b) with low pass filter #1.*

As the measurement results show the low pass filter reduces significantly the amplitudes of aliased signals. Still, it is possible that interference signals which are beyond the frequency band fold back and cause error to measurement results. The critical frequencies are located on both sides of the $f_s/2$ (200 kHz). Just above the $f_s/2$ the effect of low pass filter is limited and significant aliasing is possible. The worst possible, but very unlikely case is that the aliased interference signal from upper frequency band sums with the interference signal on lower frequency band and the sum signal exceeds the CE102 limit level. As the lower frequency band ends at 150 kHz which is 50 kHz below the $f_s/2$, the risk of incorrect measurement results is low.

4.3 Discrete Fourier Transform

After time domain measurement data acquisition with low pass filter and applicable settings on oscilloscope the frequency domain measurement result is produced by Fourier transform. Since the data is discrete, the correct Fourier transform method is the Discrete Fourier Transform (DFT) which gives the discrete frequency domain values *X(k)* as shown in equation 4.3.

$$X(k) = \sum_{n=0}^{N-1} x(n) e^{-j2\pi\, k\, n/N} \quad , \; k = 0, 1, 2, \ldots, N\text{-}1 \tag{4.3}$$

where *x(n)* are the discrete input values and N is the total number of these discrete input values (N = capture time $T \cdot$ sampling frequency f_s)

In this part of the thesis the DFT is produced with Matlab program. The syntax for DFT which is computed with efficient Fast Fourier Transform (FFT) algorithm is

```
X = fft(x)
```

Syntax shown above gives the DFT for vector x. The size of the vector X is the same as the size of vector x. To produce the DFT, which is analogous to continuous Fourier transform, the result of the equation 4.3 must be normalized i.e. divided by total number N of discrete input values. This leads to equation 4.4.

$$X_{\mathrm{c}}(k) = \frac{1}{N} \sum_{n=0}^{N-1} x(n) e^{-j2\pi\, k\, n/N} \tag{4.4}$$

The result of the DFT is a set of complex numbers. To get the amplitude spectrum (X_{as}) which corresponds to the result of the frequency domain measurement, the absolute value of the DFT result must be used. The result must also be doubled in the first half of the amplitude spectrum because above $f_s/2$ the spectrum is mirrored. The second half of the amplitude spectrum is not used, but the energy in the second half must be taken into account. Equation for X_{as} is shown below.

$$X_{\mathrm{as}}(k) = \frac{2}{N} \left| \sum_{n=0}^{N-1} x(n) e^{-j2\pi\, k\, n/N} \right| \quad , \; k = 1, 2, \ldots, \frac{N}{2} - 1 \tag{4.5}$$

Corresponding Matlab syntax is

```
Xas = 2*abs(fft(x)/N)
```

The unit for discrete input values is volt and therefore the result of the DFT is also in volts. The amplitude unit used to express the conducted EMI voltage measurement results is a dBμV. To get the corresponding measurement result the following Matlab syntax is used

```
ResultdBuV = 20*log10(Xas/10^-6)
```

Equations and Matlab syntaxes described in this subsection form the basis for TDEMI measurement method. In order to get measurement results which correspond to the results from standardized frequency domain measurements, the amplitude spectrum must be modified with corrections.

4.4 Frequency response correction

One of the frequency response corrections is already presented in equation 3.4 of this thesis. This correction F_{C1} is related to the 0.25 µF coupling capacitor in LISN. In addition to correction F_{C1} following corrections shall be used:

- Correction F_{C2} for lower frequency band (10 kHz to 150 kHz)
- Correction F_{C3} for higher frequency band (150 kHz to 10 MHz)

As discussed in the paper by Keller and Feser [8] the corrections can be calculated or measured. Precondition for calculations is that the characteristics of TDEMI measurement system are very well known. The other way to determine correction is the measurement with appropriate test signals. In this thesis corrections are determined by measurements because especially the impedance characteristics of the TDEMI measurement system are not exactly known.

Figure 4.8 shows the two comparable measurement setups which were used in correction determination. First the 80 dBµV sinusoidal test signals from signal generator were measured with spectrum analyzer and after that, corresponding measurements were performed with TDEMI measurement system.

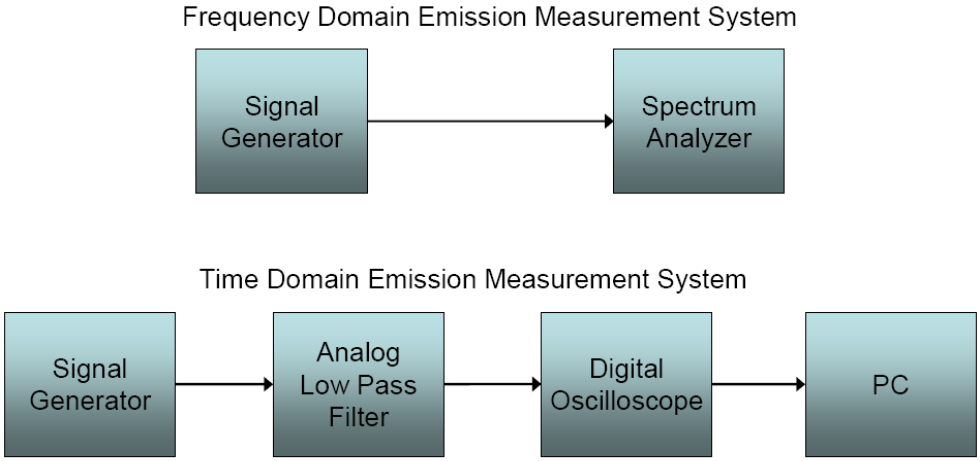

Figure 4.8 *Measurement setups used in correction determination.*

Tables 4.2 and 4.3 show the used test signal frequencies and the measurement results. The values in the *Difference* column are measured differences between frequency and time domain measurement systems. Frequency domain measurement result is the reference and therefore time domain measurement results which are higher than frequency domain measurement results lead to negative difference values.

Table 4.2 *Measured difference between spectrum analyzer and TDEMI on frequency band 10 kHz - 150 kHz.*

Frequency (kHz)	**Spectrum Analyzer (dBµV)**	**TDEMI (dBµV)**	**Difference (dB)**
10	80.50	82.47	-1.97
15	80.29	82.44	-2.15
20	80.10	82.85	-2.75
25	80.16	83.19	-3.03
30	79.96	83.06	-3.10
35	80.01	82.85	-2.84
40	80.02	82.70	-2.68
45	79.97	82.47	-2.50
50	79.91	82.15	-2.24
55	79.94	81.98	-2.04
60	79.94	81.74	-1.80
65	79.92	81.57	-1.65
70	79.93	81.37	-1.44
75	79.91	81.13	-1.22
80	79.91	80.95	-1.04
85	79.90	80.82	-0.92
90	79.88	80.59	-0.71
95	79.87	80.41	-0.54
100	79.85	80.18	-0.33
105	79.84	80.08	-0.24
110	79.85	79.89	-0.04
115	79.85	79.74	0.11
120	79.86	79.49	0.37
125	79.85	79.25	0.60
130	79.84	79.13	0.71
135	79.85	78.80	1.05
140	79.84	78.50	1.34
145	79.85	78.14	1.71
150	79.84	77.71	2.13

Table 4.3 *Measured difference between spectrum analyzer and TDEMI on frequency band 150 kHz - 10 MHz.*

Frequency (kHz)	Spectrum Analyzer (dBuV)	TDEMI (dBuV)	Difference (dB)
150	80.46	82.94	-2.48
500	80.35	82.41	-2.06
1000	80.38	81.93	-1.55
1500	80.34	80.46	-0.12
2000	80.36	79.67	0.69
2500	80.31	81.34	-1.03
3000	80.28	82.39	-2.11
3500	80.27	82.87	-2.60
4000	80.24	82.77	-2.53
4500	80.20	82.09	-1.89
5000	80.17	80.80	-0.63
5500	79.97	78.65	1.32
6000	79.92	80.45	-0.53
6500	79.86	81.44	-1.58
7000	79.82	81.74	-1.92
7500	79.80	81.17	-1.37
8000	79.76	79.96	-0.20
8500	79.73	78.02	1.71
9000	79.71	75.80	3.91
9500	79.69	76.86	2.83
10000	79.72	77.40	2.32

As the frequency resolutions of the test signals were lower compared to resolution bandwidths and frequency resolution in time domain measurements, the values for corrections F_{C2} and F_{C3} were determined by interpolation. Matlab function *interpl* was used to produce values based on measured differences between frequency and time domain measurements. Example below shows how the values for correction F_{C2} were determined by interpl function.

```
f=[10:5:150]';
xi=10:1:150;
FC2=interp1(f,Difference,xi);
```

Graphical representations of interpolated corrections F_{C2} and F_{C3} are shown in figures 4.9 and 4.10.

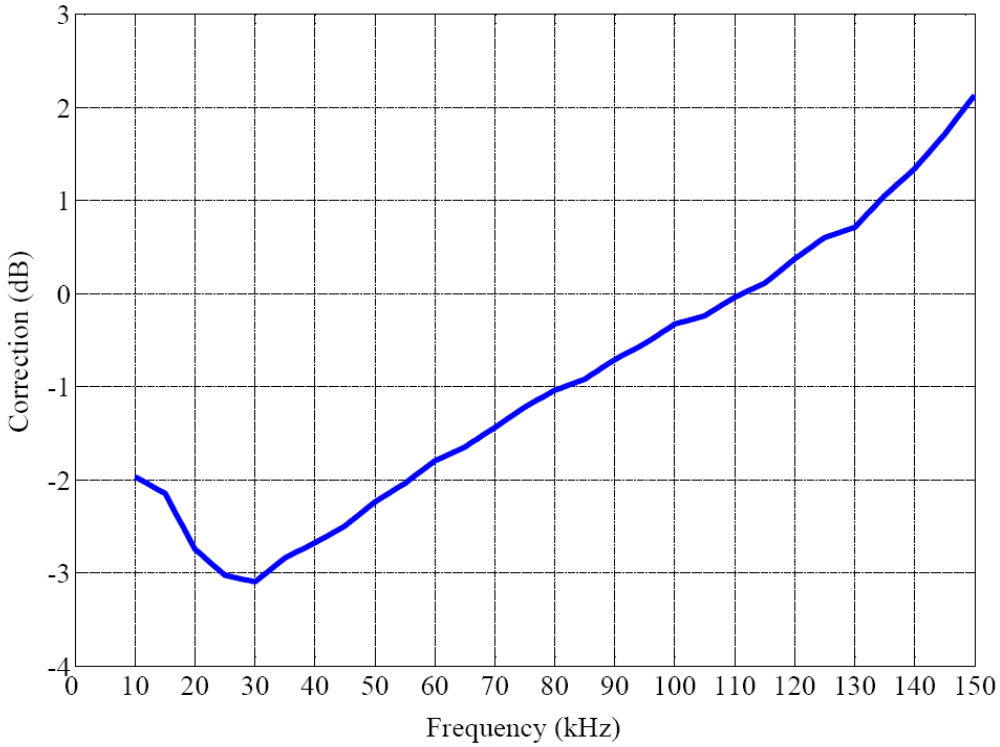

Figure 4.9 *Interpolated correction F_{C2}.*

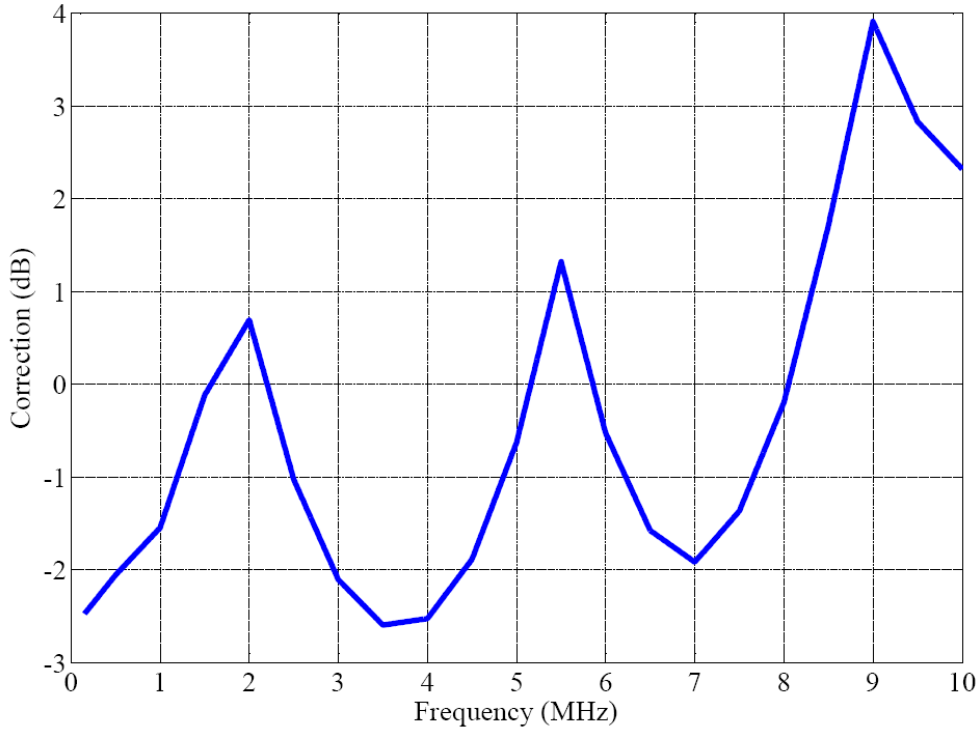

Figure 4.10 *Interpolated correction F_{C3}.*

The difference between frequency and time domain measurement results is a sum of different factors. The first obvious factor and reason for the difference is that the DFT returns the peak values while the measurement receiver or spectrum analyzer gives the RMS values. This leads to √2 (≙3 dB) difference in amplitude.

The second factor and reason for difference is the gain of low pass filters used to prevent measurement signal aliasing. Low pass filters attenuate the measurement signals as described in subsection 4.2.

The third reason for difference is the effect of different impedances. The time domain measurement system is designed for 50 Ω impedance as the frequency domain measurement system. Still there is some mismatch between different parts of the system which causes standing waves that can be seen for example in figure 4.10.

Figure 4.11 sums the reasons for the difference between frequency and time domain measurement systems.

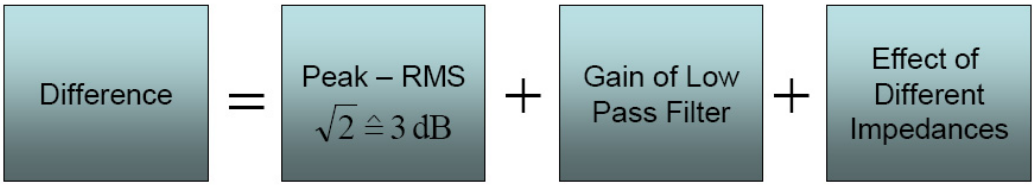

Figure 4.11 *The reasons for the difference between frequency and time domain measurements.*

4.5 First experimental measurements with basic algorithm

First EMI measurements with TDEMI measurement system were performed using the basic algorithm described in figure 1.3 on page 3 of this thesis. The equipment under test was the reference EMI source introduced in section 3.4. Both of the interference sources, brushed DC motor and DC/DC converter, were used in measurements. The references for these first measurements were the results from frequency domain measurements with Anritsu spectrum analyzer.

The first task was to check that the level of ambient noise is at least 6 dB below the limit as the standard MIL-STD-461F requires. This check was done by measurements with EUT de-energized but all of the cables connected and AC/DC power source powered. Therefore measurement results contain some interference from AC/DC power supply and from surrounding electromagnetic environment. Measurements and signal processing to find out ambient electromagnetic interference level were performed with the abovementioned basic algorithm. Results for plus and return leads seemed to be more or less identical, so the figure 4.12 represents only the result from plus lead.

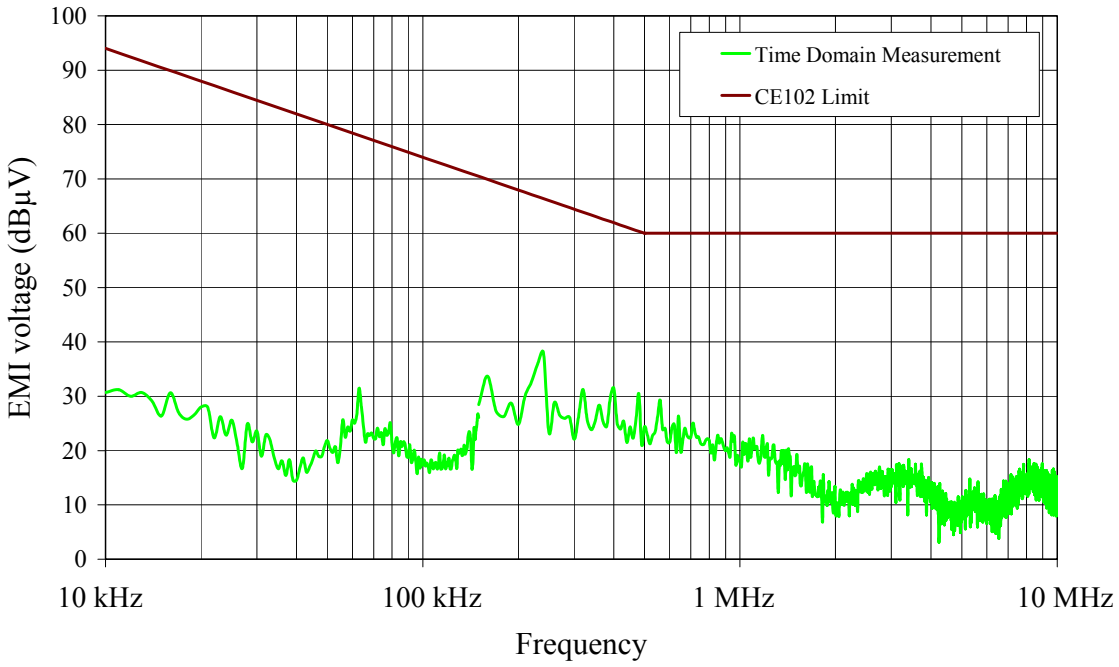

Figure 4.12 *Ambient electromagnetic interference, plus lead.*

As the figure 4.12 shows, the level of ambient electromagnetic interference fulfils the 6 dB requirement very clearly. The difference between ambient and limit line is 30 to 50 dB.

After ambient level measurements, the same measurements and signal processing with basic algorithm were performed for DC/DC power supply and brushed DC motor of the reference EMI source. Measurements were performed for both power leads (plus and return) and using two different trigger levels. Five measurements with trigger set to zero and five measurements with trigger set to a highest level which caused triggering, were performed. This means totally 80 separate measurements when measurements were done with two different capture times as described in Section 4.1. Based on these measurements, amplitude spectrums were produced with Matlab using basic algorithm. Results from Matlab were transferred to Microsoft Excel together with the frequency domain measurement results.

Results from first experimental measurements and signal processing are shown in figures 4.13 to 4.16.

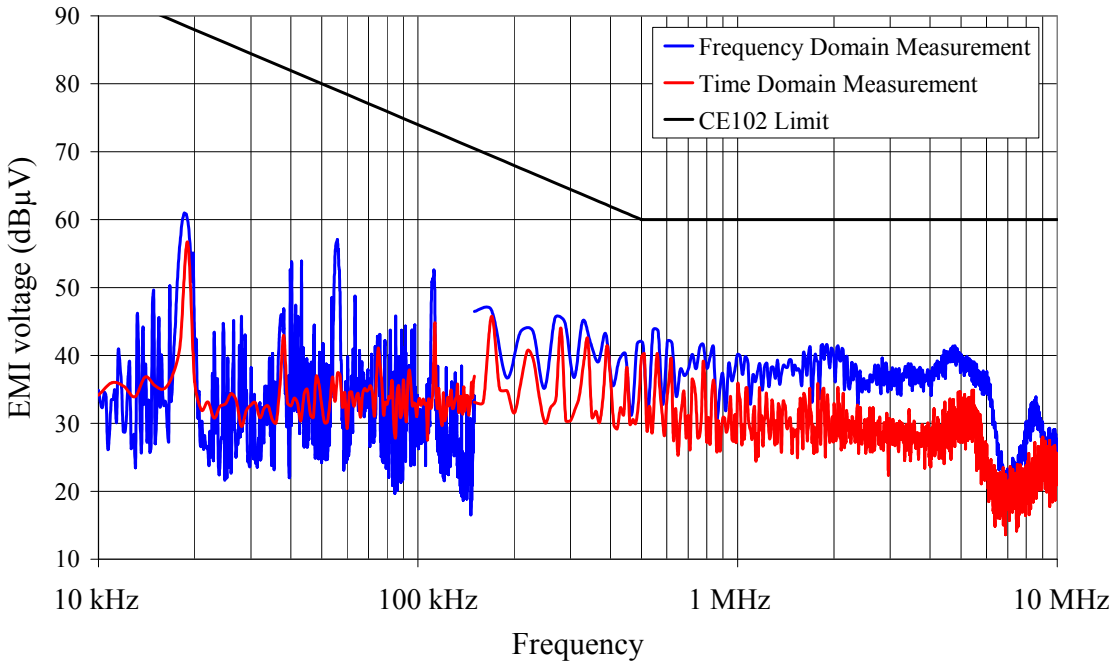

Figure 4.13 *TDEMI measurement results compared to frequency domain EMI measurement results, DC/DC converter of reference EMI source, plus lead.*

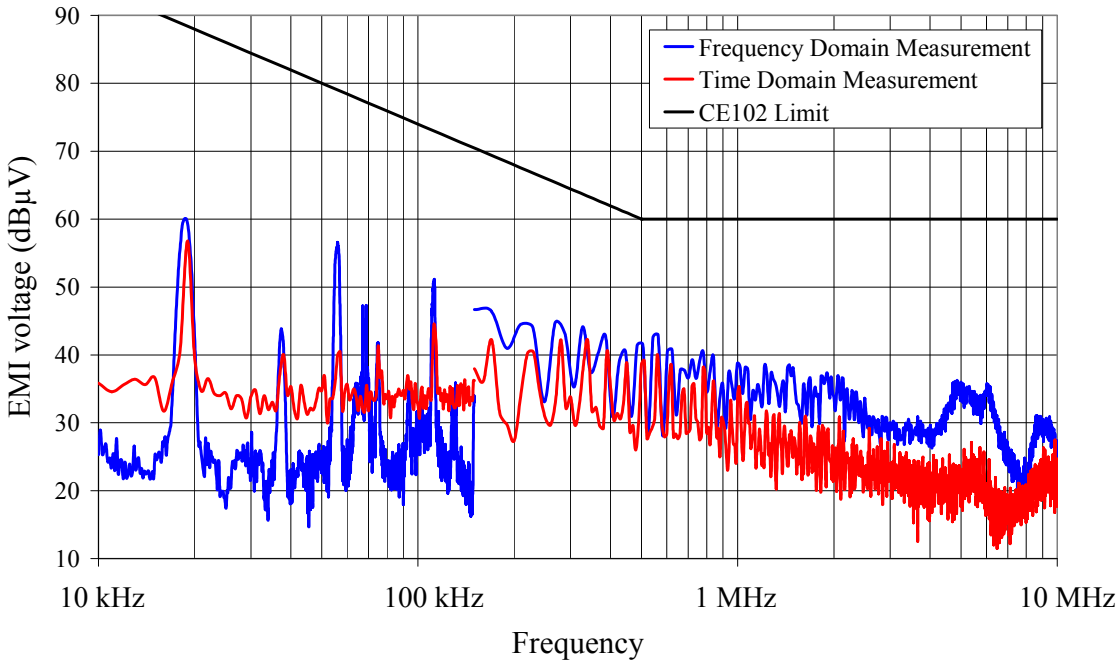

Figure 4.14 *TDEMI measurement results compared to frequency domain EMI measurement results, DC/DC converter of reference EMI source, return lead.*

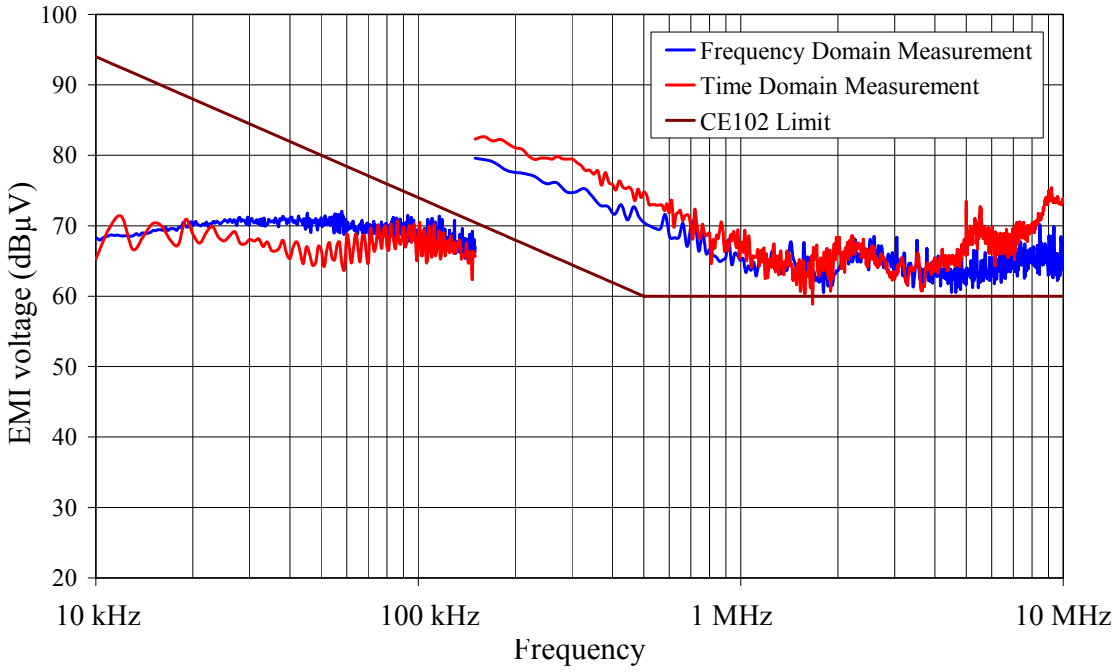

Figure 4.15 *TDEMI measurement results compared to frequency domain EMI measurement results, DC-motor of reference EMI source, plus lead.*

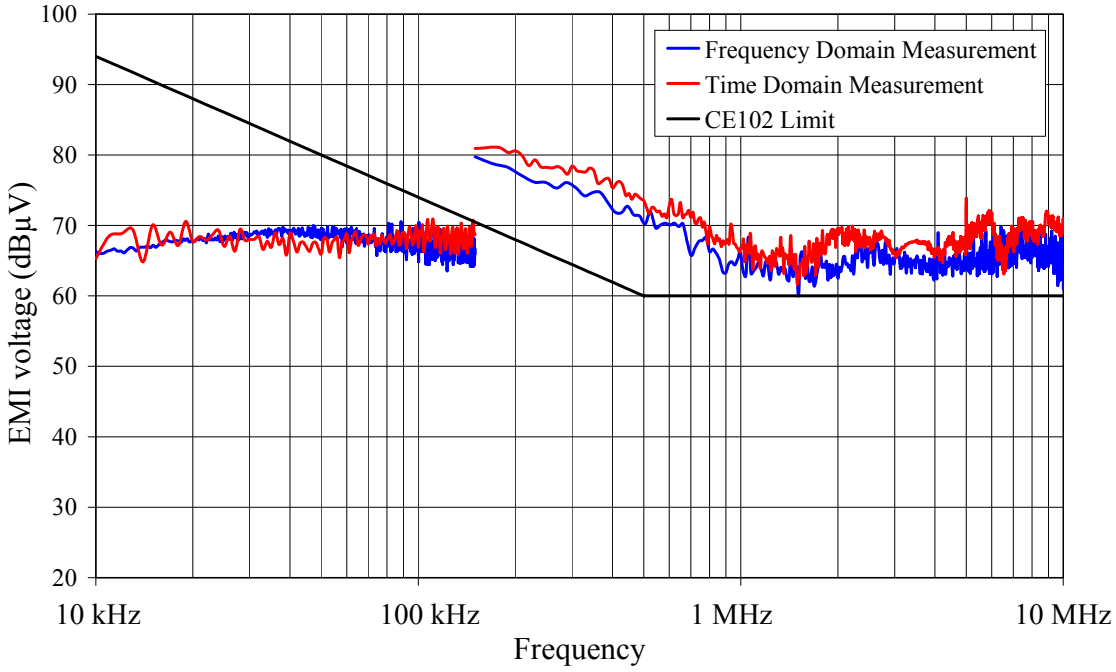

Figure 4.16 *TDEMI measurement results compared to frequency domain EMI measurement results, DC-motor of reference EMI source, return lead.*

When the results from the first experimental time domain EMI measurements with basic algorithm are compared to frequency domain EMI measurement results, it seems that the differences between results are rather small in DC motor case, but on the other hand, in DC/DC converter case the differences are significant. Reasons for the

differences are analyzed in forthcoming Chapter 5 as well as the means to improve the basic algorithm.

5 IMPROVEMENTS FOR THE BASIC ALGORITHM

In this chapter, improvements for the basic algorithm are evaluated and explored. First improvements, which are evaluated, are based on algorithms described in [6][7][8] for narrowband and broadband interference emissions. Fundamentals of these algorithms are briefly introduced in Chapter 1. In addition to these algorithms, the applicability of different window functions is studied and also some other modifications for the measurement data acquisition and DFT are evaluated.

It is essential for the TDEMI measurement method to identify the frequency and the time domain characteristics (nature) of the interference. This makes the TDEMI measurement method more laborious compared to the conventional frequency domain method, but on the other hand it provides some advantages e.g. tools for interference suppression.

In the frequency domain, interferences are typically classified as narrowband and broadband signals. This forms the basis for the improved algorithms [6][7] by Keller and Feser. Electrotechnical Vocabulary [21] gives the following definitions:

Narrowband Disturbance. *An electromagnetic disturbance, or spectral component thereof, which has a bandwidth less than or equal to that of a particular measuring apparatus, receiver or susceptible device.*

Broadband Disturbance. *An electromagnetic disturbance which has a bandwidth greater than that of a particular measuring apparatus, receiver or susceptible device.*

Note. - For some purposes particular spectral components of a broadband disturbance may be considered as narrowband disturbances.

Extremes for narrowband and broadband signals are pure sine wave and white noise. Pure sine wave with a discrete frequency is an ideal narrowband signal. In the frequency domain this signal is just a vertical line. White noise is a random signal which has a flat amplitude spectrum in the frequency domain i.e. energy of the signal is equally distributed to whole frequency band under investigation. Neither of these signals represents realistic interference signals and in practise interference signals are mixtures of different narrowband and broadband interference signals. In TDEMI measurement method this means that it may be necessary to use both narrowband and broadband algorithms for the interference signal. Algorithm for narrowband signals is used for "peaks" and the algorithm for the broadband signals is used for broader "hillocks".

5.1 Algorithm for narrowband interference

Algorithm for the narrowband interference signals is presented in [6] and the basic idea of it is described in Chapter 1 of this thesis. The algorithm is based on Flat Top windowing of the captured measurement data to reduce the scallop loss. The scallop loss is the loss caused by spectral leakage which occurs when the peak of the narrowband signal is located between DFT steps. Scallop loss causes widening and amplitude attenuation of the narrowband peaks. Flat Top windowing reduces the widening of the peak but like all other window functions, with the exception of the rectangular window, it attenuates the amplitude. Figure 5.1 shows the Flat Top window compared to the rectangular window.

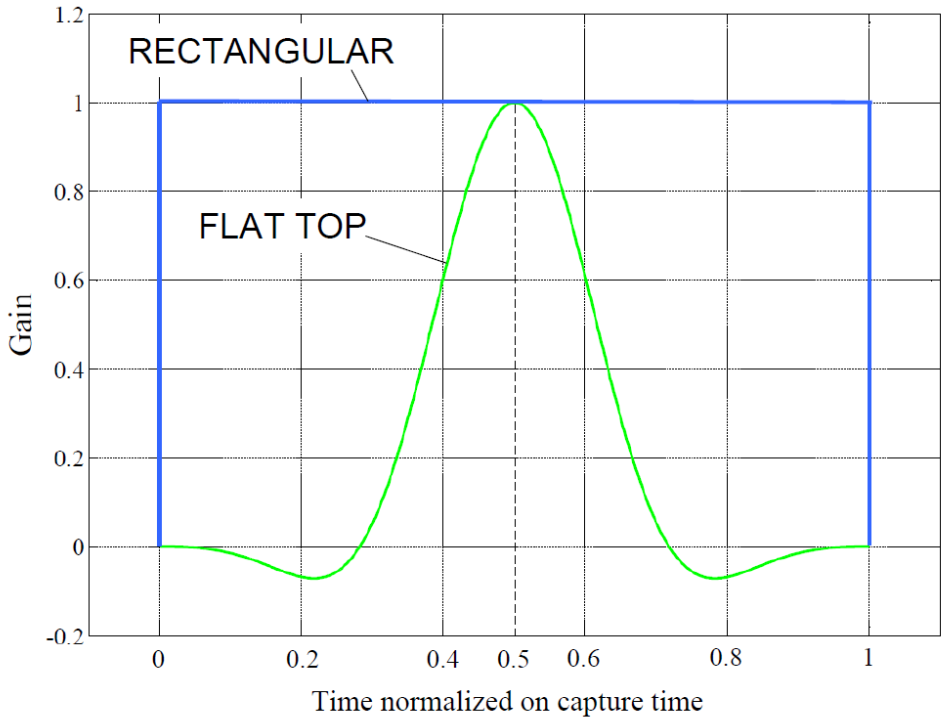

Figure 5.1 *Rectangular and Flat Top window functions.*

Actually, if the length of the rectangular window is equal to the length of the capture time, the rectangular window is not a "real" window function as it has no impact on captured measurement data.

The attenuation caused by windowing is called coherent gain G_C. Table 5.1 shows the coherent gain values and corresponding scale factors for typical window functions. The term coherent gain is a little bit confusing as the value is always equal to one or smaller than one. Therefore the term coherent gain loss is used in some publications. To get the correct amplitude values in frequency domain, amplitudes of narrowband peaks shall be corrected (multiplied) by scaling factor after DFT.

Table 5.1 *Coherent gain values for typical window functions.*

Window Function	Coherent Gain G_C	Scaling Factor (1 / G_C)
Rectangular Window	1	1
Flat Top Window	0.22	4.545
Blackman Window	0.42	2.38
Hanning Window	0.5	2
Hamming Window	0.54	1.852

Following demonstration shows how the Flat Top windowing can be used to correct amplitude of narrowband peak. In the demonstration two 80 dBµV sinusoidal test signals of frequencies 30.0 kHz and 30.5 kHz are first measured with TDEMI measurement system and with the basic algorithm described in Chapter 4. Test signal frequencies are chosen so that the 30.0 kHz signal matches to the DFT steps and 30.5 kHz is located between 1 kHz DFT steps 30.0 kHz and 31.0 kHz.

Basic algorithm gives correct amplitude value for the 30.0 kHz test signal but the amplitude for the 30.5 kHz test signal is approximately 3 dBµV lower than the correct amplitude. 30.5 kHz peak is also widened. Aforementioned facts indicate scallop loss. Results are shown in Appendix 3.

In the next phase of the demonstration, both of the test signals are windowed with Flat Top window before DFT. Figure 5.2 shows the effect of Flat Top windowing in the time domain.

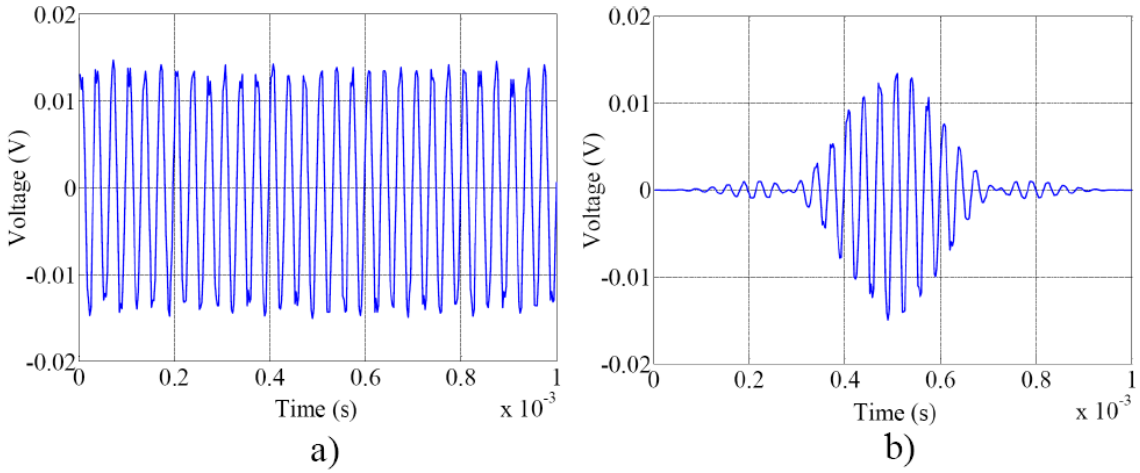

Figure 5.2 *Captured 30.5 kHz test signal* ***a)*** *before windowing* ***b)*** *after windowing with Flat Top window function.*

The effect of the windowing is that the peaks are broader in the frequency domain but the so-called side slopes around the peaks are lower. Amplitudes of the peaks are also lower, approximately 67 dBµV. Results are shown in Appendix 3.

As in the algorithm for narrowband interference [6][7], the next step is the correction of coherent gain. This is done by multiplying amplitude spectrums by scaling factor ($1/G_C = 4.545$). After this, both signals have correct amplitude values as shown in

Appendix 3. This proves that the algorithm for narrowband interference can be used to correct the amplitudes of narrowband peaks, at least peaks of discrete frequency signals.

The reason why Flat Top window is so efficient for discrete frequency signals can be seen from figure 5.3, which shows the frequency responses of rectangular and Flat Top windows. These frequency responses are produced by Matlab's Window Design and Analysis Tool and the applied parameters are according to the previous demonstration (sampling frequency 400 kHz and length of the window 400).

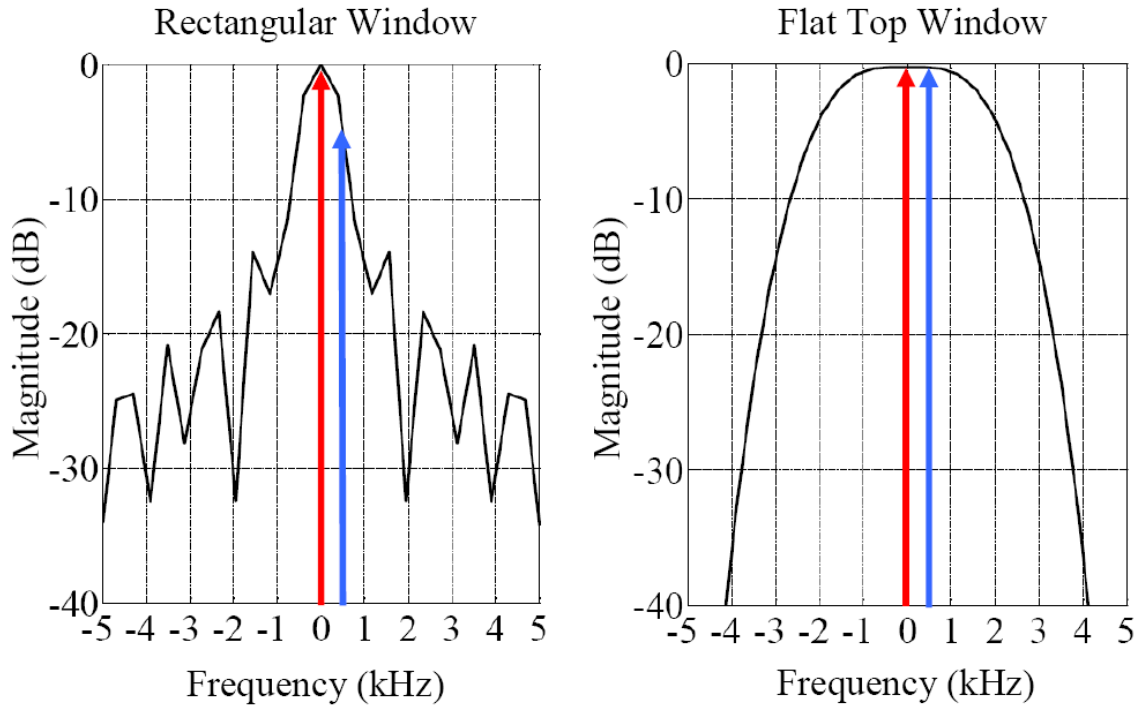

Figure 5.3 *Frequency responses of rectangular and Flat Top windows. Coherent gains are compensated.*

The 3 dB bandwidth of rectangular window is 0.879 kHz while corresponding 3 dB bandwidth of Flat Top window is 3.711 kHz. This means that in the previous demonstration the rectangular window attenuates the 30 kHz signal (red arrows) less than it attenuates the 30.5 kHz signal (blue arrows). In the case of Flat Top window the attenuation is practically the same for both signals because of broader bandwidth. Broader bandwidth of the Flat Top window is not always a benefit; it may overestimate the amplitudes of the signals in some cases. This can happen for example in the case of narrowband noise.

According to Keller and Feser [8] narrowband signals are sinusoidal oscillations of a discrete frequency or periodic pulses with a repetition frequency higher than the measurement bandwidth. 30 kHz and 30.5 kHz test signals applied in previous demonstration fulfil this definition but what about the differential mode interference voltage caused by DC/DC converter of reference EMI source? In figure 5.4 the interference voltage of DC/DC converter is plotted in time domain.

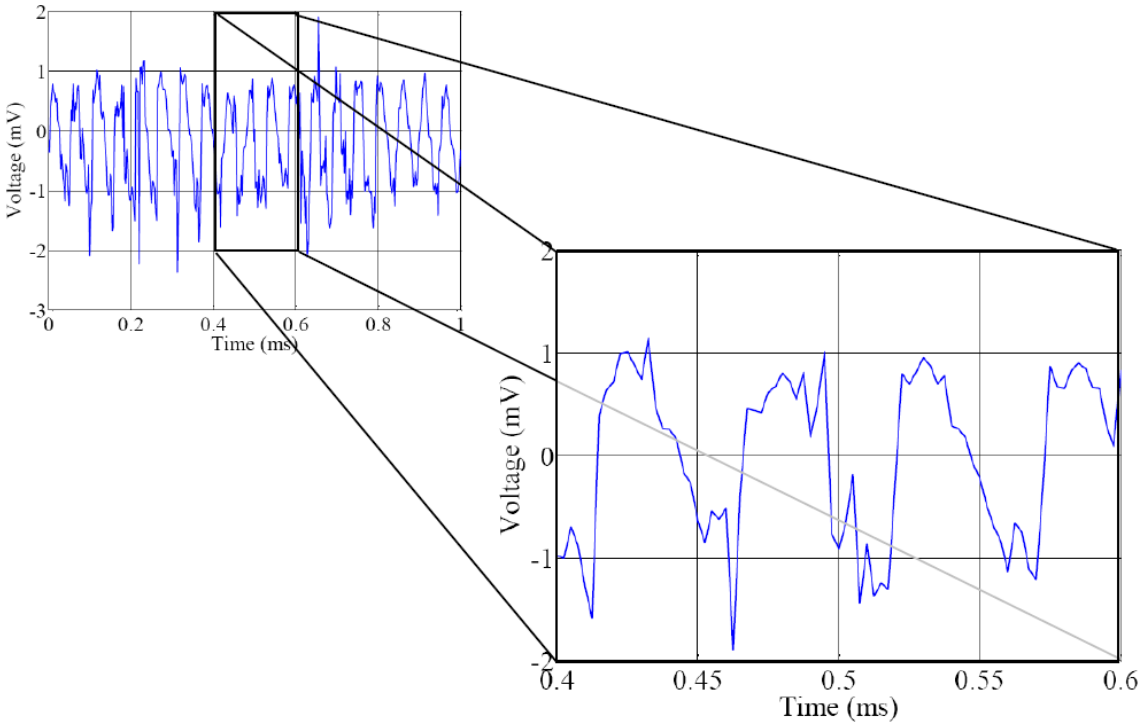

Figure 5.4 *Differential mode interference voltage caused by DC/DC converter of reference EMI source.*

As it can be seen from figure 5.4 the interference signal contains periodic pulses and the fundamental repetition frequency of the pulses, which is just below 20 kHz, is higher than the measurement bandwidths (1 kHz and 10 kHz). Based on this, the interference signal can be classified into narrowband signals according to Keller and Feser, but on the other hand it is obvious that the interference signal contains several other frequencies. Actually the energy of the interference is widely distributed in the measurement frequency band which is clearly visible in figures 4.13 and 4.14. This is in conflict with the narrowband interference's (disturbance's) definition in the Electrotechnical Vocabulary [21], but it notes that for some purposes particular spectral components of a broadband interference may be considered as narrowband disturbances. This may be applicable in this case.

Based on aforementioned facts, it seems that the Keller's and Feser's algorithm for narrowband interference could be the correct choice to improve amplitude accuracy of TDEMI measurement. In the first TDEMI measurements with the basic algorithm, results show that the TDEMI measurement method gives too low amplitude values.

The applicability of the Flat Top window based algorithm for narrowband interference is now evaluated. In the first phase of the evaluation, the same captured interference measurement data from DC/DC converter, which is used with the basic algorithm, is multiplied with a Flat Top window. For the lower frequency band (10 kHz - 150 kHz), the length of the used Flat Top window is 400 points. This is equal to the length of the captured interference signal which is used in DFT. Figure 5.5 shows an

example of original captured interference signal and corresponding Flat Top windowed signal.

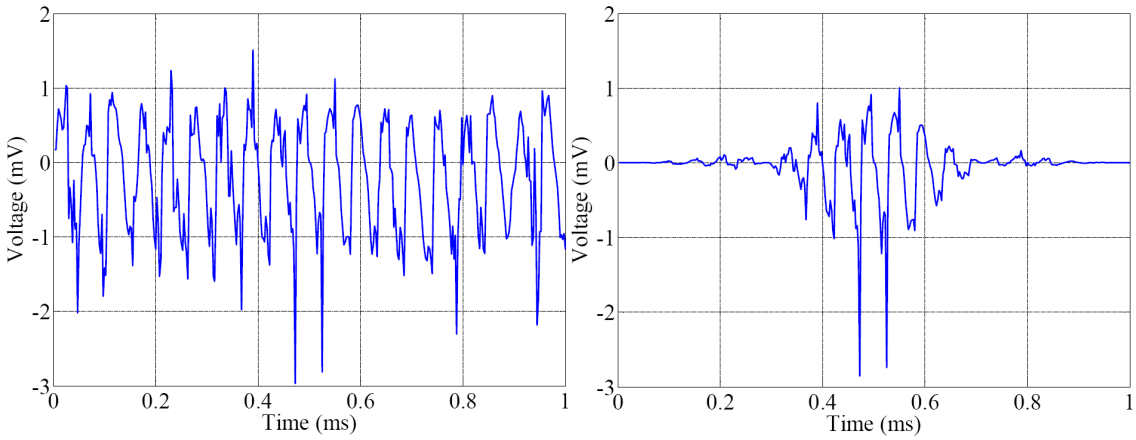

Figure 5.5 a) *Interference signal caused by DC/DC converter of reference EMI source, capture time 1 ms* ***b)*** *Same signal after Flat Top windowing.*

For frequency band 150 kHz - 10 MHz, the length of the Flat Top window is 2000 points. An example of original captured interference signal is shown in figure 5.6 together with a Flat Top windowed signal.

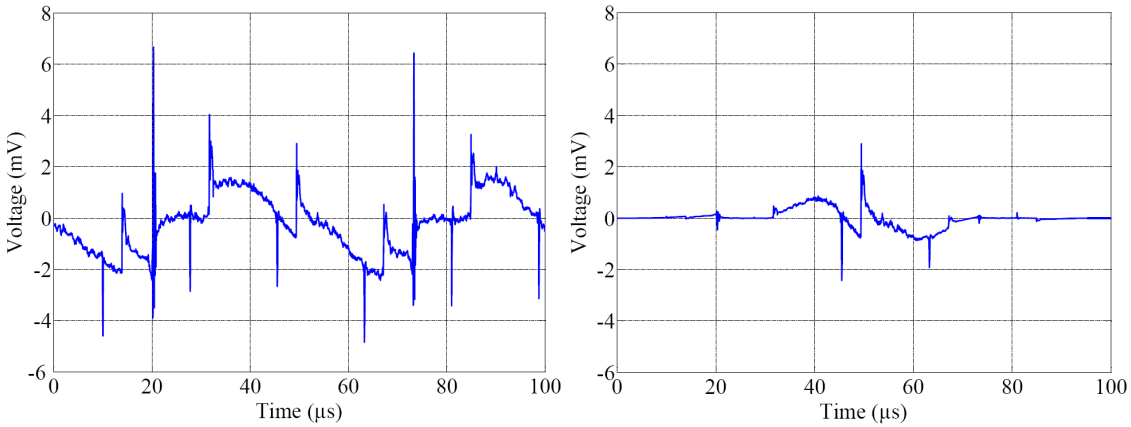

Figure 5.6 a) *Interference signal caused by DC/DC converter of reference EMI source, capture time 100 µs* ***b)*** *Same signal after Flat Top windowing.*

From the figure 5.6 it can be seen very clearly that the result of Flat Top windowing and presumably also the result of DFT depends on how the window function and the interference signal are located, related to each other in the time domain. In the figure 5.5 the Flat Top window attenuates the highest peaks which occur at 20 µs and at 74 µs. These peaks are likely to cause the highest amplitudes (peaks) also in the frequency domain. In the lower frequency band, when the capture time is longer compared to the repetition period of interference signal, the effect of Flat Top window is not so significant (see figure 5.5).

After Flat Top windowing the same basic algorithm which is introduced in Chapter 4 is used. The effect of coherent gain is also taken into account. In the figure 5.7 it can be seen that the Flat Top windowing reduces the difference between frequency domain and time domain measurement results at lower frequencies, but above 1 MHz the difference between frequency and time domain measurement results is still significant (max. 10 dBµV).

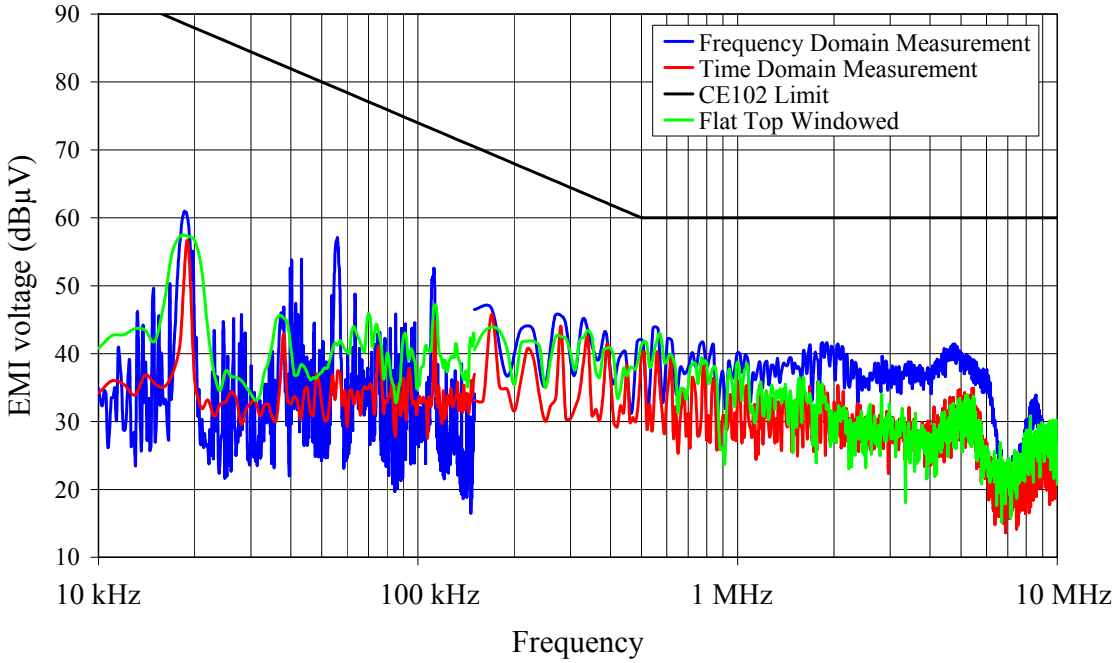

Figure 5.7 *TDEMI measurement results compared to frequency domain EMI measurement results, DC/DC converter of reference EMI source, plus lead.*

Next possible improvement for the algorithm is "a variable phase shift" between Flat Top window and interference signal. This means that the Flat Top window is moved in the time domain in relation to the interference signal, and by that way all parts of the time domain signal are taken into account. The effect of this possible improvement is demonstrated with six different Flat Top windowed signals which are represented in the Appendix 4. This demonstration applies only for the upper frequency band 150 kHz – 10 MHz, so the possible improvements will be seen at frequencies above 150 kHz. The result after DFT is shown in figure 5.8.

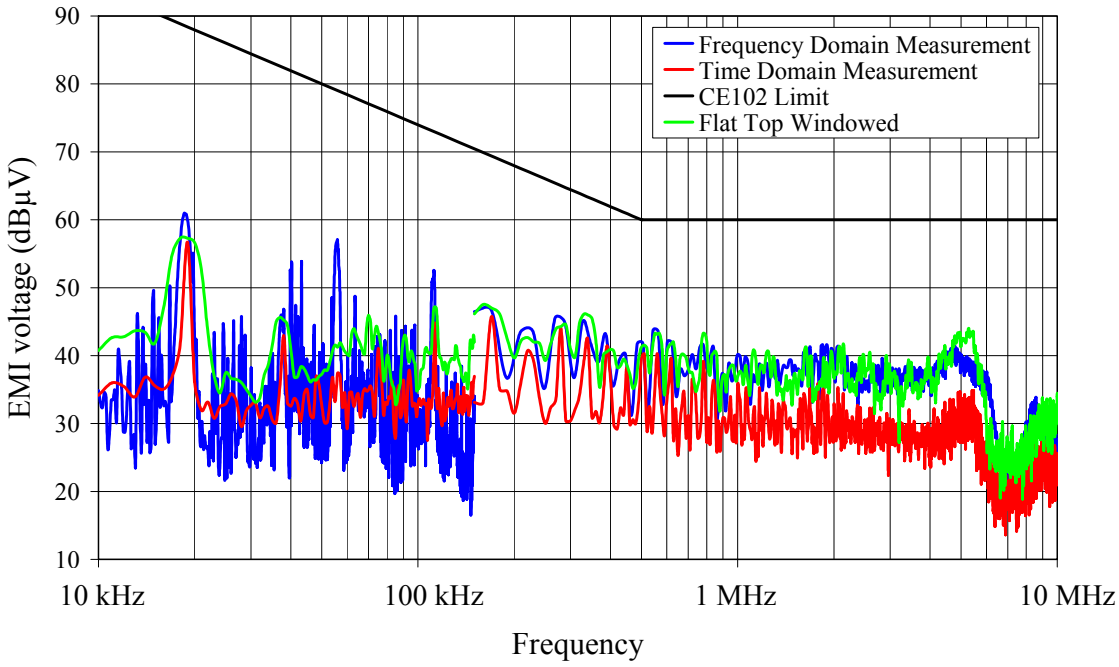

Figure 5.8 *TDEMI measurement results compared to frequency domain EMI measurement results, DC/DC converter of reference EMI source, plus lead, Flat Top windowing applied to six overlapped time domain signals (see Appendix 4).*

Flat Top windowing and variable phase shift seems to be efficient solution. Now the difference between frequency and time domain measurement results is rather small on frequency band 150 kHz to 10 MHz.

In the original algorithm for narrowband interference [6][7], the last phase is the replacement of the peak amplitudes from the TDEMI basic algorithm with the amplitudes from the Flat Top window based results. This seems to be unnecessary in this case and perhaps in other cases too, because the amplitude value is the most important criterion in EMI measurements. The exact form and shape of the amplitude spectrum is not so relevant.

The above described variable phase shift method is close to the overlapping method which is used in the Welch periodogram. In the Welch periodogram the time domain signal is first divided into overlapping segments and then the segments are windowed before Fourier transform of separate segments. The result of the Welch periodogram is the average of the Fourier transforms. The difference between overlapping method and variable phase shift is that in the variable phase shift the Flat Top windowing is applied to separate time domain signals which are not in the same phase while the overlapping method is typically applied to one time domain signal. The reason why the overlapping method is not used in this thesis is that the digital oscilloscope used does not allow capturing data with suitable length and sampling frequency. Therefore overlapping must be done by moving the trigger in the time axis and by capturing several data sets.

As the interference signal from the DC/DC converter is quite stationary, the difference between overlapping and variable phase shift is rather small. The figure 5.7 is a result of maximum of separate DFTs while the result of the Welch periodogram is average of separate DFTs.

5.2 Applicability of other window functions

Even though the results with the Flat Top window based algorithm are quite satisfying for the narrowband interference as shown in subsection 5.1.1, the applicability of other window functions is also evaluated within this research. The amount of different window functions is enormous and it is almost impossible to evaluate all of them. Several good overviews concerning different window functions and their applicability for different purposes can be found from scientific publications, such as from the papers [22][23], and also from application notes and tutorials by measurement instrument manufacturers, for example from tutorials [24][25].

In this research 13 different window functions are chosen for evaluation. These window functions, listed in the Table 5.2, represent well known and very typical window functions which are used in signal processing. The interference signals used in the evaluation are the same differential mode interference signals from the DC/DC converter which are used in subsection 5.1.1. The exact window functions are produced with Matlab's Window Design & Analysis Tool, using the same parameters (sampling frequency and length of the measurement data) as used in actual time domain measurements.

Results of the evaluation of different window functions are shown in Appendix 5. Following information and results are shown in the Appendix 5:

1. Time and frequency domain responses of the particular window function (on lower measurement frequency band 10 kHz-150 kHz → sampling frequency 400 kHz and length 400)
2. 3 dB bandwidth values from Window Design & Analysis Tool on both frequency bands (10 kHz-150 kHz and 150 kHz-10 MHz)
3. Calculated coherent gain values (values from Matlab's Window Design & Analysis Tool)
4. Results from the time domain EMI measurement method with and without windowing the time domain measurement data. Results from the frequency domain measurement are also shown as a reference.

The assessment of the applicability of evaluated window functions can be found from the Table 5.2. The assessment is based on visual examination of measurement results.

Table 5.2 *Evaluated window functions and assessment of their applicability.*

Window Function	3 dB Bandwidths (kHz)	Applicability
Hamming	1.270 / 12.207	Poor
Hann	1.367 / 13.428	Poor
Blackman	1.563 / 15.896	Poor
Blackman-Harris	1.855 / 18.311	Moderate
Chebyshev	1.758 / 18.311	Moderate
Gaussian (α = 4)	2.051 / 20.752	Good
Gaussian (α = 5)	2.637 / 25.635	Very good
Gaussian (α = 6)	3.125 / 31.738	Good
Nuttall	1.855 / 18.311	Moderate
Bohman	1.660 / 15.896	Moderate
Parzen	1.758 / 17.090	Moderate
Tukey (α = 1)	1.367 / 13.428	Good
Triangular	1.270 / 12.207	Poor

According to the results, Gaussian and Tukey windows seem to be possible alternatives to the Flat Top window, at least in this case. The overall trend is that all of the evaluated window functions give better results than no-windowing (rectangular window).

The disadvantage of the use of window functions is that they decrease frequency resolution. Flat Top window which has a wide main lobe in the frequency domain (3 dB bandwidth 3.72 bins / 6 dB bandwidth 4.58 bins) widens the peaks strongly. The way to keep the frequency resolution equal to the measurement receiver is to increase capture time *T*. Keller and Feser [8] define following formula 5.1 for the minimum capture time $T_{\min}$:

$$T_{\min} = \frac{\alpha_{\text{window}}}{B_{6\,\text{dB receiver}}}, \tag{5.1}$$

where α_{window} is the 6 dB bandwidth of the applied window function (in bins) and $B_{6\ \text{dB receiver}}$ is the 6 dB bandwidth of the measurement receiver (in hertz) which is used in the frequency domain measurements.

6 dB bandwidth values for window functions can be found from literature, for example from [22][24]. 6 dB bandwidth can also be determined with Matlab's Window Design & Analysis Tool. For the Flat Top window, the formula 5.1 gives 4.58 times longer capture time compared to the basic algorithm. On the lower measurement frequency band from 10 kHz to 150 kHz this means 4.58 milliseconds capture time instead of one milliseconds capture time. The effect of this longer capture time is demonstrated in the figure 5.9.

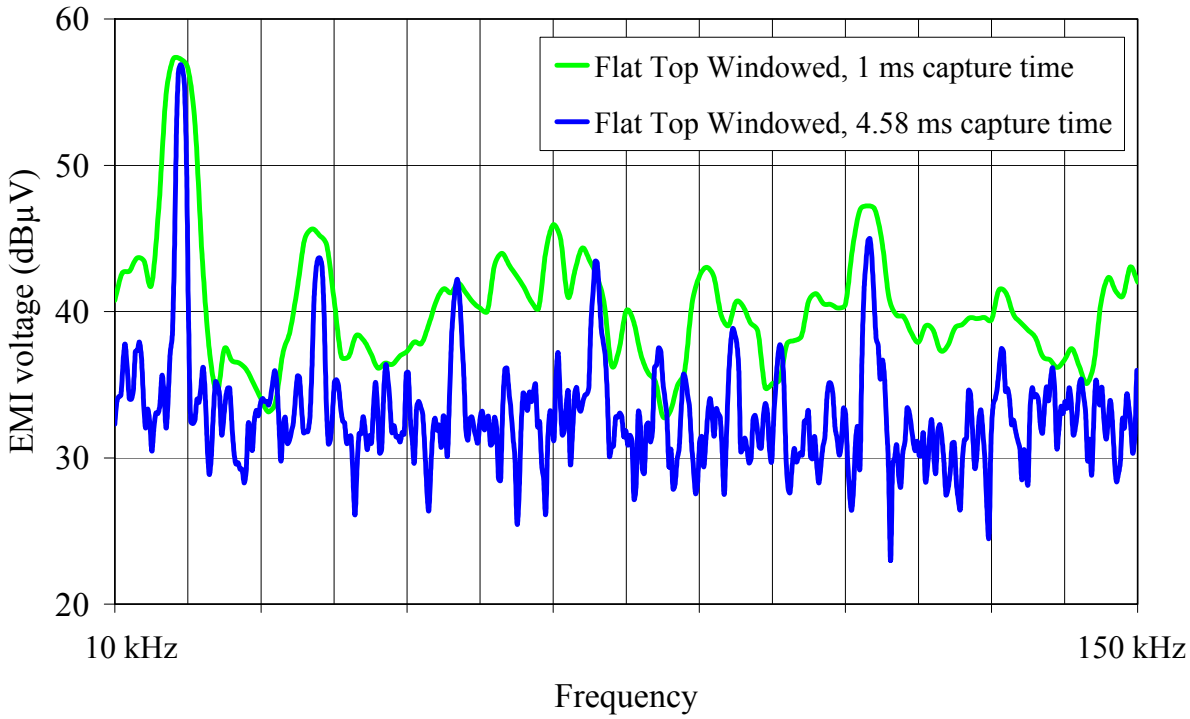

Figure 5.9 *The effect of longer capture time. Interference signal from the DC/DC converter of the reference EMI source.*

As the demonstration shows, the longer capture time improves the frequency resolution, but it has no significant impact on the maximum amplitude level. As the amplitude level of the interference signal is the most important thing in EMI measurements, the need for longer capture times must be considered case by case. If the frequency resolution is required to be equal to the frequency domain measurement, the need for longer capture time is obvious.

5.3 Algorithm for broadband interference

The knowledge of the pulse response characteristics of the measurement receiver (or spectrum analyzer) and the TDEMI measurement system forms the basis for the broadband algorithm. Both, measurement receiver and TDEMI measurement system, give typically “incorrect results” for broadband signals and those results deviate from the theoretical and true ones. Despite this fact, more important than true results, is to identify differences between pulse response characteristics of the frequency and time domain EMI measurement methods. Based on these differences, TDEMI algorithm for broadband signals, which gives results equal to the frequency domain EMI measurement results, shall be constructed.

Even though obtaining the true measurement result for broadband interference signal, which correlates to result of an ideal receiver, is not in the scope of this research, following demonstration is presented. This demonstration shows how the TDEMI and also frequency domain EMI measurement methods can give incorrect results.

The signal used in the demonstration is a square wave signal whose repetition frequency is 4 kHz and amplitude 10 mV (=80 dBµV). The square shape of the pulse determines the envelope of the spectrum and the repetition frequency 4 kHz determines the distance between the frequency components in the spectrum.

Figure 5.10 shows the spectrum of the signal up to 10 MHz. Spectrum is produced with LTSpice program.

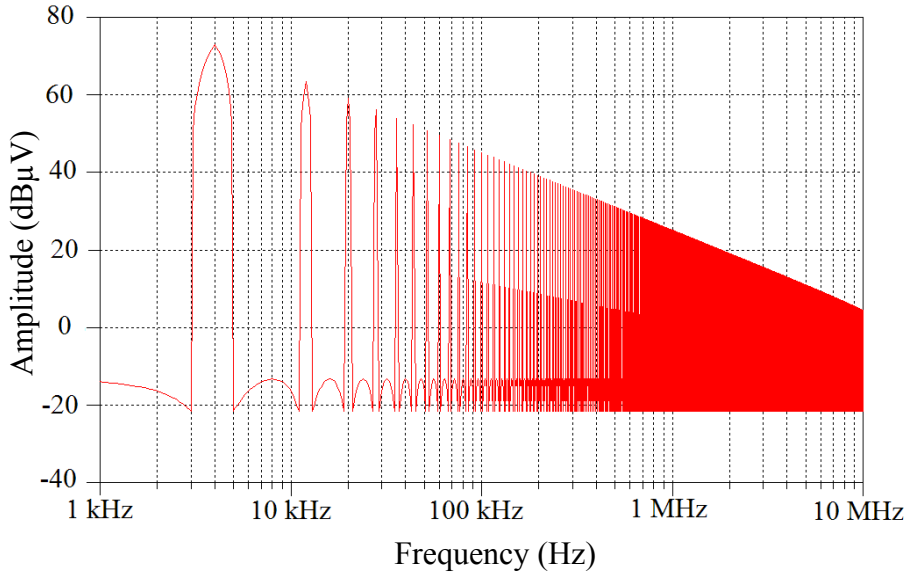

Figure 5.10 *Spectrum of a 4 kHz square wave signal.*

According to theory the envelope of the square wave signal falls 20 dB / decade and the odd harmonics are dominant. These facts can be seen from the figure 5.10.

The 4 kHz frequency is higher than the frequency resolution bandwidth and the DFT step on the lower measurement frequency band from 10 kHz to 150 kHz. This means that the signal is narrowband on this frequency band and the TDEMI and the frequency domain measurement system should give correct results.

Next, the Fourier transform of the 4 kHz square wave signal is produced with LTSpice for lower frequency band from 10 kHz to 150 kHz. Sample size (400) and sampling frequency f_s (400 kHz) are equal to the TDEMI algorithm. Figure 5.11 shows the result of the Fourier transform for frequency band from 10 kHz to 150 kHz.

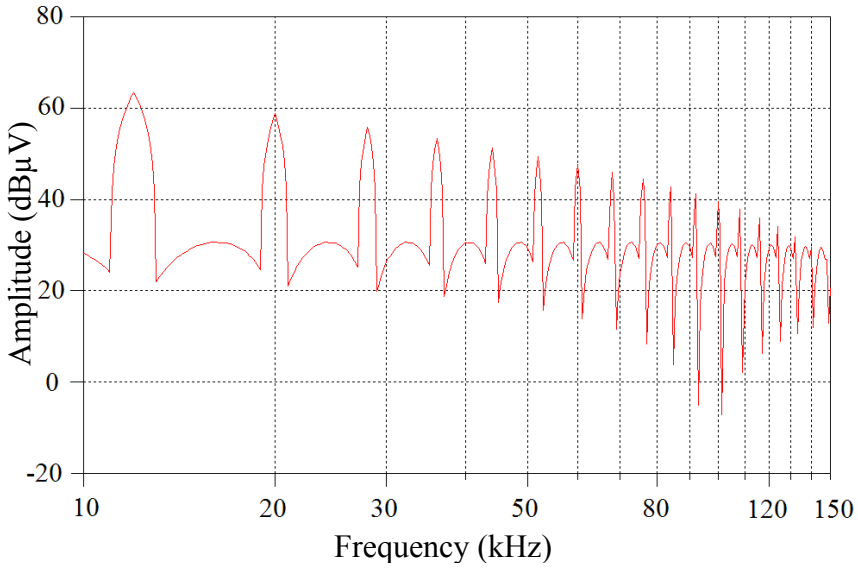

Figure 5.11 *Spectrum of a 4 kHz square wave signal. Simulated TDEMI measurement result for lower frequency band (10 kHz – 150 kHz).*

Result shown in figure 5.11 seems to be correct and equal to the figure 5.10. For the upper frequency band, from 150 kHz to 10 MHz, the 4 kHz square wave signal represents broadband signal as the 4 kHz frequency is significantly lower than the resolution bandwidth and the DFT step which both are 10 kHz. Figure 5.12 shows the result of Fourier transform for the upper frequency band. Sample size (2000) and sampling frequency f_s (20 MHz) are equal to the TDEMI basic algorithm also in this case.

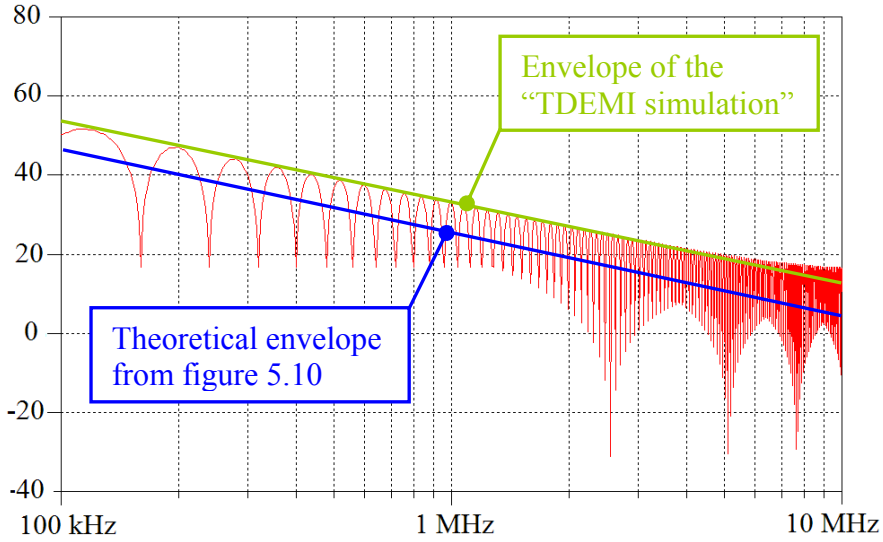

Figure 5.12 *Spectrum of a 4 kHz square wave signal. Simulated TDEMI measurement result for upper frequency band (150 kHz – 10 MHz).*

Now, a significant difference between theoretical and "simulated TDEMI" envelopes can be noted. The reason for this difference is that only one pulse or part of the pulse is located in the captured time period T and the DFT based algorithm "does not know" when the next pulse is coming. TDEMI algorithm expects that the pulse repeats at the same time point during next capture time T period and this leads to incorrect results.

With broadband signal, when the repetition frequency is equal to or smaller than the DFT step size, the repetition period T_r is equal to or longer than the capture time T. In these cases (cases b and c in figure 5.13) the TDEMI produces same incorrect result and result is independent of the repetition frequency.

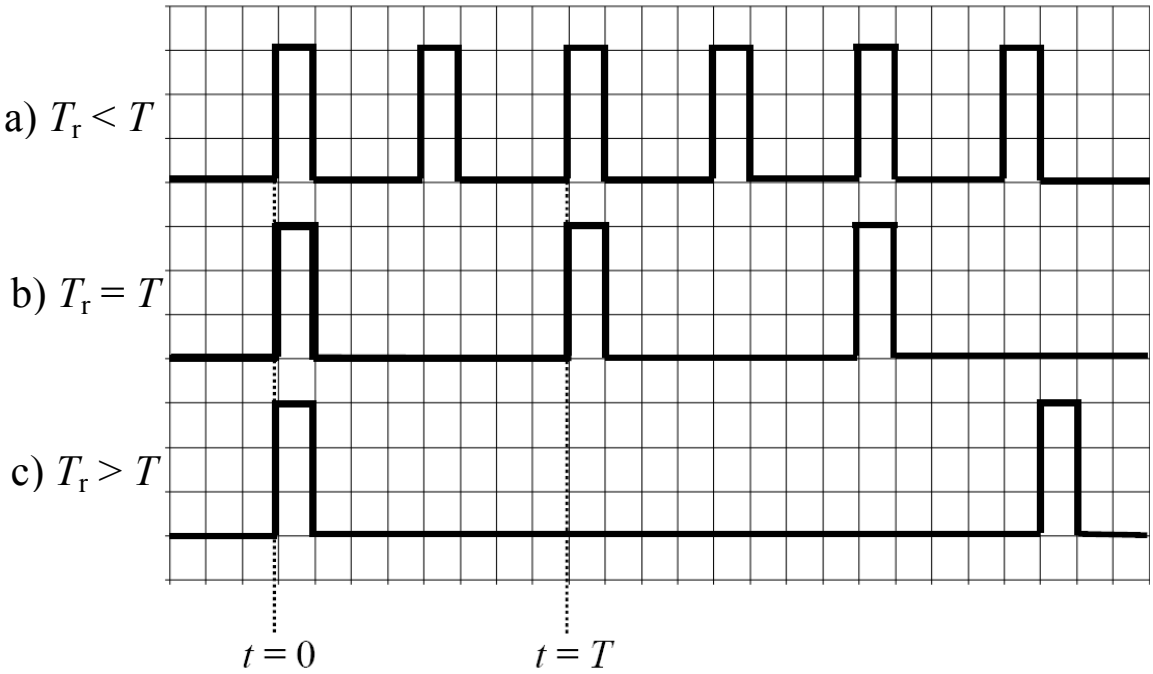

Figure 5.13 *Pulses with different repetition periods T_r and the capture time T.*

With narrowband signal, when the repetition frequency is higher than the DFT step size, the repetition period T_r is shorter than the capture time T (case a in figure 5.13). In this case the TDEMI algorithm produces correct result.

When the TDEMI result of broadband signal is compared to the theoretical one, the difference between results increases when the repetition frequency decreases. The increase of the difference is 20 dB / decade. When the signal is narrowband, the difference between TDEMI result and theoretical result is zero. The point where the difference begins to be remain zero is in time domain $t = T$ and in the frequency domain $f = 1/T$.

Based on the above mentioned pulse response characteristics a curve that defines the response of the TDEMI algorithm can be produced. Figure 5.14 shows the pulse response curve for the TDEMI algorithm which uses 100 µs capture time. From this curve the amplitude difference between result of TDEMI algorithm and theoretical result can be obtained.

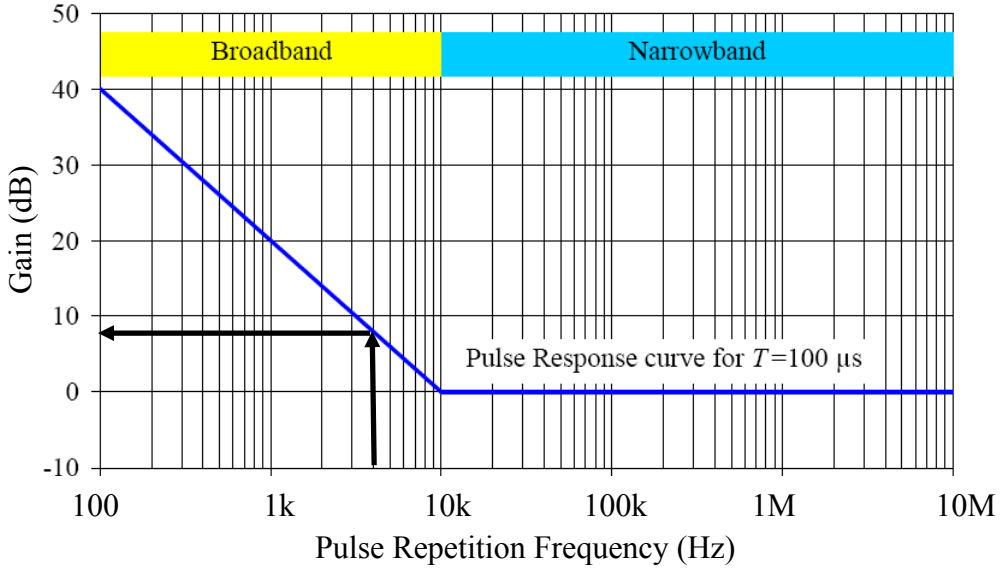

Figure 5.14 *Pulse response curve of TDEMI algorithm, capture time T = 100 µs, response for the 4 kHz signal is shown with the arrows.*

The difference (gain in the figure 5.14) seems to correlate to the difference shown in figure 5.12.

Same kind of pulse response curve can be produced to EMI measurement receiver or spectrum analyzer, but in this case the phenomenon shall be studied in the frequency domain. The typical graphical definitions for narrowband and broadband signals are shown in figure 5.15

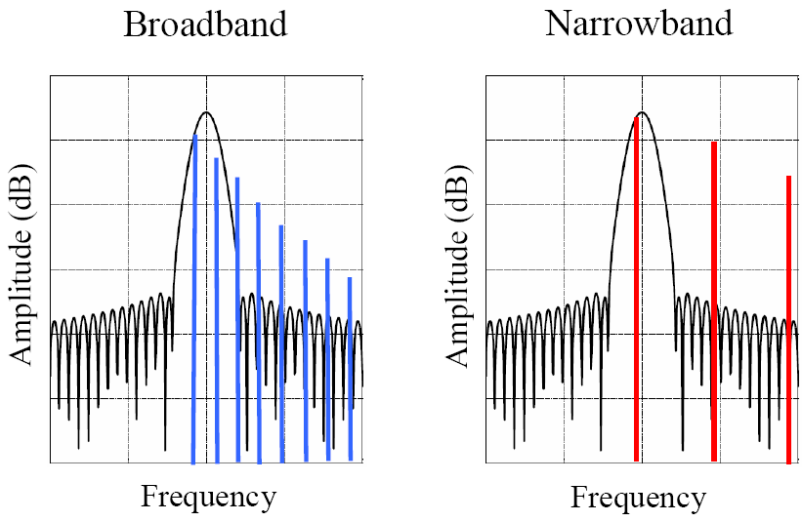

Figure 5.15 *Broadband and narrowband signals in the frequency domain.*

The signal is broadband when more than one spectral component (line) is located inside the IF filter's pass-band and the signal is narrowband when only one spectral component is located inside the IF filter's pass-band. In case of broadband signal the EMI receiver gives incorrect amplitude value because the spectral components in the IF filter's pass-band are summed.

EMC standards define the resolution bandwidths (RBW) that shall be used in the measurements. The resolution bandwidth $B_{6\text{ dB receiver}}$ is the 6 dB bandwidth of the IF band-pass filter in EMI receiver. When the EMI receiver's pulse repetition characteristics are analyzed, more important than the 6 dB (or 3 dB) bandwidth is the impulse bandwidth B_{i}, of IF band-pass filter which determines when the pulsed signal changes from broadband to narrowband. The equation 5.2 for the impulse bandwidth B_{i} can be found from the CISPR 16-1 standard [26]:

$$B_i = \frac{V_{\text{out}}}{2 \cdot G \cdot A_{\text{v-t}}}, \tag{5.2}$$

where V_{out} is output voltage of the band pass filter, G is the gain of the band pass filter and $A_{\text{v-t}}$ is the impulse area of the pulse (for a square wave $A_{\text{v-t}} = \tau_{\text{in}}$ x V_{in}).

Graphical definitions for the above-mentioned terms are shown in figure 5.16.

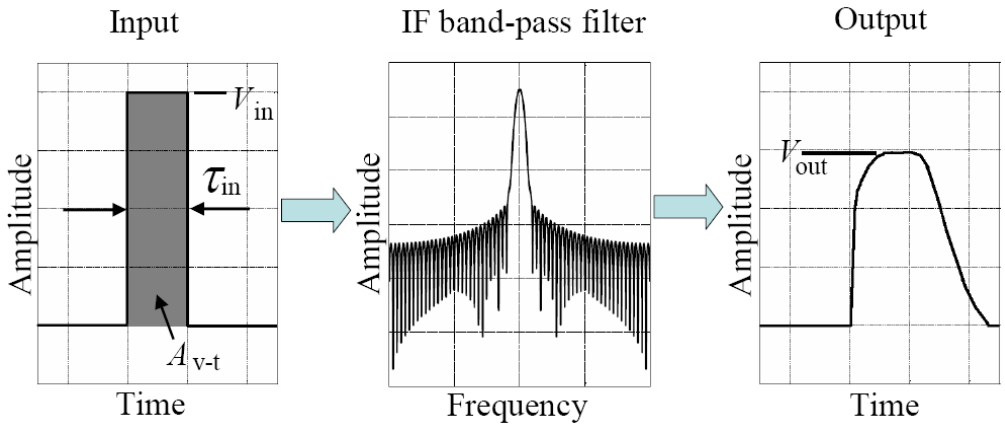

Figure 5.16 *Definition of the terms used in impulse bandwidth calculation.*

It is possible that two IF band-pass filters with a same 6 dB or 3 dB bandwidth have different impulse bandwidth which leads to different measurement results. The reason for the different impulse bandwidth is probably different shape factor of the IF band-pass filter. According to [26] the impulse bandwidth of the EMI receiver IF pass-band filter is 1.05 times greater than the 6 dB bandwidth and 1.31 times greater than the 3 dB bandwidth of the filter. The impulse bandwidth can also be measured as described in the F. Ball's article [27].

As the impulse bandwidth B_{i} of the IF band-pass filter is slightly greater than the 6 dB bandwidth, the pulse response curve of EMI receiver is not equal to the pulse response curve of TDEMI algorithm even though the RBW setting corresponds to the DFT step size. Figure 5.17 shows the minor differences between pulse response curves when RBW is 10 kHz and DFT step is 10 kHz (T = 100 μs).

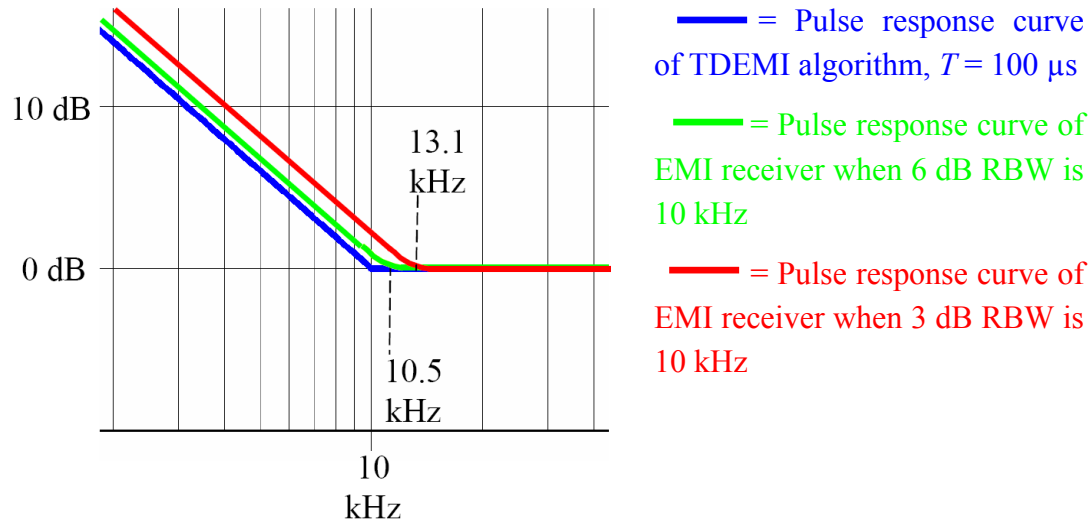

Figure 5.17 *Pulse response curves in the vicinity of 10 kHz.*

Both pulse response curves of the EMI receiver are very close to the pulse response curve of the TDEMI algorithm when the peak detector is used. Pulse response curves of quasi-peak and average detectors are more complicated as described in [7][8] and those curves differ from the previous curves. In these cases the pulse response correction curve $PC(f_{prf})$ described in the figure 1.6 is needed to correct the result of TDEMI algorithm. Pulse response correction curve is based on the differences between pulse response curves of quasi-peak or average detector and the TDEMI algorithm.

As the MIL-STD-461F requires only peak detector, the difference between TDEMI algorithm and EMI receiver is small, maximum couple of dB. Based on this fact, the basic algorithm introduced in the Chapter 4 seems to be a sufficient solution for broadband interference. If a more accurate approach is needed, detailed characteristics of an EMI receiver shall be available and more measurements with pulsed signals shall be conducted. This is not in the scope of this thesis, but it is one possible topic for further research, to improve TDEMI measurement method.

6 STATISTICAL ANALYSIS OF TIME DOMAIN CONDUCTED EMI MEASUREMENT RESULTS

6.1 Uncertainty and statistical evaluation of time domain conducted EMI measurement results

A measurement result is complete only if it includes the related uncertainty and the confidence level for the uncertainty. This fact is quite often forgotten in EMC measurement reports and the uncertainty evaluation is missing. The reason for this may be the fact that the evaluation of uncertainty in EMC measurements is quite difficult and laborious task.

The methods to evaluate the uncertainty in measurements are discussed in the *Guide to the Expression of Uncertainty in Measurement* [28]. The definitions and terms related to uncertainty, which are used in this thesis, are based in this publication. The uncertainty related especially to EMC measurements is discussed in British NIS81 publication *The Treatment of Uncertainty in EMC Measurements* [29].

NIS81 publication gives the typical expression for the conducted EMI measurement result:

y dBµV ± U dB for a level of confidence of approximately 95 %, (k=2)

The uncertainty U in the above expression is the so-called expanded uncertainty and it is a combination of separate uncertainties caused by different uncertainty sources. Different uncertainty sources in the frequency domain conducted EMI measurements are related to:

- Measurement receiver or spectrum analyzer
- LISN
- Cables and attenuators
- Mismatches in cable connections
- Repeatability and statistical properties.

In the time domain conducted EMI measurements uncertainty sources are related to:

- Digital oscilloscope
- LISN
- Cables and low-pass filters
- Mismatches in cable connections
- Repeatability and statistical properties.

The expanded uncertainty U is based on the uncertainty budget where above mentioned different uncertainties are collected. The method to determine the expanded uncertainty is described in [28].

The properties of different uncertainties can be can be determined by two different methods. The method called **Type A evaluation method** is based on evaluation of uncertainty of measurement by the statistical analysis of series of observations. The method called **Type B evaluation method** is evaluation of uncertainty by other means than Type A evaluation method. The type B evaluation method is typically based on information from equipment specifications, calibration certificates and reference data from handbooks.

In this research the Type A evaluation method is applied in analysis of repeatability of time domain EMI measurements. This repeatability is part of the uncertainty budget and it can be divided to two different parts. The first part is related to repeatability of the measurement method and measurement equipment and the second part is related to statistical properties of the interference from EUT. The evaluation of total expanded uncertainty, which includes also other uncertainty sources, is not in the scope of this research.

The first step in the statistical evaluation is that the experimental standard deviation *s(q)* is calculated based on several measurement results. The equation for the experimental standard deviation is

$$s(q) = \sqrt{\frac{1}{(n-1)} \sum_{j=1}^{n} \left(q_j - \overline{q}\right)^2} \,, \tag{6.1}$$

where $\overline{q}$ is the arithmetic mean (average) of the individual measurement results (q_j) and the n is number of the independent measurement results.

According to [26] the standard uncertainty $u(\overline{q})$ is the standard deviation of the mean if the number n of repeated measurements is large enough.

$$u(\overline{q}) = s(\overline{q}) = \frac{s(q)}{\sqrt{n}} \tag{6.2}$$

According to publication *EA-4/02 Expression of the Uncertainty of Measurement in Calibration* [30] the number of repeated measurements is large enough if more than 10 repeated measurements are performed and used in calculation of experimental standard deviation.

6.2 Statistical analysis of the time domain conducted EMI measurement results

In this research three different signal types are used in statistical analysis of the time domain conducted EMI measurement results. These signal types are:

1. Interference signal from the DC/DC converter of the reference EMI source (realistic narrowband EMI signal)
2. Discrete 135 kHz sinusoidal signal from signal generator (close to ideal narrowband signal)
3. Interference signal from the brushed DC motor of the reference EMI source (realistic broadband EMI signal)

The algorithm for narrowband interference signals, introduced in Chapter 5, is used for signal types 1 and 2. The basic algorithm introduced in Chapter 4 is used for signal type 3. Measurements with above-mentioned algorithms are repeated 20 times (n = 20). This ensures that the following analysis is as statistically reliable as practical.

Based on results from algorithms, the experimental standard deviation and the standard uncertainty for each DFT step is produced for each signal type. This means 141 different values in the frequency band from 10 kHz to 150 kHz and 986 different values in the frequency band from 150 kHz to 10 MHz. Obviously, for the discrete 135 kHz signal (signal type 2) only the lower frequency band (10 kHz to 150 kHz) is measured because there is nothing but ambient noise on the upper frequency band.

6.2.1 Statistical analysis of the signal type 1

Figures 6.1 and 6.2 show the experimental standard deviation and the standard uncertainty of the results from 20 repeated time domain measurements of the interference from DC/DC converter (signal type 1).

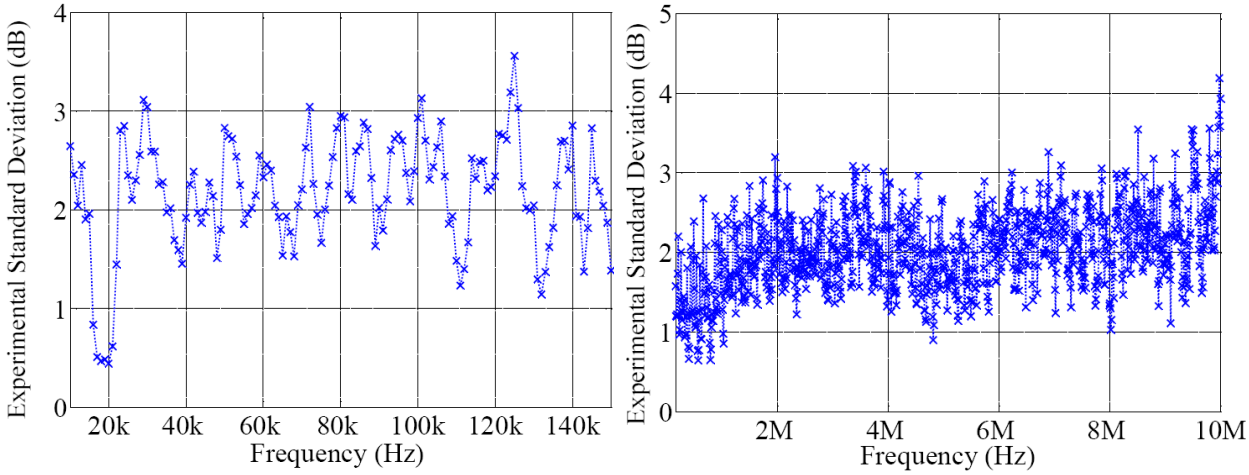

Figure 6.1 *The experimental standard deviation of the measurement results, interference signal from DC/DC converter.*

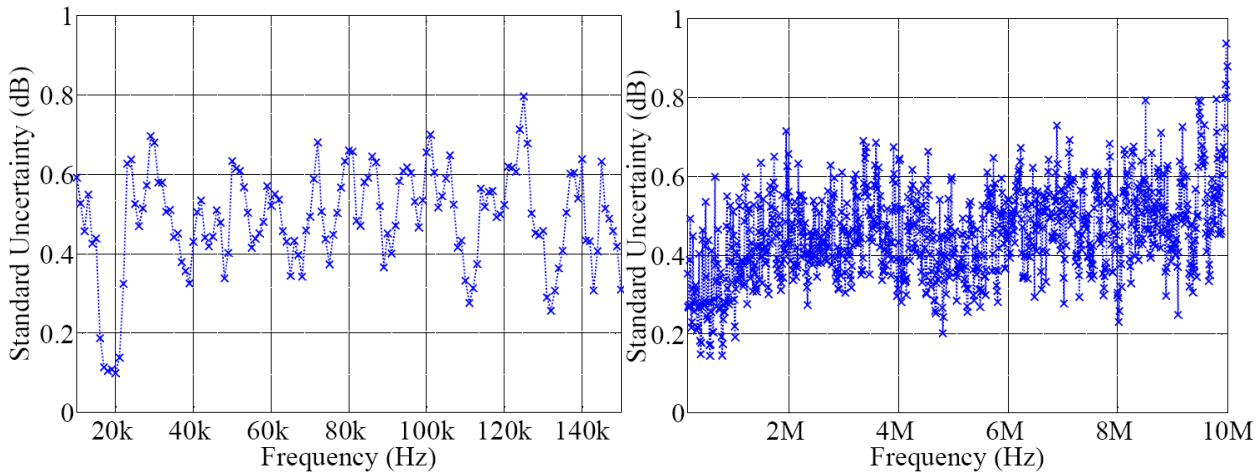

Figure 6.2 *The standard uncertainty of the measurement results, interference signal from DC/DC converter.*

Histograms in figure 6.3 show how the individual measurement results (data points) deviate from the arithmetic mean values. For the lower frequency band from 10 kHz to 150 kHz this means 2820 individual data points (20 x 141) and for the upper frequency band from 150 kHz to 10 MHz 19720 individual data points (20 x 986). Figure 6.3 shows also ideal normal distribution curves for equal size data. These normal distribution curves are plotted with red solid line.

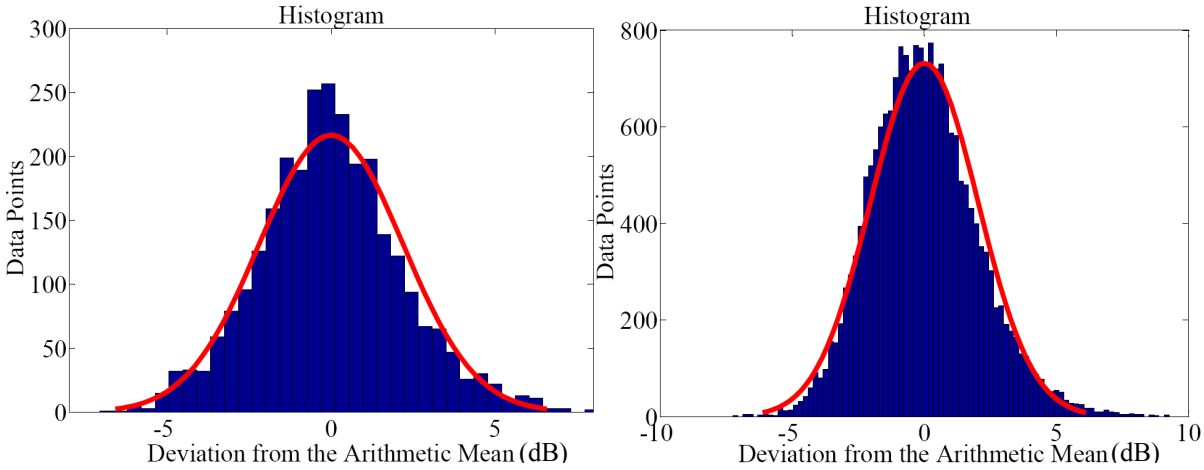

Figure 6.3 a) *Histogram of individual measurement results, 10 kHz - 150 kHz / 2820 data points* ***b)*** *Histogram of individual measurement results, 150 kHz - 10 MHz / 19720 data points.*

As it can be seen from the histograms, the distribution of individual measurement results is close to normal distribution. This fact can also be seen from the normal probability plots shown in figure 6.4.

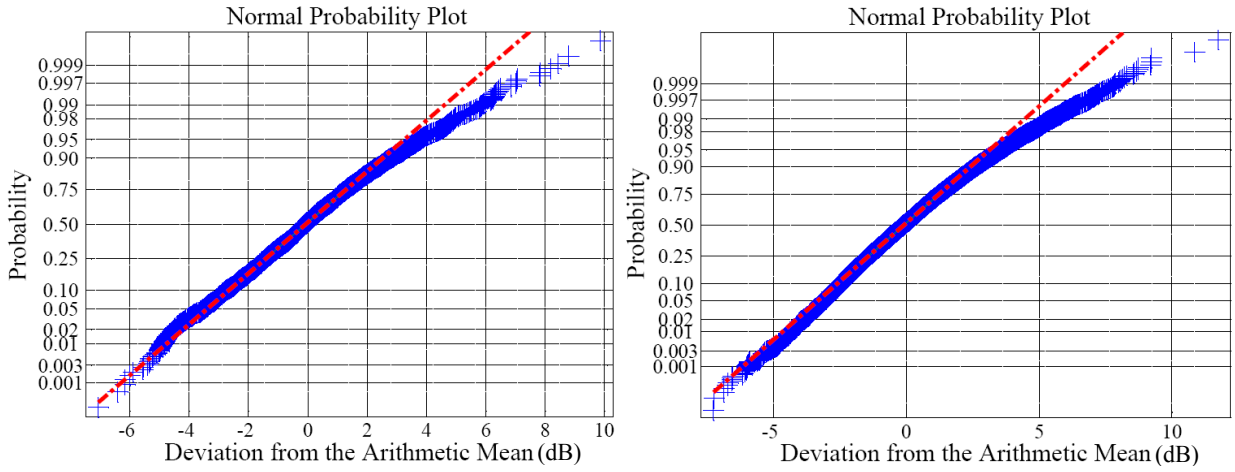

a) b)

Figure 6.4 a) *Normal probability plot of individual measurement results, 10 kHz - 150 kHz / 2820 data points* ***b)*** *Normal probability plot of individual measurement results, 150 kHz - 10 MHz / 19720 data points.*

Deviations from the arithmetic mean of the individual measurement results are marked with blue plus marks (+) and the result from an ideal normal distribution is marked with red dash-dot line.

6.2.2 Statistical analysis of the signal type 2

Figure 6.5 shows the experimental standard deviation and the standard uncertainty of the discrete 135 kHz sinusoidal signal (signal type 2).

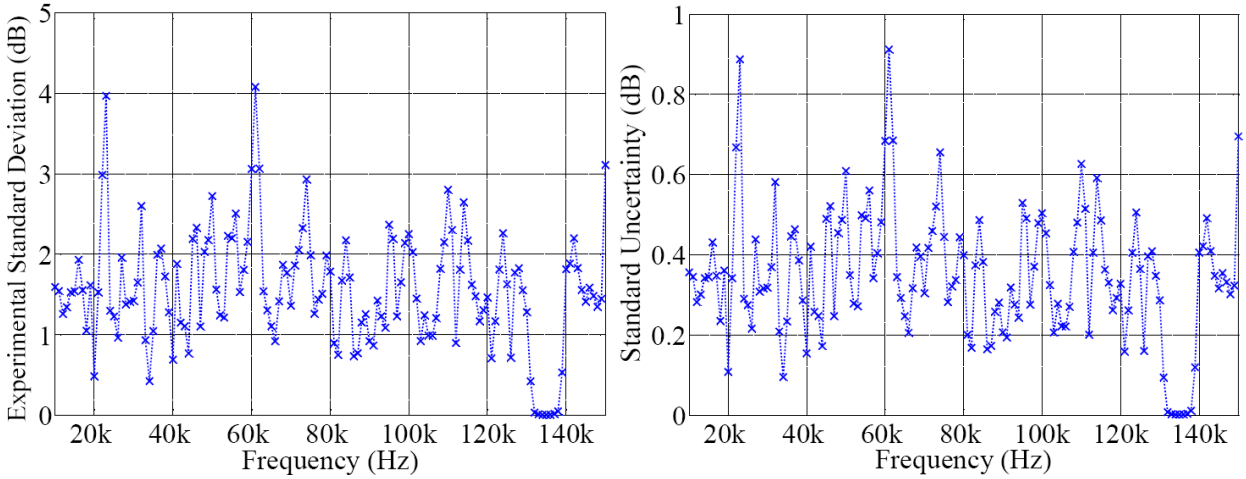

a) b)

Figure 6.5 a) *The experimental standard deviation of the discrete 135 kHz sinusoidal signal b) Standard uncertainty of the discrete 135 kHz sinusoidal signal.*

Histogram and normal probability plot in figure 6.6 show how the individual measurement results (data points) deviate from the arithmetic mean value.

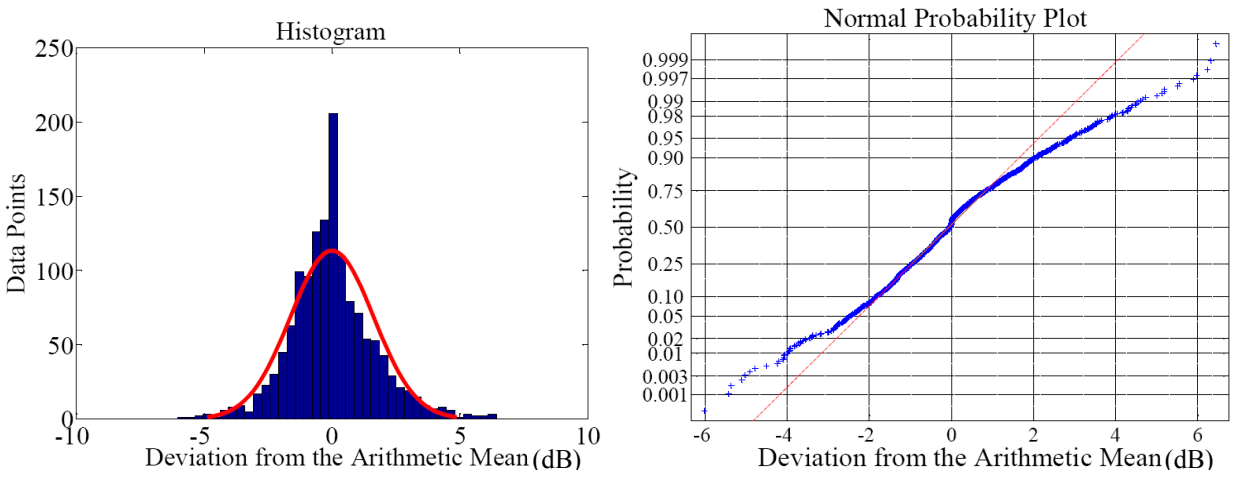

Figure 6.6 a) *Histogram of individual measurement results, 10 kHz - 150 kHz / 2820 data points* ***b)*** *Normal probability plot of individual measurement results, 10 kHz - 150 kHz / 2820 data points.*

Figure 6.6 tells that the distribution of individual measurement results of discrete signal is also quite close to normal distribution.

6.2.3 Statistical analysis of the signal type 3

Figures 6.7 and 6.8 show the experimental standard deviation and the standard uncertainty of the results from 20 repeated time domain measurements of the interference from DC motor (signal type 3).

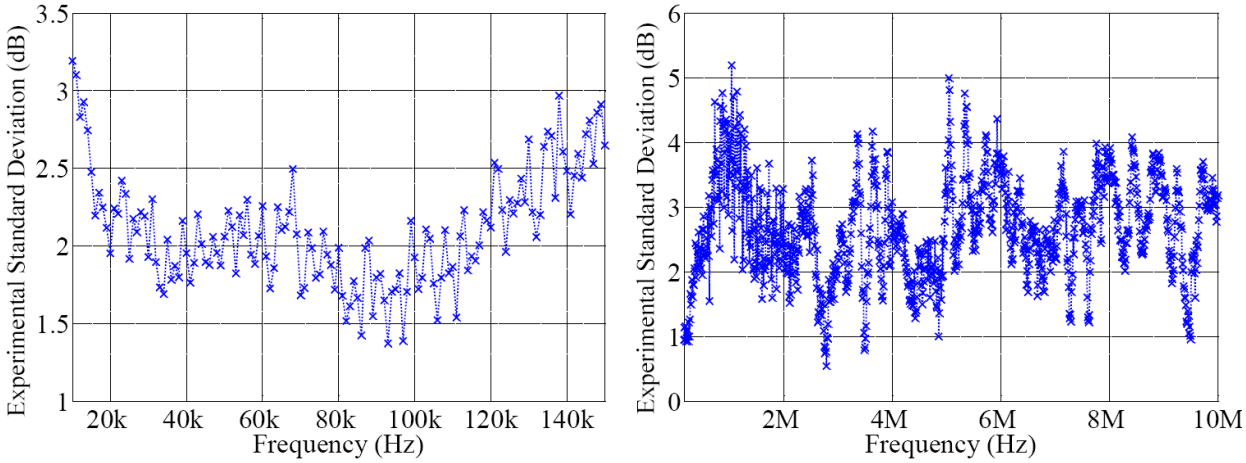

Figure 6.7 *The experimental standard deviation of the measurement results, interference signal from DC motor.*

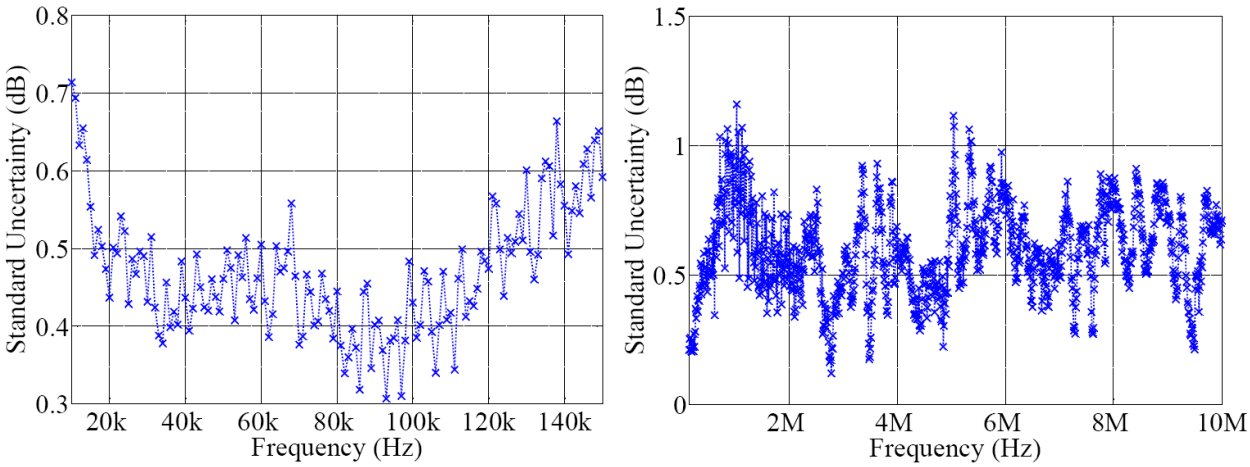

Figure 6.8 *The standard uncertainty of the measurement results, interference signal from DC motor.*

Histograms in figure 6.9 show how the individual measurement results (data points) deviate from the arithmetic mean value.

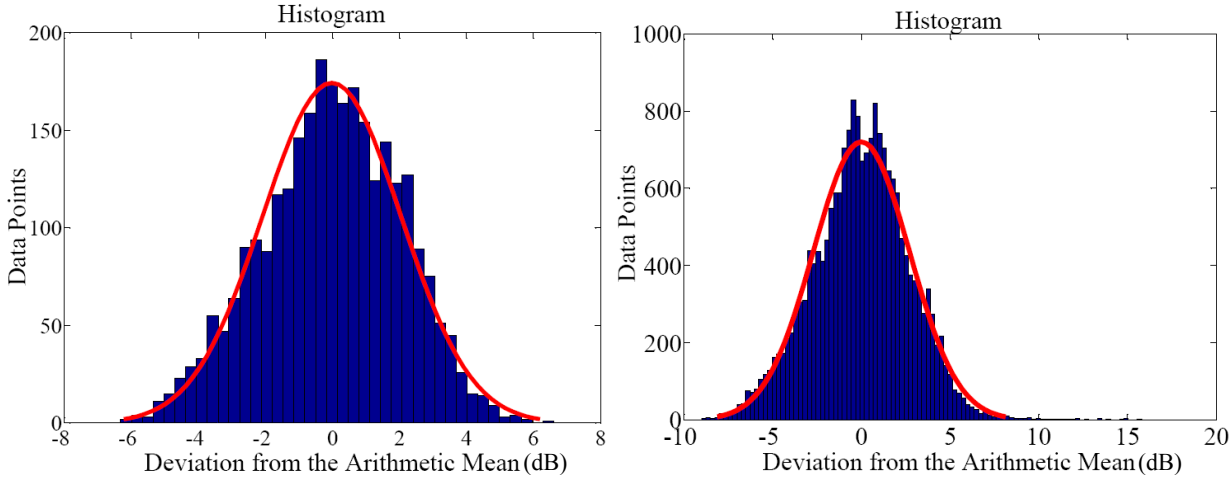

a) b)

Figure 6.9 a) *Histogram of individual measurement results, 10 kHz - 150 kHz / 2820 data points* ***b)*** *Histogram of individual measurement results, 150 kHz - 10 MHz / 19720 data points.*

Corresponding normal probability plots are shown in figure 6.10.

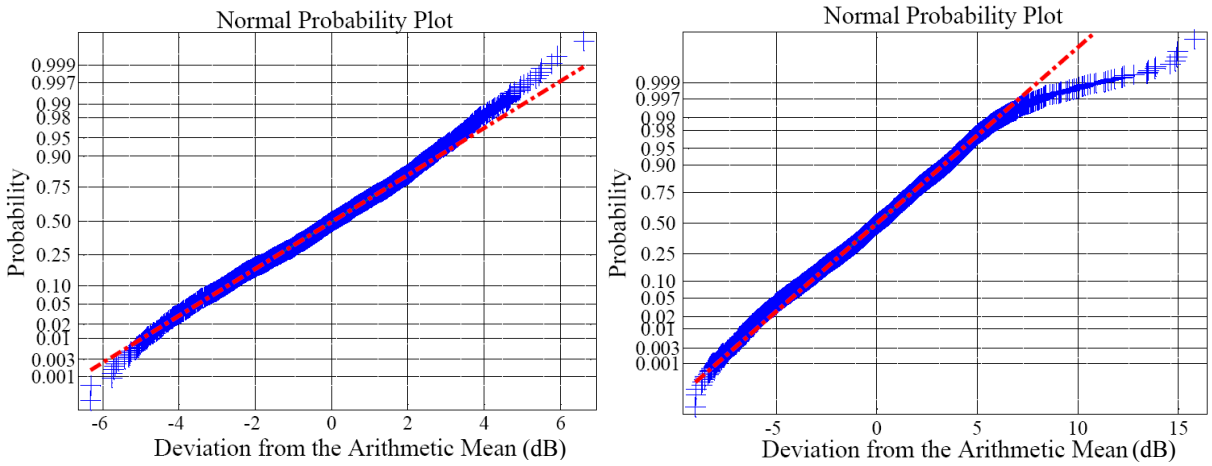

a) b)

Figure 6.10 a) *Normal probability plot of individual measurement results, 10 kHz - 150 kHz / 2820 data points* ***b)*** *Normal probability plot of individual measurement results, 150 kHz - 10 MHz / 19720 data points.*

6.3 Summary of the statistical analysis

Performed statistical analysis indicates that the characteristics of the measured interference signal have a very strong influence on the uncertainty and the repeatability. Uncertainty caused by measurement equipment and method itself is relatively low. This can be seen from the evaluation of measurement results of narrowband signals (signal types 1 and 2). If the interference signal contains narrowband component or components which have a stable frequency and amplitude, the values of the experimental standard deviation and standard uncertainty of the measurement results are very low on these frequencies. In the figures 6.1 and 6.2, there is a dip in the graphs of the experimental standard deviation and standard uncertainty just below 20 kHz. The experimental standard deviation is around 0.5 and standard uncertainty is around 0.1. On the same frequency there is the highest interference peak. The same phenomenon can be seen from the figure 6.5 where the experimental standard deviation and the standard uncertainty are close zero on frequencies close to 135 kHz. Outside the frequencies of the narrowband signals the maximum values of the experimental standard deviation are 3 to 4 dB.

Evaluation of broadband interference signals shows that the maximum level of experimental standard deviation of the measurement results is 4 to 5 dB and maximum level of standard uncertainty is 1 dB. Higher values are obvious, as the interference signal is quite unstable and contains random components.

Above-mentioned facts tell that the repeatability of the EUT is more significant than the repeatability of the measurement system itself.

According to analysis it seems also that the distributions of individual measurement results from repeated measurements are very close to the normal distribution. This can be seen from the histograms and from normal probability plots. Based on this fact, it

seems that it is possible to use the logarithmic dB values of standard uncertainty in the calculation of the total expanded uncertainty. This and the overall use of logarithmic dB values in the evaluation of uncertainty of EMC measurements are strongly questioned by Bronaugh and Osburn. According to their paper [31] the logarithmic dB terms can be used only if the lognormal distribution is applied with the logarithmic terms. Normal distribution should be used only with linear (additive) data. Bronaugh and Osburn allow still to use normal distribution with logarithmic terms, if the logarithmic dB values are distributed normally, which seems to be the situation with the evaluated data in this research.

7 COMPARISON OF TIME DOMAIN EMISSION MEASUREMENT SYSTEM AND STANDARD FREQUENCY DOMAIN EMISSION MEASUREMENT SYSTEM

Comparative measurements for the reference EMI source were carried out in the Finnish Army Materiel Command's EMC laboratory in Riihimäki. The purpose of this measurement session was to check how the results from the time domain EMI measurement system correspond to the results from standard frequency domain measurement system. The measurements were performed in a semi-anechoic chamber with non-conductive table. Photograph of the measurement setup is shown in Figure 8.1.

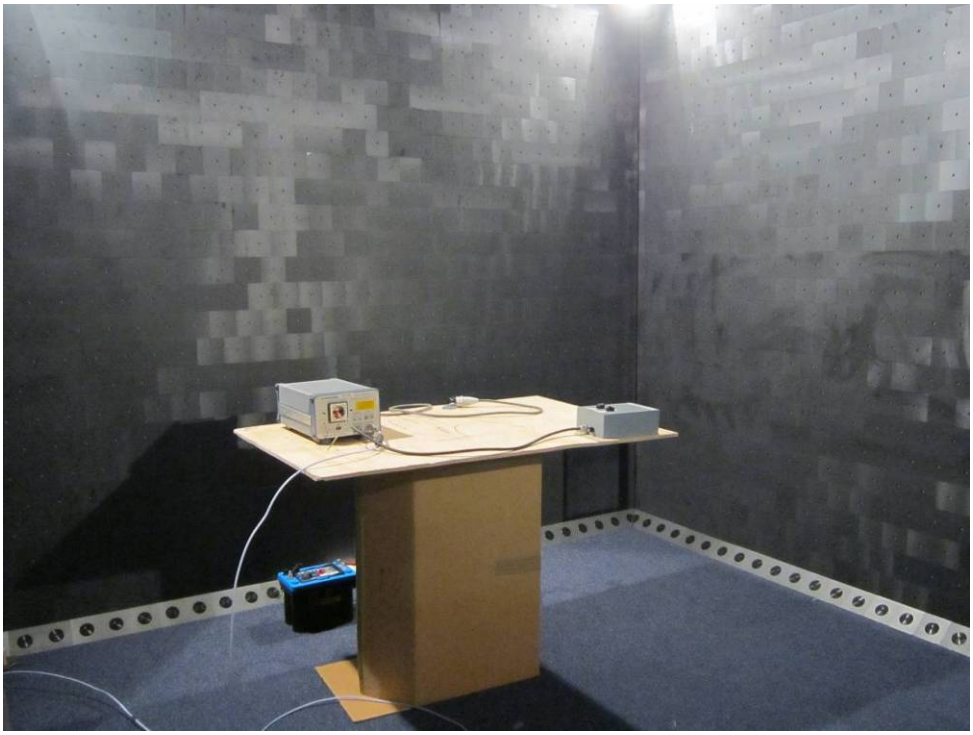

Figure 8.1 *Measurement setup in semi-anechoic chamber in the Finnish Army Materiel Command's EMC laboratory.*

Interference from the DC motor of the reference EMI source was used in this examination because the interference from DC motor can be processed with basic algorithm, without special window functions which make the time domain measurement process more time consuming. Figures 8.2 and 8.3 show the results of the frequency

domain measurements at Riihimäki, together with the measurement results from previous frequency and time domain measurements (results shown in Chapter 4).

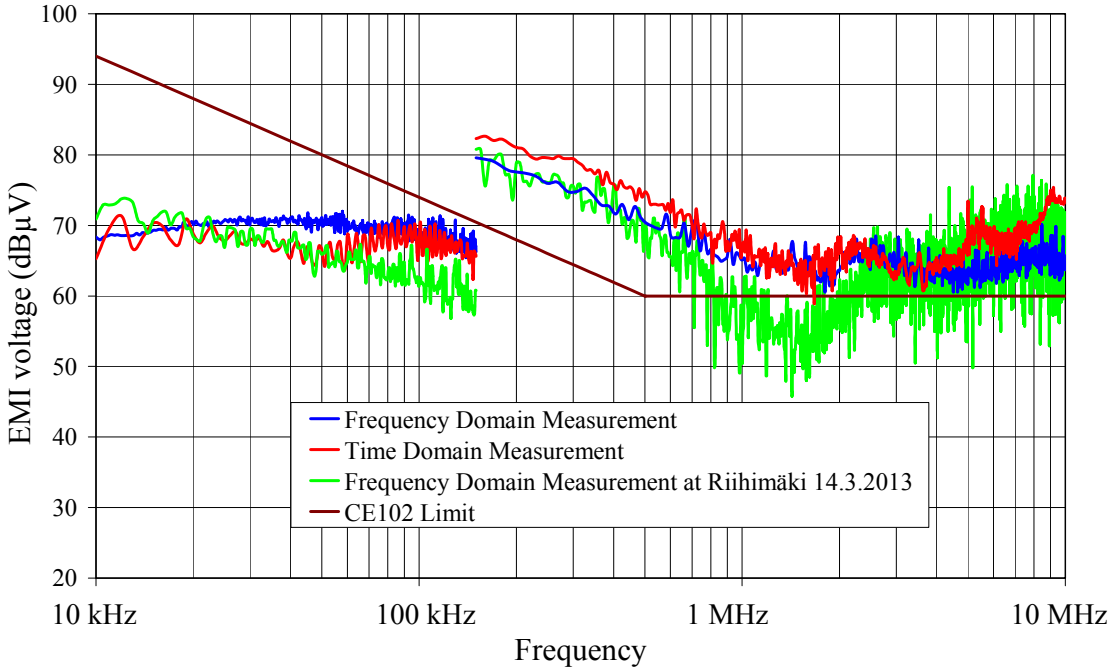

Figure 8.2 *TDEMI measurement results and frequency domain EMI measurement results, DC-motor of the reference EMI source, plus lead.*

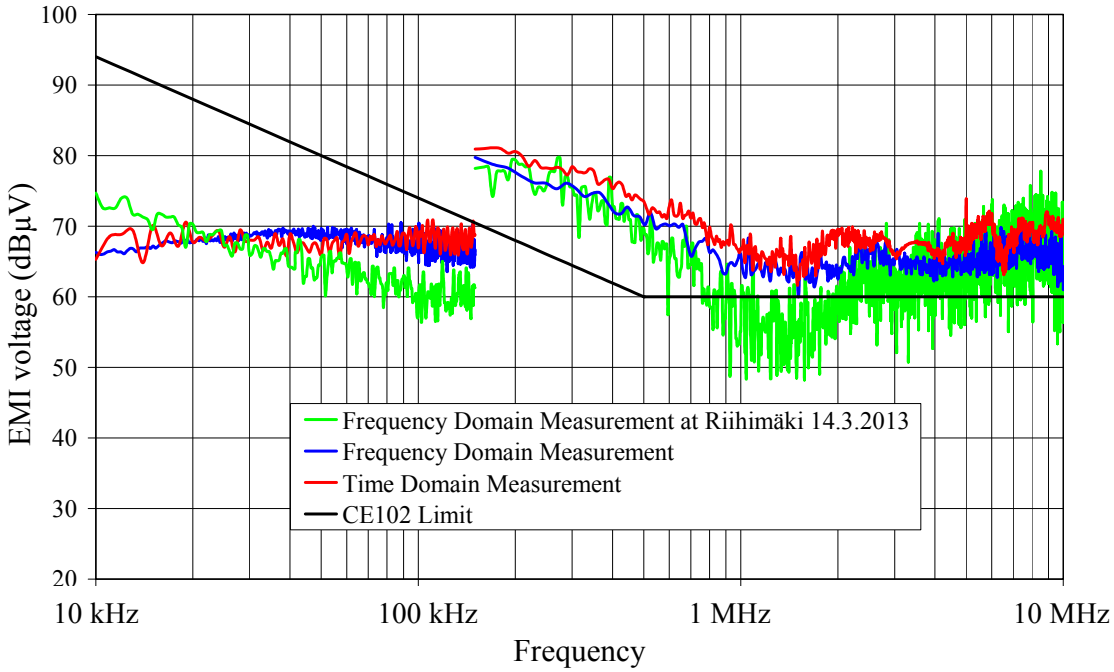

Figure 8.3 *TDEMI measurement results and frequency domain EMI measurement results, DC-motor of the reference EMI source, return lead.*

Results of the frequency domain measurements at Riihimäki deviated from the previous measurement results significantly. As the EUT was the same reference EMI source which has been used in all of the measurements and the measurement receiver was similar to the receiver which has been used in previous measurements, the only possible reason for the difference was the LISN.

The effect of different LISN was checked by repeating time domain EMI measurements with the LISN which was available at Riihimäki. Results are shown in figures 8.4 and 8.5.

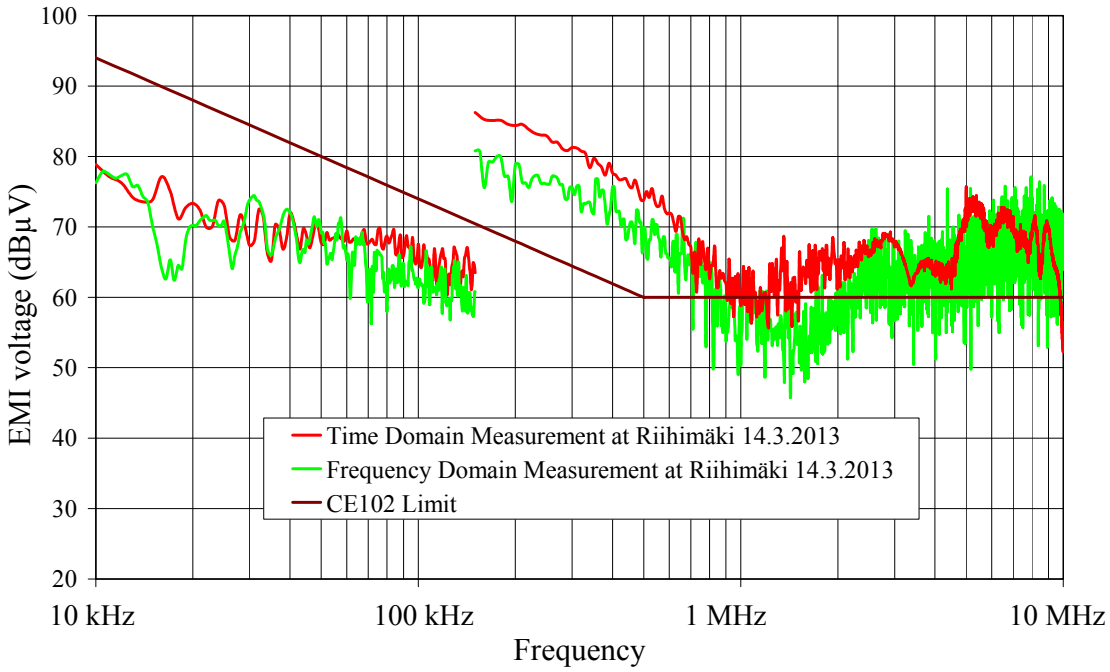

Figure 8.4 *TDEMI measurement results and frequency domain EMI measurement results, both measurements at Riihimäki 14.3.2013, DC-motor of the reference EMI source, plus lead.*

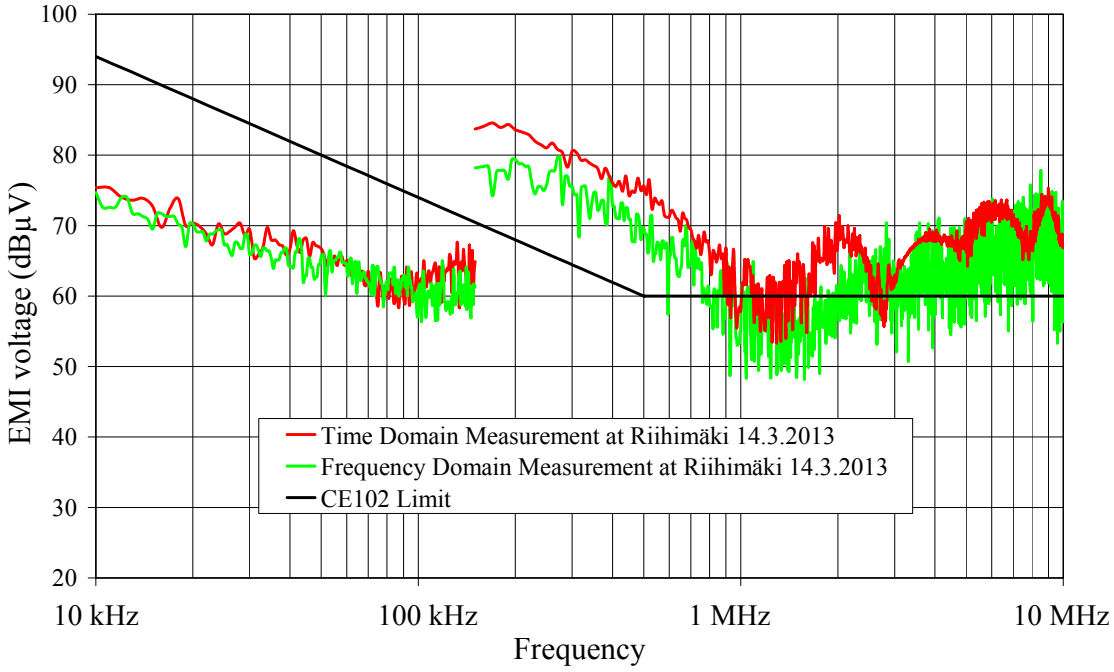

Figure 8.5 *TDEMI measurement results and frequency domain EMI measurement results, both measurements at Riihimäki 14.3.2013, DC-motor of the reference EMI source, return lead.*

The results shown in figures 8.4 and 8.5 proved that the different LISN was the main reason for the difference between measurement results. The LISN which was available at Army Materiel Command EMC laboratory at Riihimäki was also same kind of 50 µH / 50 Ω LISN like the other LISN which is used in this research. The deviation caused by the LISN was a small surprise but on the other hand it was a valuable finding.

Comparative measurements performed at the Army Materiel Command's EMC laboratory proved that the time domain conducted EMI measurement itself is reliable and measurements are repeatable. The differences between measurement equipment are a significant source for uncertainty and this has to keep in mind when comparative measurements are carried out.

8 CONCLUSIONS

The aim of this research was to study the feasibility of the TDEMI measurement method in MIL-STD-461F compliance measurements. The EMI measurement method studied as an example was the conducted emission measurement method CE102. The essential part of the research was measurements of the reference EMI source which contained sources for narrowband and broadband interference.

Chapter 4 describes the process of building the TDEMI measurement system including the physical parts and the Discrete Fourier Transform (DFT) based basic algorithm. The process of building the TDEMI measurement system turned out to be laborious and time consuming effort, requiring lot of different measurements and simulations. The first EMI measurements with the built TDEMI measurement system showed that the measured level of ambient electromagnetic interference clearly fulfilled the MIL-STD-461F requirement. The results for broadband interference were close to frequency domain measurement results, but in case of narrowband interference, the difference between the TDEMI and frequency domain measurement results was greater. Despite this difference, the TDEMI measurement method proved to be a developable alternative for the frequency domain measurements, but very much attention must be paid to the correct data acquisition including anti-aliasing filtering. Aliasing is probable source for measurement errors, but the effects of aliasing can be reduced by effective low-pass filtering, as shown in section 4.2. Determination of the frequency response corrections for TDEMI measurement system should also be done very carefully, so that the different frequency responses of the TDEMI measurement system and frequency domain measurement system are taken into account.

Chapter 5 introduces the improvements for the basic algorithm. The first improvement is the Flat Top window based algorithm for narrowband interference. This algorithm proved to be efficient for narrowband interference signals when the time domain characteristics of the narrowband interference were taken into account. When the Flat Top window based algorithm is used, it very important that the all parts of the interference signal are taken into account when the frequency domain result is produced by the DFT. Demonstration in section 5.1 shows how the Flat Top window based algorithm may give incorrect results if the algorithm is used negligently.

In addition to Flat Top window function, thirteen other window functions were evaluated with the narrowband interference. This evaluation is described in section 5.2 and in Appendix 5. The evaluation showed that the Flat Top window is not the only window function which can be used to improve basic algorithm in case of narrowband interference. Gaussian and Tukey window functions proved to be also applicable. The

overall disadvantage of the use of window functions is that they decrease frequency resolution. This can be compensated by increasing the capture time T as demonstrated in section 5.2.

Section 5.3 introduces the algorithm for broadband interference. This algorithm is based on pulse response characteristics of TDEMI measurement system and frequency domain measurement system. Demonstration in section 5.3 revealed that both measurement systems may give incorrect results for broadband interferences. The difference between TDEMI and frequency domain results depends on the detector type used in frequency domain measurements. The difference is typically greatest when the average detector is used and also noticeable with the quasi-peak detector. In these cased the TDEMI measurement system overestimates the amplitude. The peak detector gives results which are close to TDEMI measurement results and the possible difference is caused by impulse bandwidth of EMI measurement receiver. Even the resolution bandwidth of EMI receiver (RBW) is equal to DFT step in TDEMI measurement system, the impulse bandwidth may be significantly greater. As the MIL-STD-461F requires the peak detector to be used in frequency domain measurements, the basic algorithm proved to be reasonable solution.

In Chapter 6 the statistical properties of TDEMI measurement system was evaluated. The evaluation focused to the repeatability of time domain EMI measurements. The repeatability is part of the total uncertainty budget and it can be divided to two different parts. The first part is related to repeatability of the measurement method and measurement equipment and the second part is related to statistical properties of the interference from EUT. The evaluation of total expanded uncertainty, which includes also other uncertainty sources, was not in the scope of this research. Evaluation with Type A evaluation method proved that the repeatability of the EUT is more significant than the repeatability of the measurement system itself. Results of statistical evaluation were close to the results presented in [9] and the conclusion was that the repeatability of the TDEMI measurement system itself is high.

The last task in the research was the comparison of time domain emission measurement system and standard frequency domain emission measurement system. This was done by measurements at the Finnish Army Materiel Command's EMC laboratory. The reference EMI source was measured with the standard frequency domain measurement system and the results were compared to the results of TDEMI measurements which were performed earlier. Results showed that there was a significant difference between results. TDEMI measurements for the reference EMI source were repeated at the Finnish Army Materiel Command's EMC laboratory and the results, which were closer to the frequency domain measurement results, revealed that the reason for the difference was mainly the LISN. This LISN was not the same as used earlier, but still according to the standard.

The conclusion of the research is that the TDEMI measurement method and system is a feasible alternative for the frequency domain measurement system in MIL-STD-461F CE102 measurements. In most of the practical cases the TDEMI measurement

method is more time consuming than the CE102 frequency domain measurement, but if the interference signal contains infrequent phenomena, TDEMI measurement method may save time. These kinds of signals were not used in this research, so the exact numbers for saving in time can not be presented. The undisputed benefit of the TDEMI measurement method is that the measurement equipment is cheaper than the equipment used in frequency domain measurement. On the other hand the building of TDEMI measurement system is laborious task and it requires lot of specific knowledge.

Even though the TDEMI measurement method seems to give results which are close to the frequency domain measurement results, it can still be improved by further research. The possible further research areas are application of different window functions in the algorithm for narrowband interference and transient measurements with the TDEMI measurement method. Also the algorithm for broadband interference can be improved by more detailed modelling of pulse response characteristics of TDEMI and frequency domain measurement methods.

9 REFERENCES

[1] MIL-STD-461F. Department of defense interface standard. Requirements for the control of electromagnetic interference characteristics of subsystems and equipment. December 2007.

[2] Bronaugh, E. L. An advanced electromagnetic interference meter for the twenty-first century. 8th International Zurich Symposium on Electromagnetic Compatibility, Zurich, Switzerland, 1989. Paper no. 42H5. pp. 215-219.

[3] Bronaugh, E. L. & Oshurn, J. D. M. New ideas in EMC instrumentation and measurement. 10th International Zurich Symposium on Electromagnetic Compatibility, Zurich, Switzerland, 1993. Paper no. 58JI. pp. 323-326.

[4] Schütte, A. & Karner, H.C. Comparison of time domain and frequency domain electromagnetic susceptibility testing. IEEE International Symposium on Electromagnetic Compatibility, Chicago, USA, August 22-26, 1994. pp. 64-67.

[5] Sikora, P. A. An EMI receiver design using modern digital techniques. 11th International Zurich Symposium on Electromagnetic Compatibility, Zurich, Switzerland, March 7-9, 1995. Paper no. 86N2. pp. 453-458.

[6] Keller, C. & Feser, K. Fast emission measurement in time domain. In 14th International Zurich Symposium on Electromagnetic Compatibility, Zurich, Switzerland. February 20-22, 2001. Paper no. 70K7.

[7] Keller, C. & Feser, K. A new method of emission measurement. IEEE International Symposium on Electromagnetic Compatibility EMC 2002. Minneapolis, MN, USA. August 19-23, 2002. pp. 599-604. Vol.2.

[8] Keller, C. & Feser, K. Fast emission measurement in time domain. IEEE Transactions on Electromagnetic Compatibility 49(2007)4. pp. 816-824.

[9] Krug, F. & Russer, P. The Time-Domain Electromagnetic Interference Measurement System. IEEE Transactions on Electromagnetic Compatibility 45(2003)2. pp. 330-338.

[10] Krug, F. Braun, S. Kishida, Y & Russer, P. A novel digital quasi-peak detector for time-domain measurements. 33rd European Microwave Conference, Munich, Germany, October 7-9, 2003. pp. 1027-1030. Vol.3.

[11] Krug, F. & Russer, P. Signal processing methods for time domain EMI measurements. IEEE International Symposium on Electromagnetic

Compatibility EMC '03, Istanbul, Turkey, May 11-16, 2003. pp. 1289-1292. Vol.2.

[12] Krug, F. Hermann, T. & Russer, P. Signal processing strategies with the TDEMI measurement system. Proceedings of the 20th IEEE Instrumentation and Measurement Technology Conference IMTC '03, Vail, CO, USA, May 20-22, 2003. pp. 832-837.

[13] Krug, F. & Russer, P. Statistical evaluations of time-domain EMI measurements. IEEE International Symposium on Electromagnetic Compatibility EMC '03, Istanbul, Turkey. May 11-16, 2003. pp. 1265 – 1268. Vol.2.

[14] Pontt, J., Olivares, R., Carrasco, H., Keller, V., López, M., Robles, H., Díaz, S., Toro, A. & Fuentes, C. Developing a simple, modern and cost effective system for EMC pre-compliance measurements of conducted emissions. European Conference on Power Electronics and Applications, Aalborg, Denmark, September 2-5, 2007. pp. 1 – 7.

[15] Braun, S., Aidam, M. & Russer, P. Development of a multiresolution time domain EMI measurement system that fulfills CISPR 16-1. IEEE International Symposium on Electromagnetic Compatibility EMC 2005, Chicago, IL, USA, August 8-12, 2005. pp. 388-393. Vol. 2.

[16] Braun, S. Hoffmann, C., Frech, A & Russer, P. A realtime time-domain EMI measurement system for measurements above 1 GHz. IEEE International Symposium on Electromagnetic Compatibility, 2009, EMC 2009, Austin, Texas, USA, August 17-21, 2009. pp. 143-146.

[17] Hoffmann, C. Braun, S. & Russer, P. A broadband time-domain EMI measurement system for measurements up to 18 GHz. European Conference on Electromagnetic Compatibility, 2010, EMC Europe 2010, Wroclaw, Poland, September 13-17, 2010. pp. 1-4.

[18] Braun, S. An overview of emission measurements in time-domain. In Proceedings of the 2009 International Symposium on EMC EMC'09, Kyoto, Japan, July 20-24, 2009. pp. 681-684.

[19] Russer, P. EMC measurements in the time-domain. General Assembly and Scientific Symposium, 2011 XXXth URSI, Istanbul, Turkey, August 13-20, 2011. pp. 1-35.

[20] Westenberger, H. Use of time domain methods for CISPR16 compliant EMI measurements. IEEE International Conference on Microwaves, Communications, Antennas and Electronics Systems COMCAS 2009, Tel Aviv, Israel, November 9-11, 2009. pp. 1-4.

[21] International Standard IEC 60050, Chapter 161. International Electrotechnical Vocabulary (IEV). 1998.

[22] Harris, F. J. On the use of windows for harmonic analysis with the discrete Fourier transform. Proceedings of the IEEE, vol 66, no. 1, pp. 51-83. 1978.

[23] Gade, S. Herlufsen, H. Use of Weighting Functions in DFT/FFT Analysis (Part I), Brüel & Kjær, Technical Review, No. 3, 1987, pp. 19-21.

[24] Tutorial: The Fundamentals of FFT-Based Signal Analysis and Measurement in LabVIEW and LabWindows/CVI. National Instruments, June 8, 2009. Available from http://www.ni.com/white-paper/4278/en. Referred 28.2.2013.

[25] Tutorial: Optimizing FFTs using window functions. National Instruments, December 6, 2011. Available from http://www.ni.com/white-paper/4844/en. Referred 28.2.2013.

[26] CISPR 16-1, Specification for radio disturbance and immunity measuring apparatus and methods – Radio disturbance and immunity measuring apparatus. International Electrotechnical Commission. 1999.

[27] Ball, F. Measure the real impulse bandwidth. Article in the Microwaves & RF Magazine. January 1987. pp. 93-96.

[28] Evaluation of measurement data - Guide to the expression of uncertainty in measurement. First edition. Joint Committee for Guides in Metrology (JCGM/WG 1). September 2008. Available from http://www.bipm.org/utils/common/documents/jcgm/JCGM_100_2008_E.pdf. Referred 3.4.2013.

[29] NIS81:1994, The treatment of uncertainty in EMC measurements. NAMAS Executive, National Physical Laboratory, England.

[30] EA-4/02, Expression of the Uncertainty of Measurement in Calibration. European co-operation for Accreditation. December 1999.

[31] Bronaugh, E. Osburn, J. Estimating EMC measurement uncertainty using logarithmic terms (dB). IEEE International Symposium on Electromagnetic Compatibility, 1999. Seattle, WA, USA, August 2-6, 1999. pp. 376 – 378.

APPENDIX 1

Circuit Diagram for Reference EMI Source

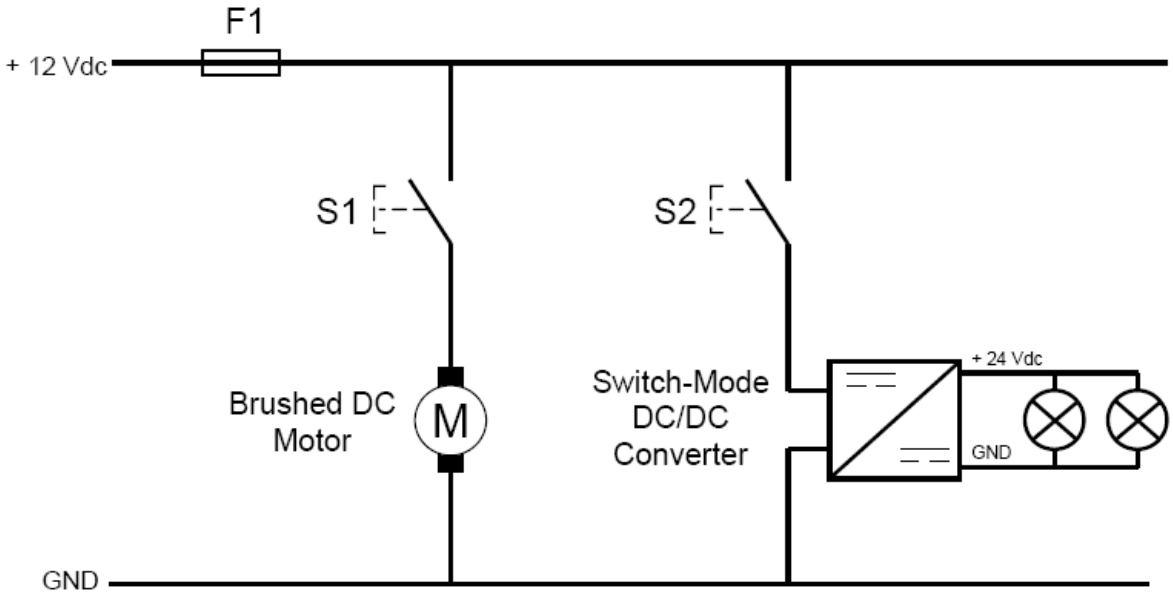

APPENDIX 2

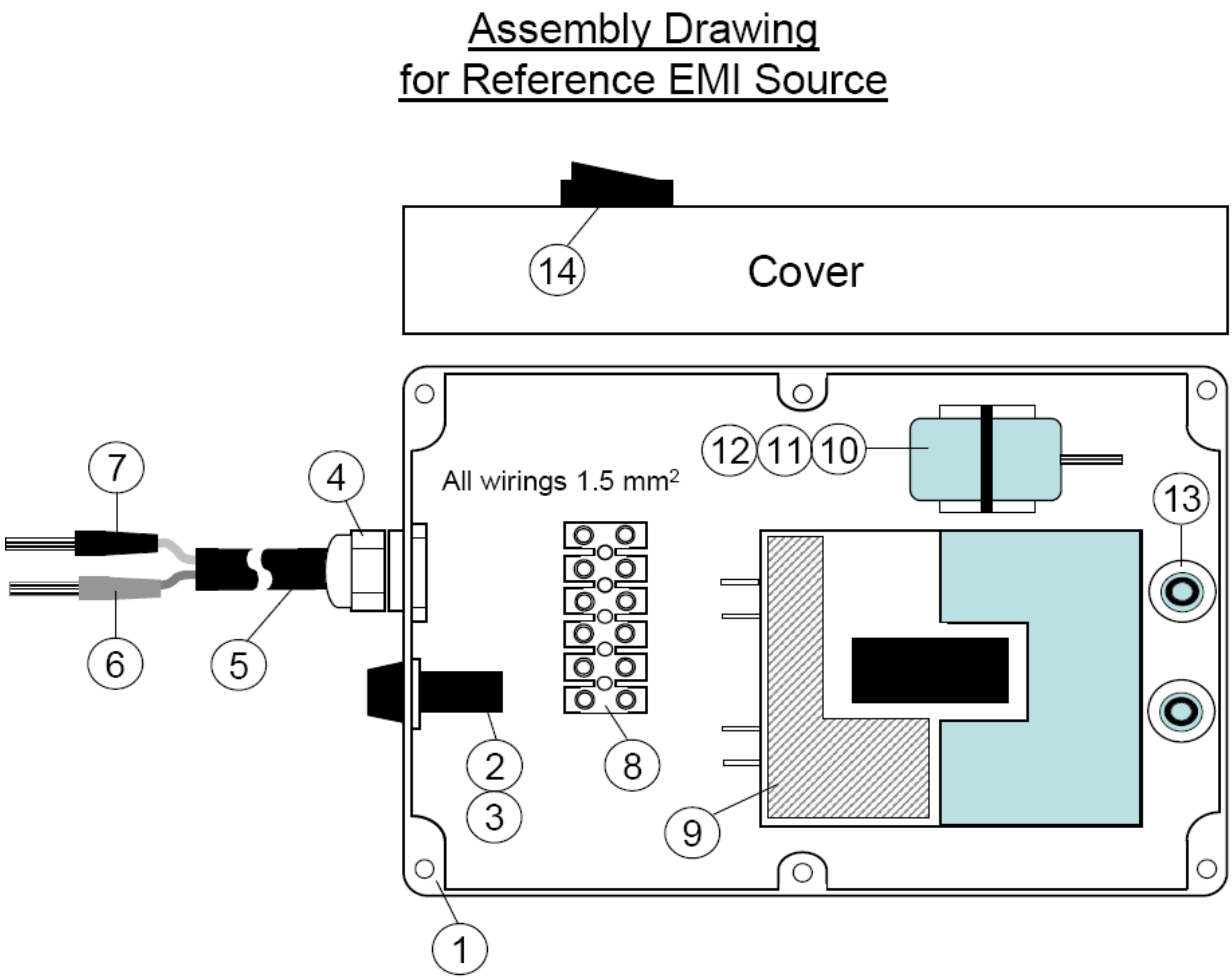

Part #	Name	Type
1	Plastic enclosure with screws	N/A
2	Fuse holder	Biltema 35-652
3	Fuse	10 A
4	Cable feed through	Biltema 350101
5	Cable (length 1 meter)	H07RN-F 3G1.5mm²
6	Banana plug (red)	BULA 20K
7	Banana plug (black)	BULA 20K
8	Terminal block	N/A
9	DC/DC converter	N/A
10	DC motor	N/A
11	Cable tie	N/A
12	Mounting plate for cable tie	N/A
13	2 X 24 V 21 W bulb	BA15s
14	2 X Switch	Biltema 43209

APPENDIX 3

Amplitude spectrum of a 30 kHz sinusoidal signal without Flat Top windowing before DFT

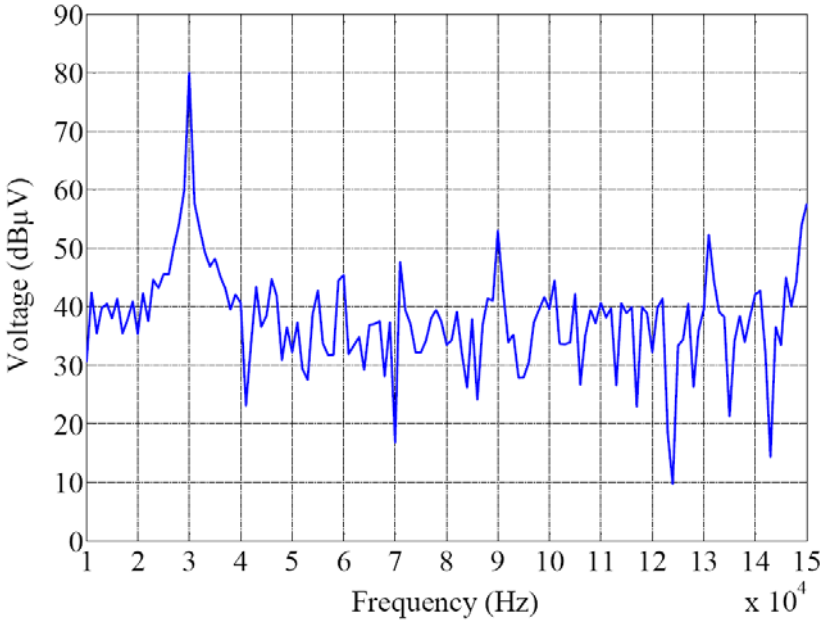

Amplitude spectrum of a 30 kHz sinusoidal signal with Flat Top windowing before DFT. Coherent gain included.

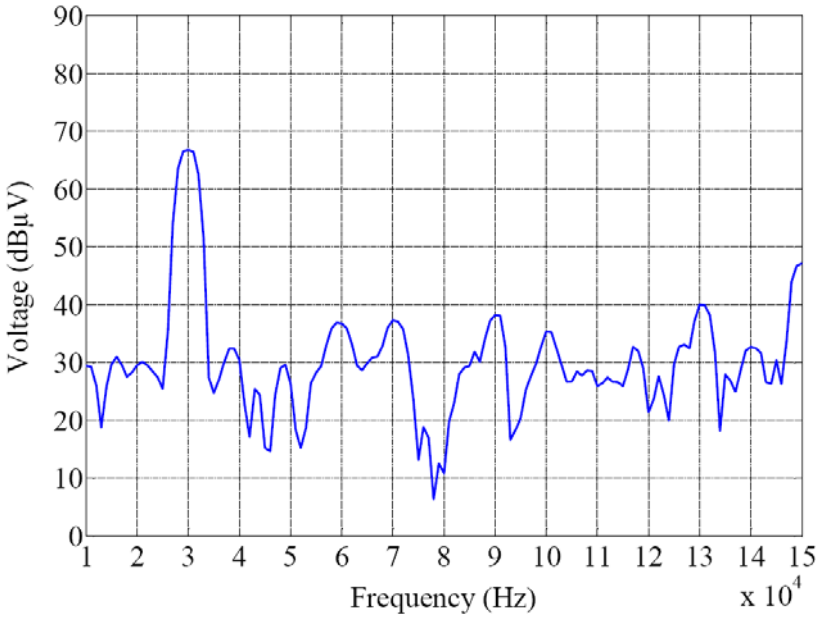

Amplitude spectrum of a 30 kHz sinusoidal signal with Flat Top windowing before DFT. Coherent gain compensated.

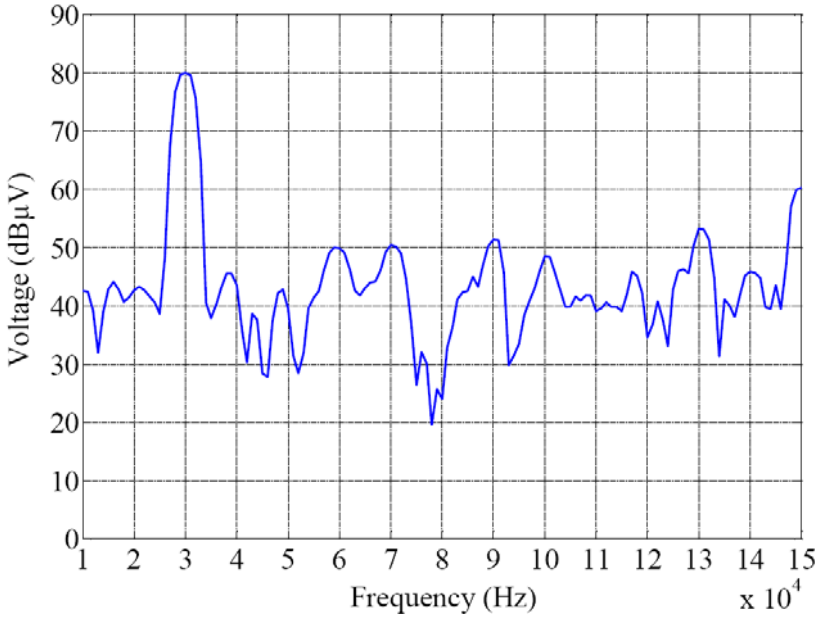

Amplitude spectrum of a 30.5 kHz sinusoidal signal without Flat Top windowing before DFT

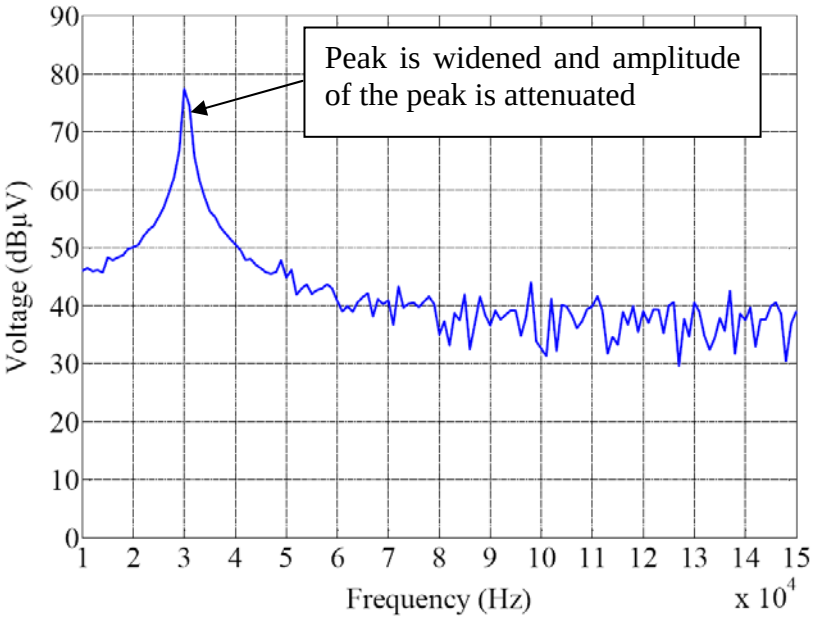

Amplitude spectrum of a 30.5 kHz sinusoidal signal with Flat Top windowing before DFT. Coherent gain included.

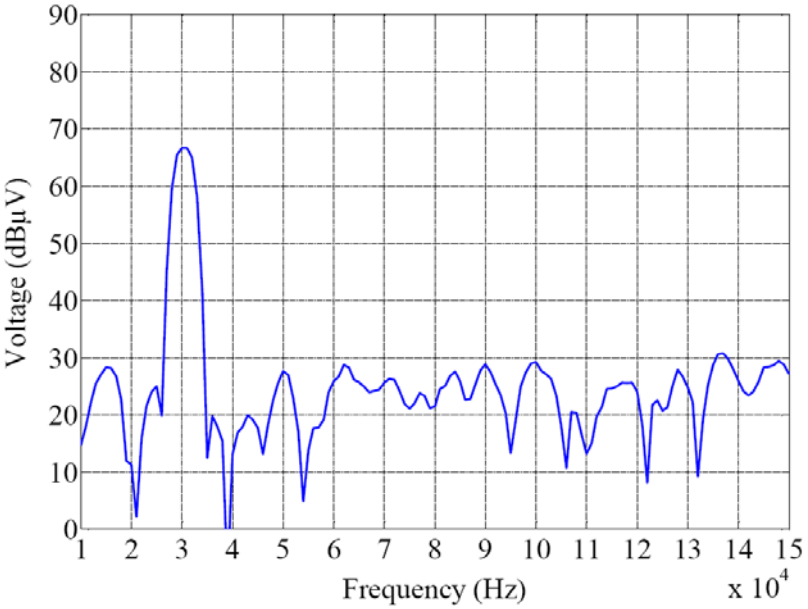

Amplitude spectrum of a 30.5 kHz sinusoidal signal with Flat Top windowing before DFT. Coherent gain compensated.

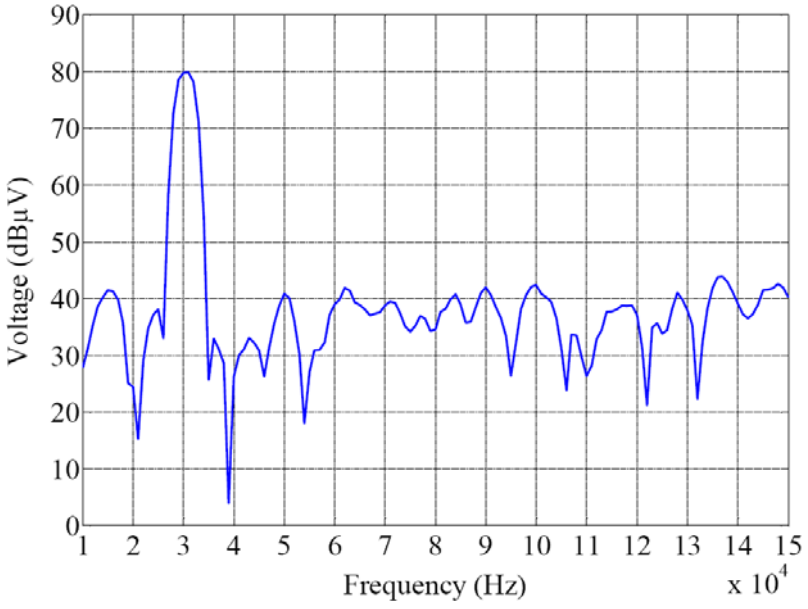

APPENDIX 4

Original Signal 1

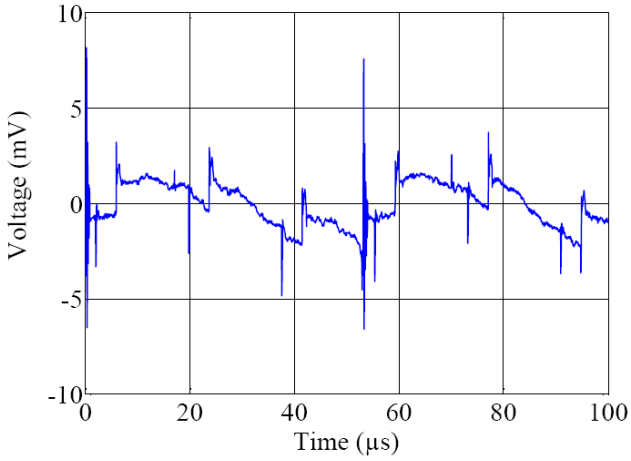

Flat Top Windowed Signal 1

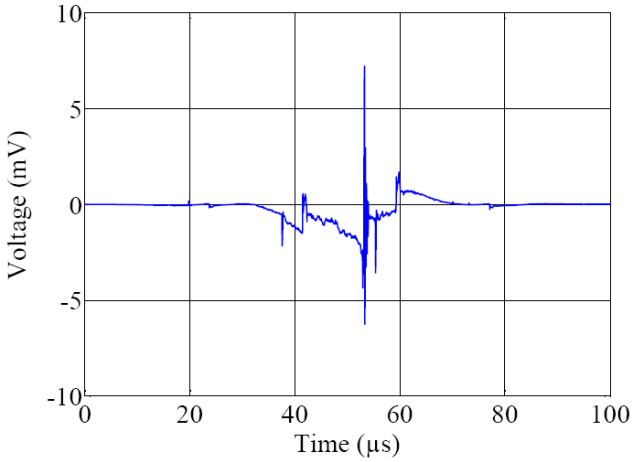

Original Signal 2

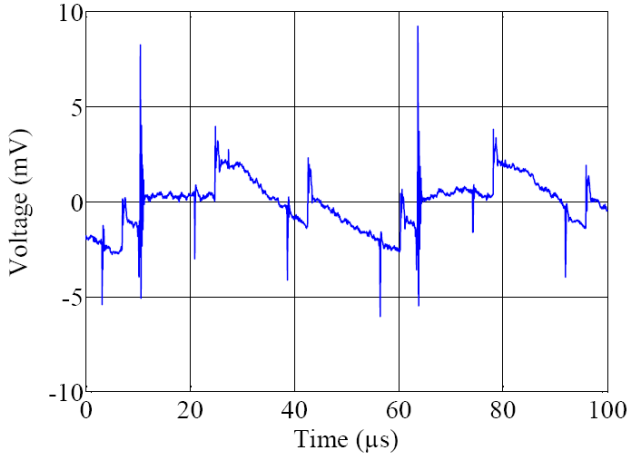

Flat Top Windowed Signal 2

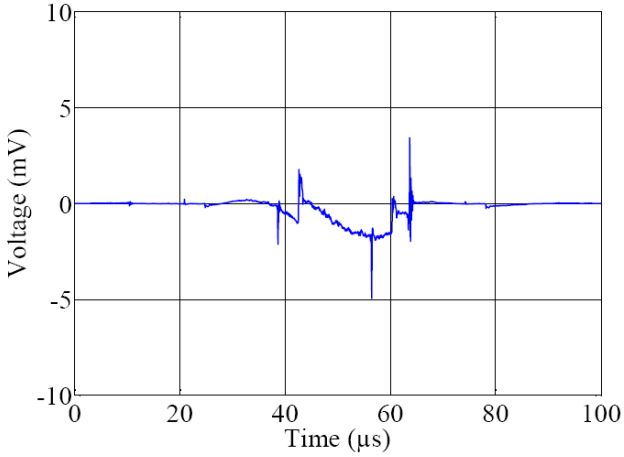

Original Signal 3

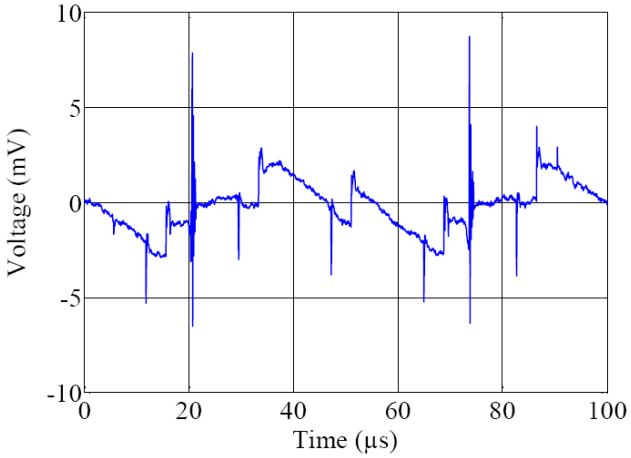

Flat Top Windowed Signal 3

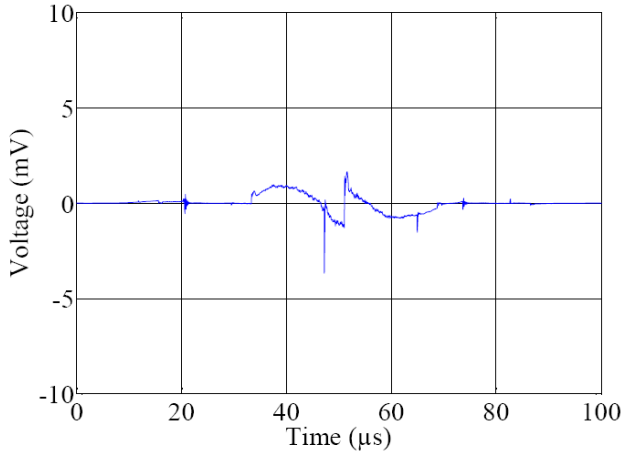

Original Signal 4

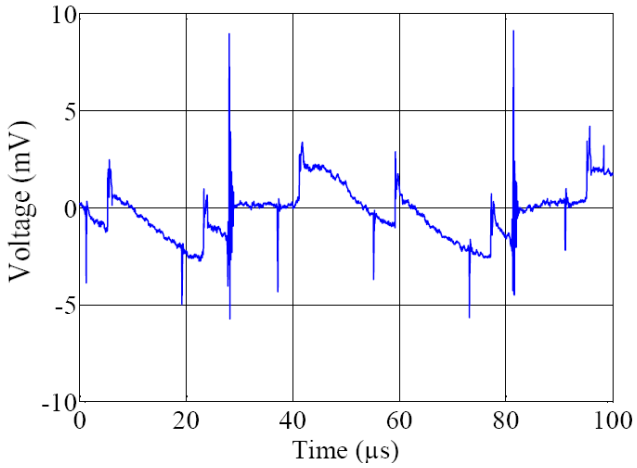

Flat Top Windowed Signal 4

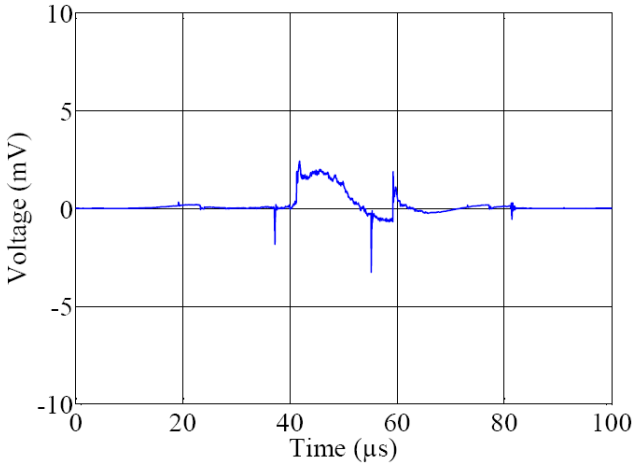

Original Signal 5

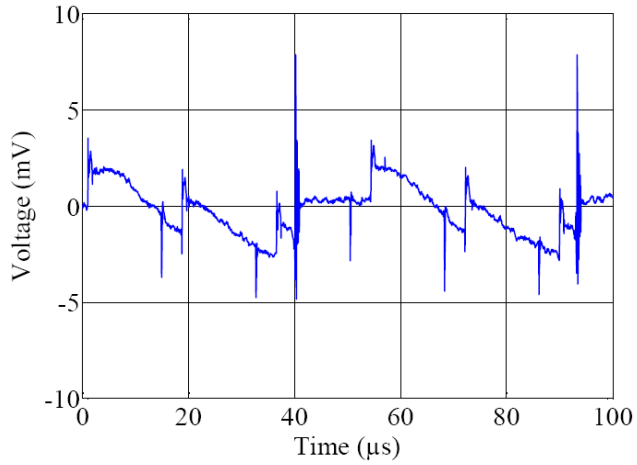

Flat Top Windowed Signal 5

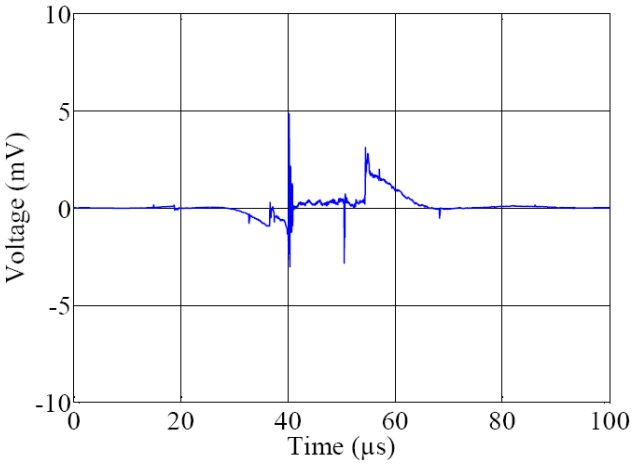

Original Signal 6

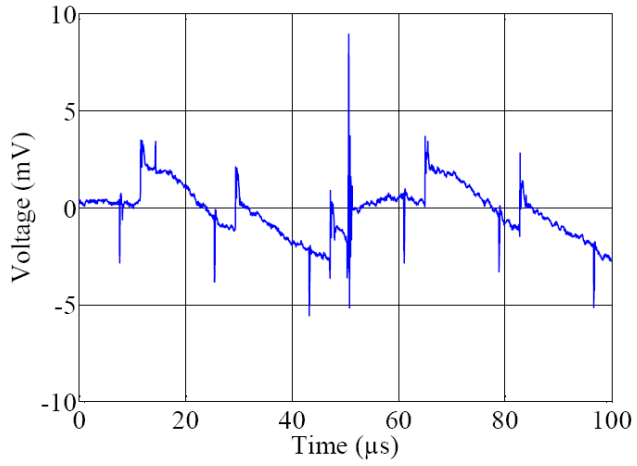

Flat Top Windowed Signal 6

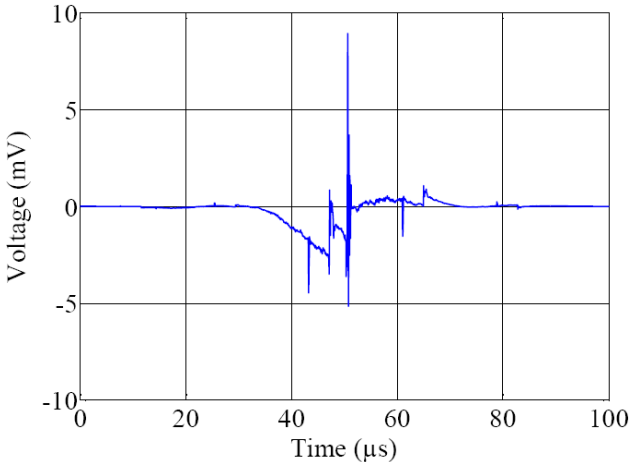

APPENDIX 5

HAMMING WINDOW

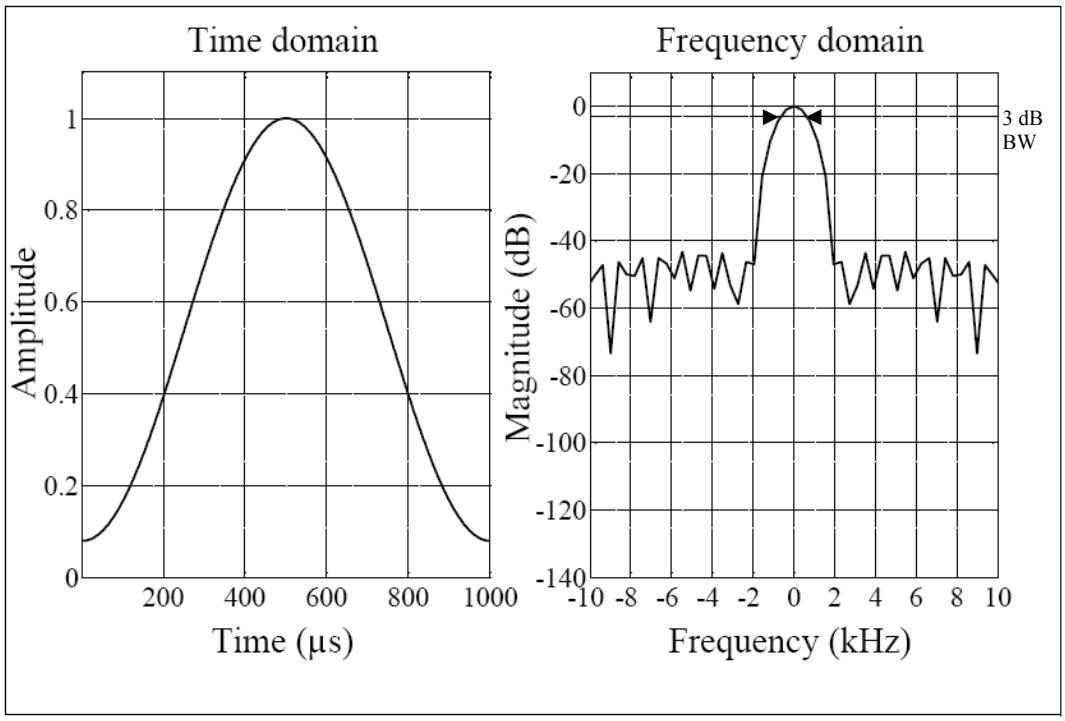

Frequency Range	3 dB Bandwidth (kHz)	Coherent Gain
10 kHz – 150 kHz	1.270	0.539
150 kHz – 10 MHz	12.207	0.540

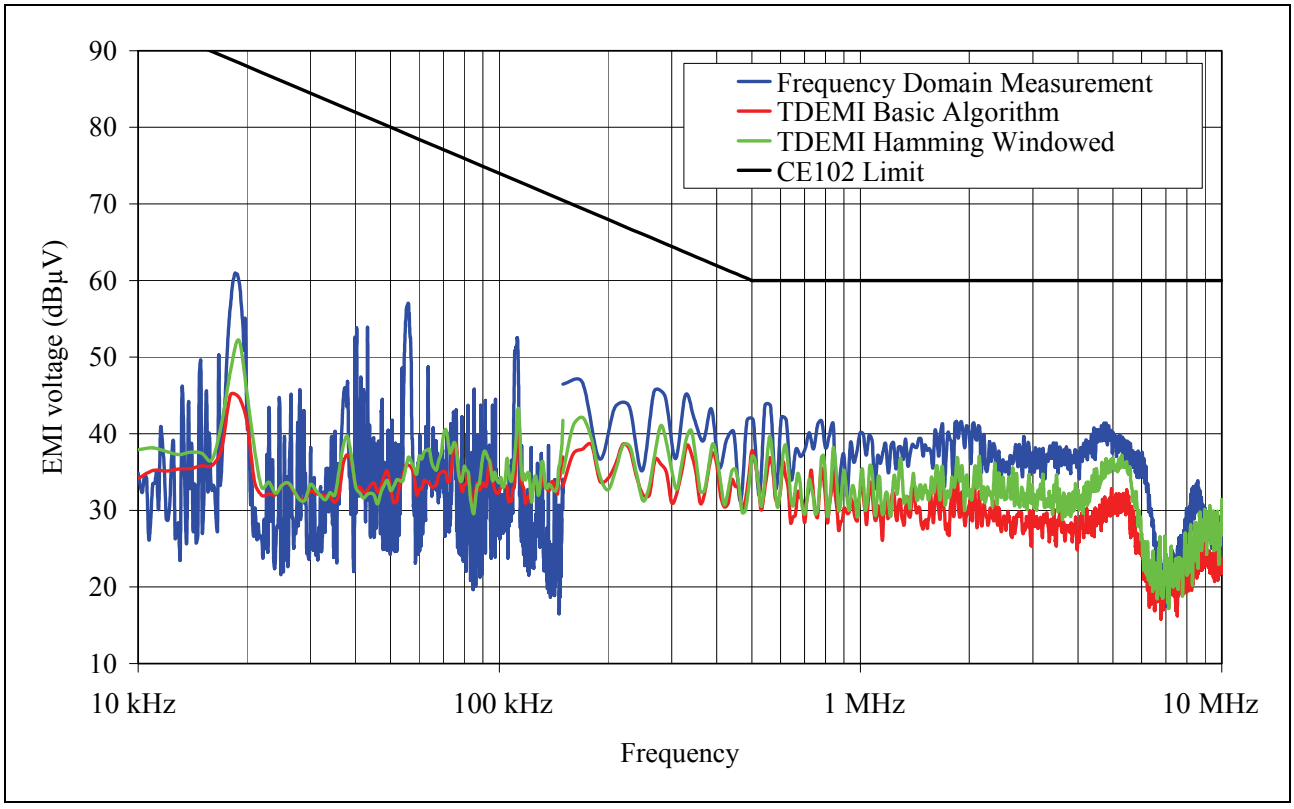

HANN WINDOW

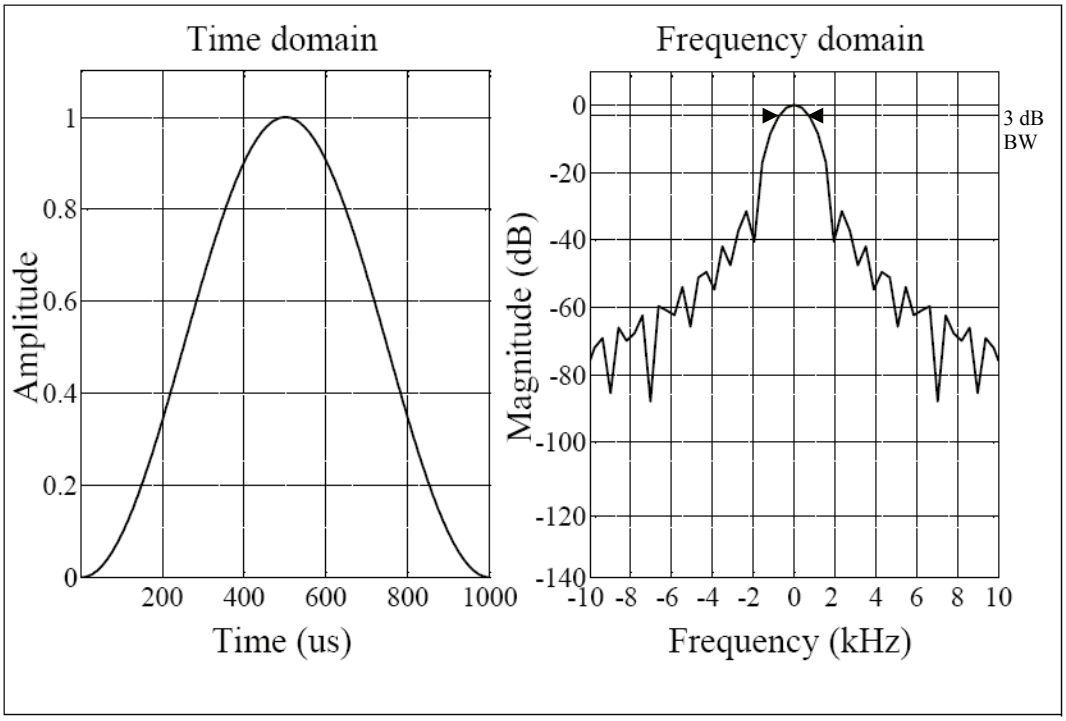

Frequency Range	3 dB Bandwidth (kHz)	Coherent Gain
10 kHz – 150 kHz	1.367	0.499
150 kHz – 10 MHz	13.428	0.500

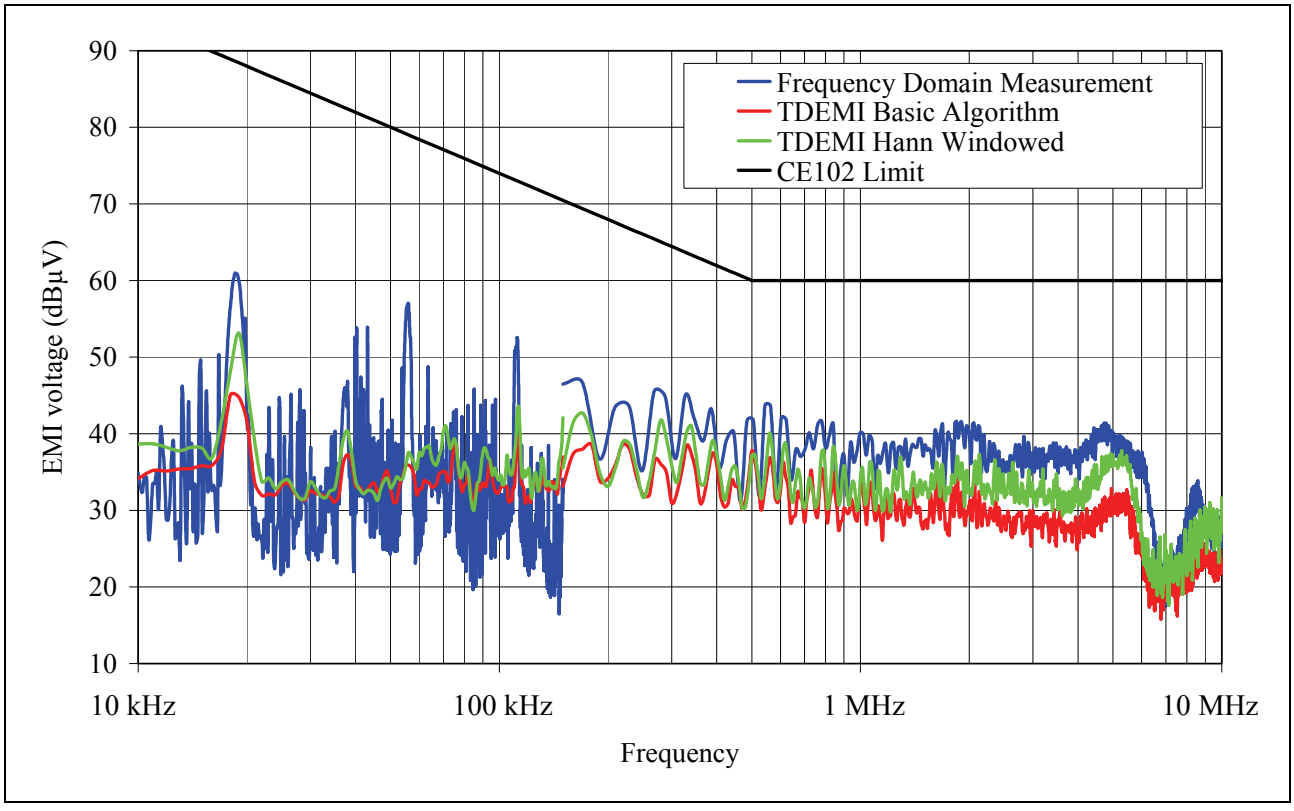

BLACKMAN WINDOW

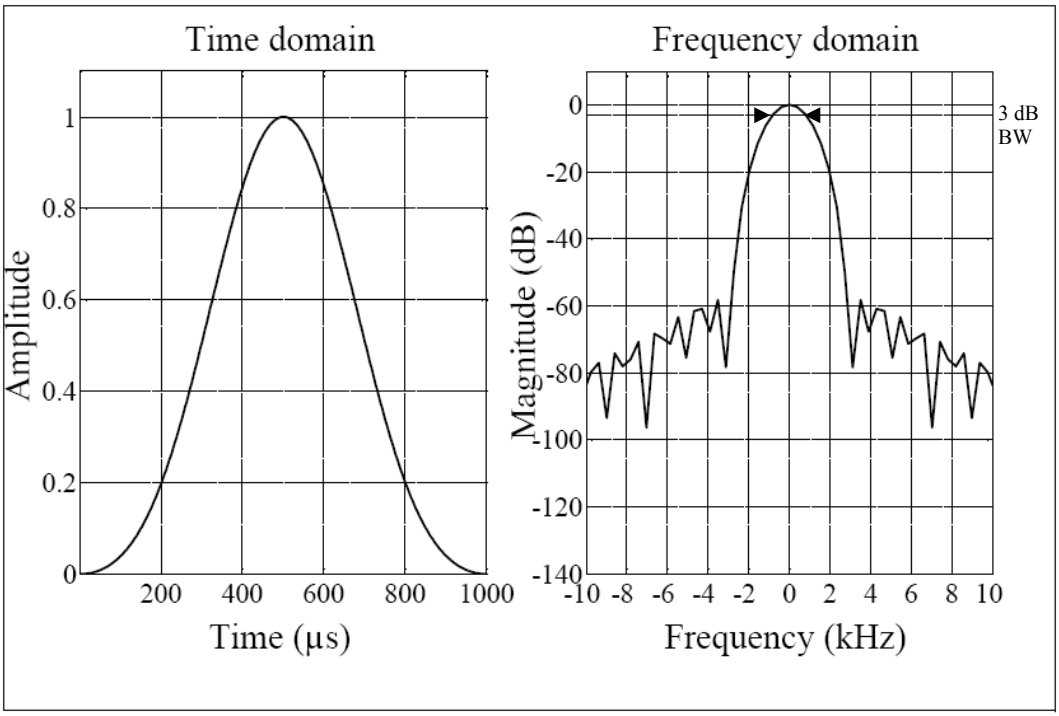

Frequency Range	3 dB Bandwidth (kHz)	Coherent Gain
10 kHz – 150 kHz	1.563	0.419
150 kHz – 10 MHz	15.896	0.420

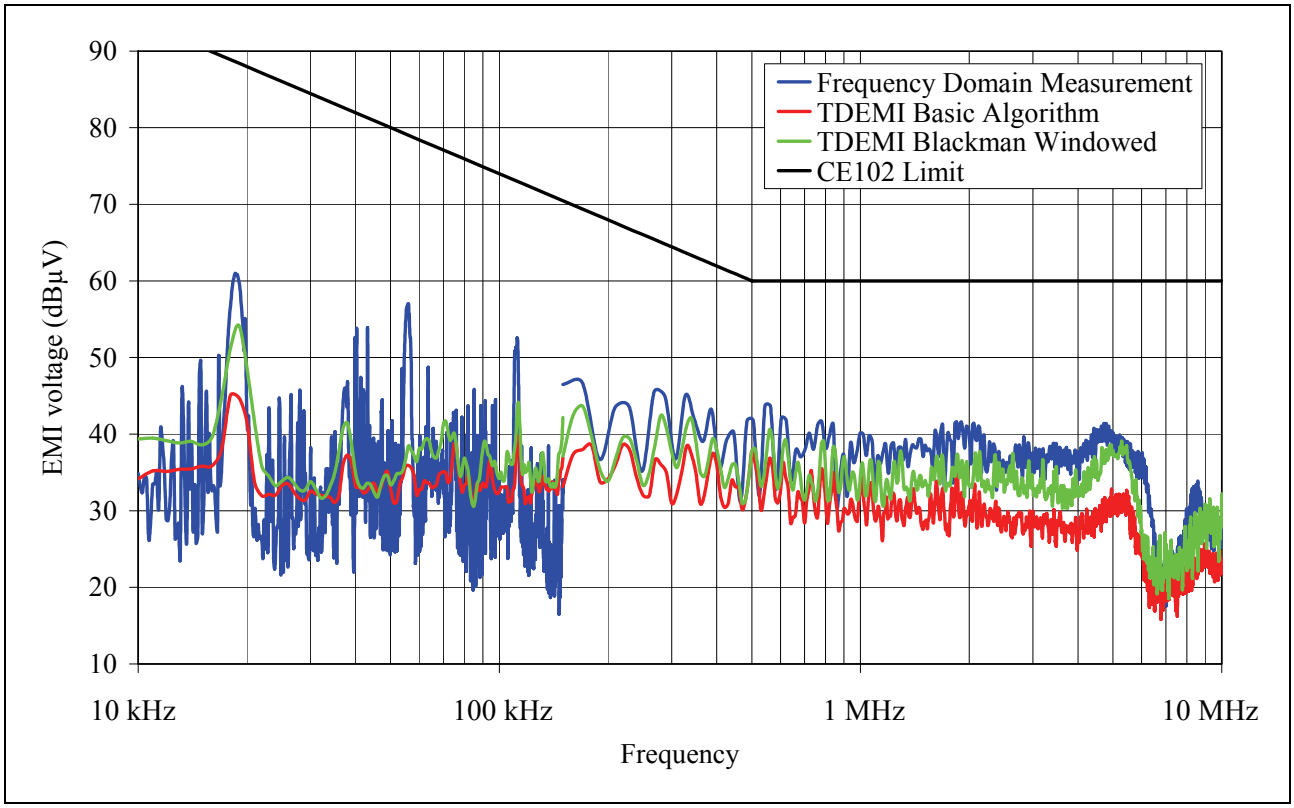

BLACKMAN-HARRIS WINDOW

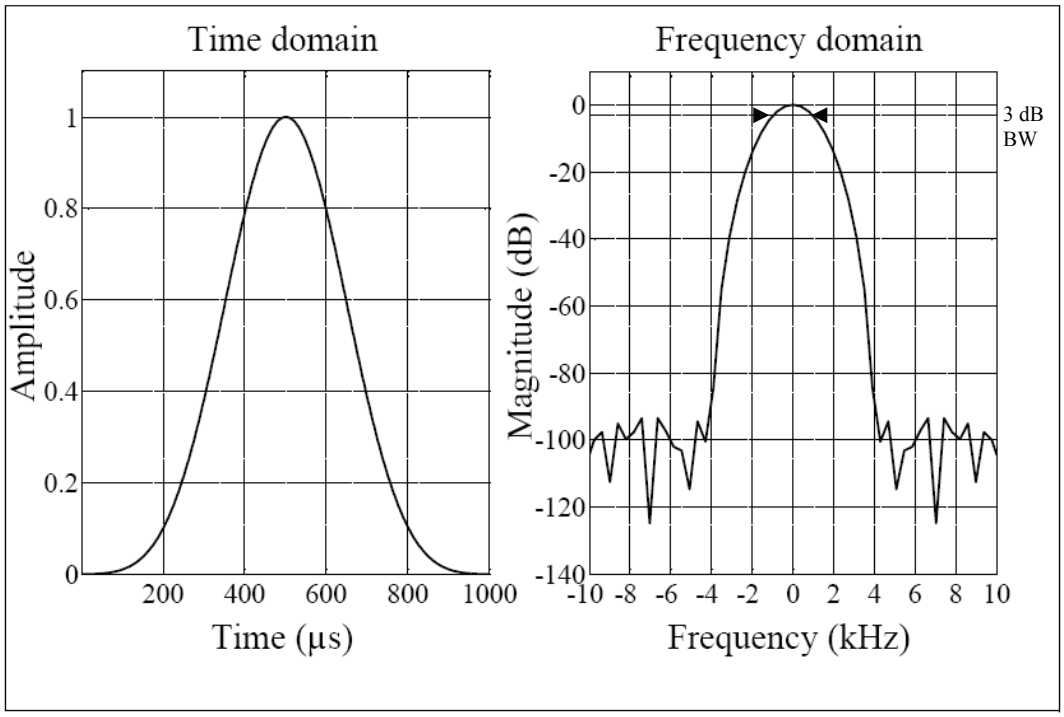

Frequency Range	3 dB Bandwidth (kHz)	Coherent Gain
10 kHz – 150 kHz	1.855	0.358
150 kHz – 10 MHz	18.311	0.358

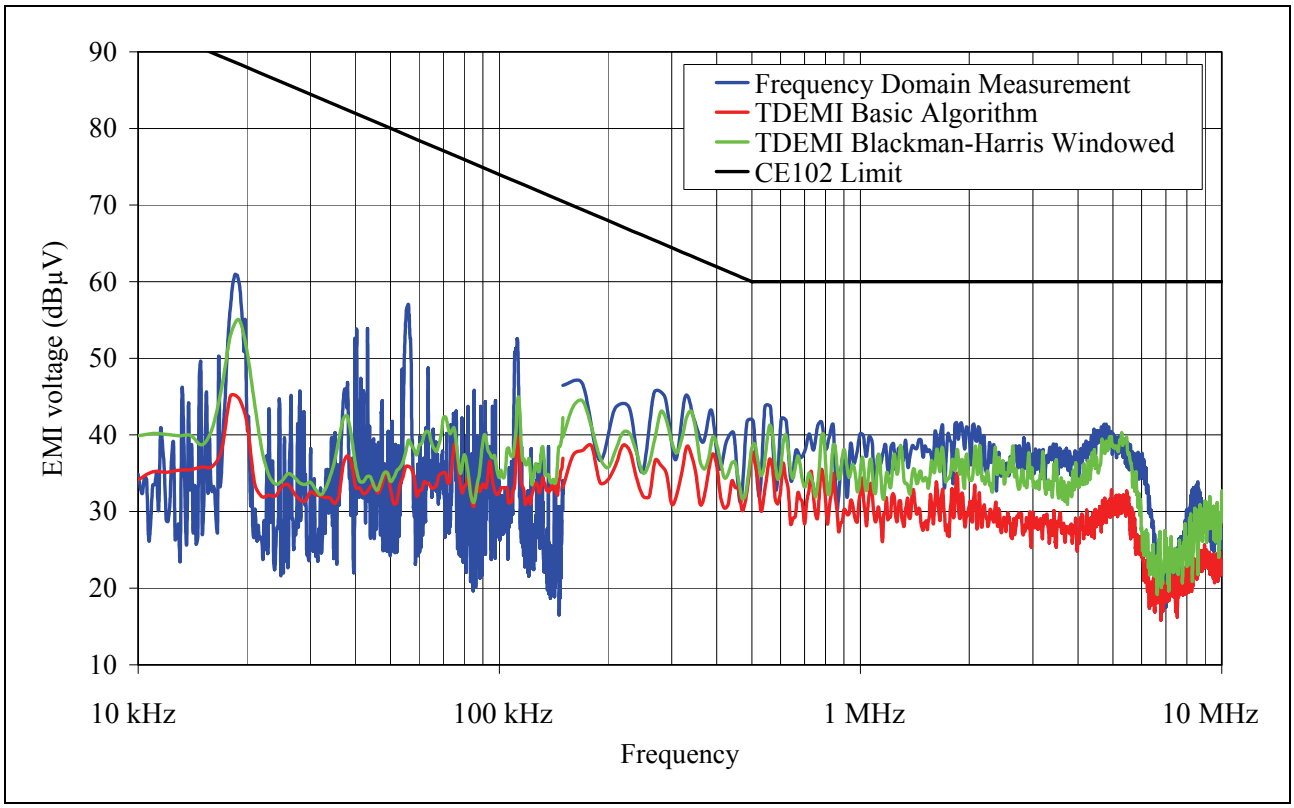

CHEBYSHEV WINDOW

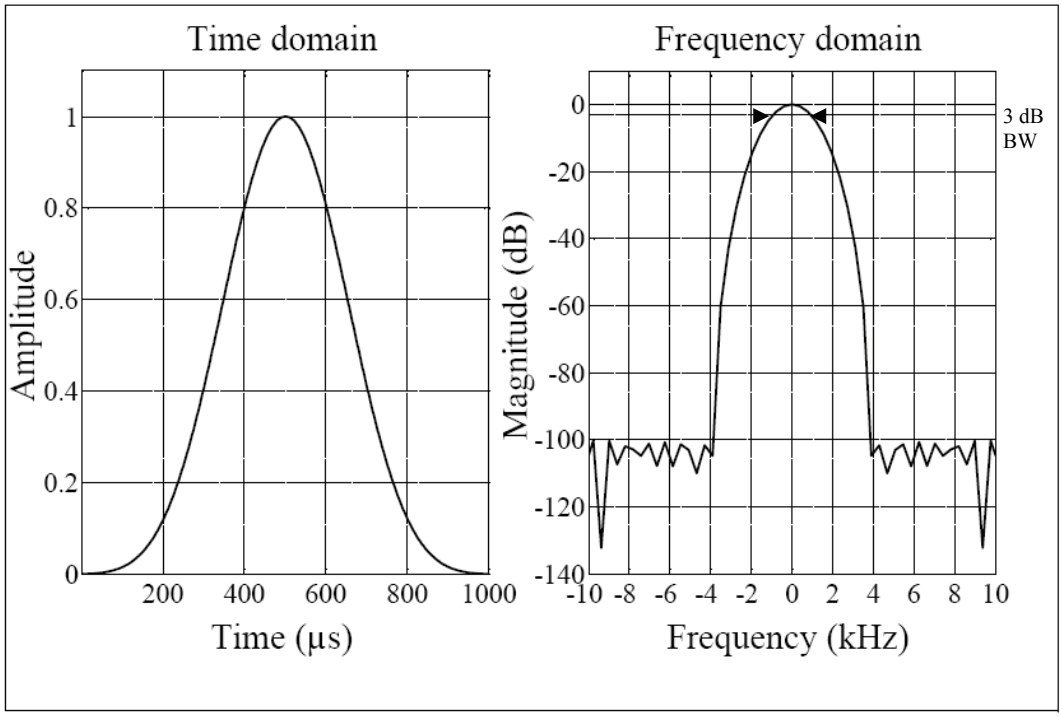

Frequency Range	3 dB Bandwidth (kHz)	Coherent Gain
10 kHz – 150 kHz	1.758	0.370
150 kHz – 10 MHz	18.311	0.370

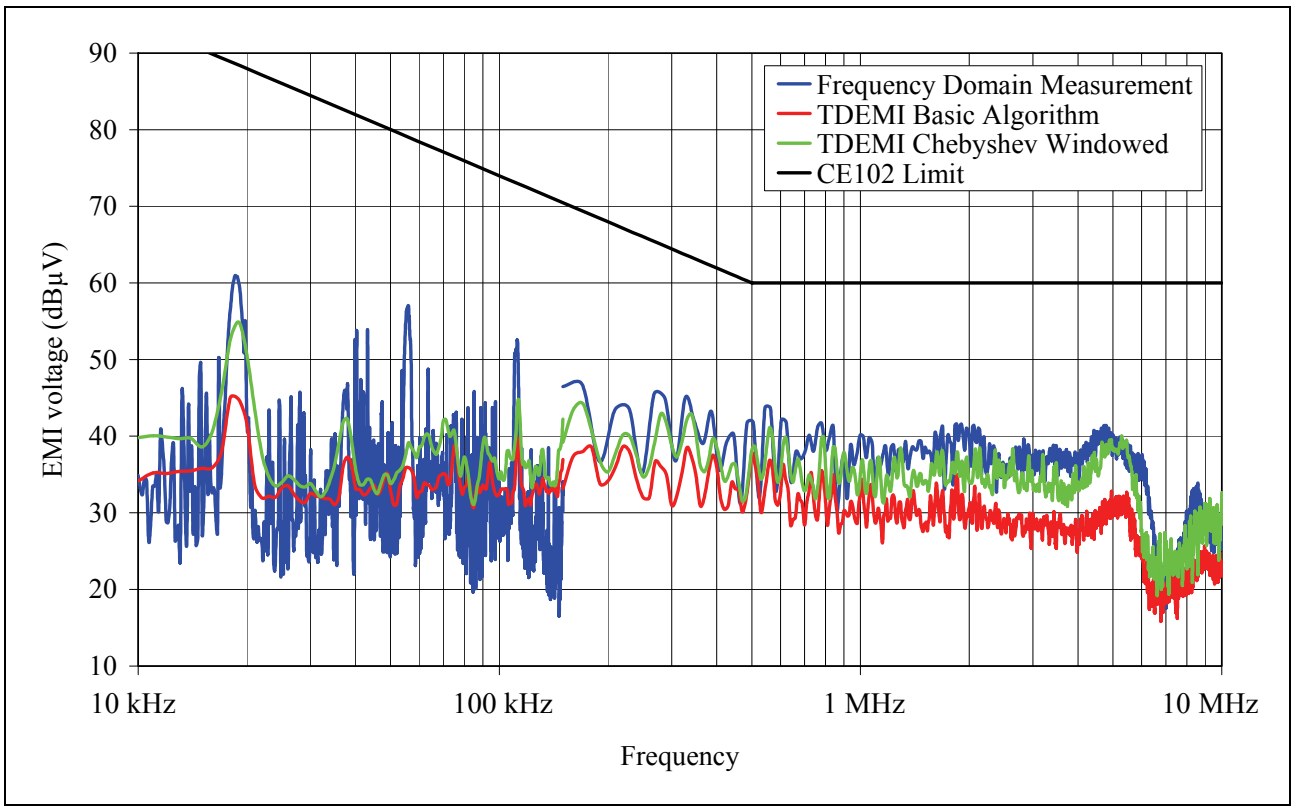

GAUSSIAN WINDOW (α = 4)

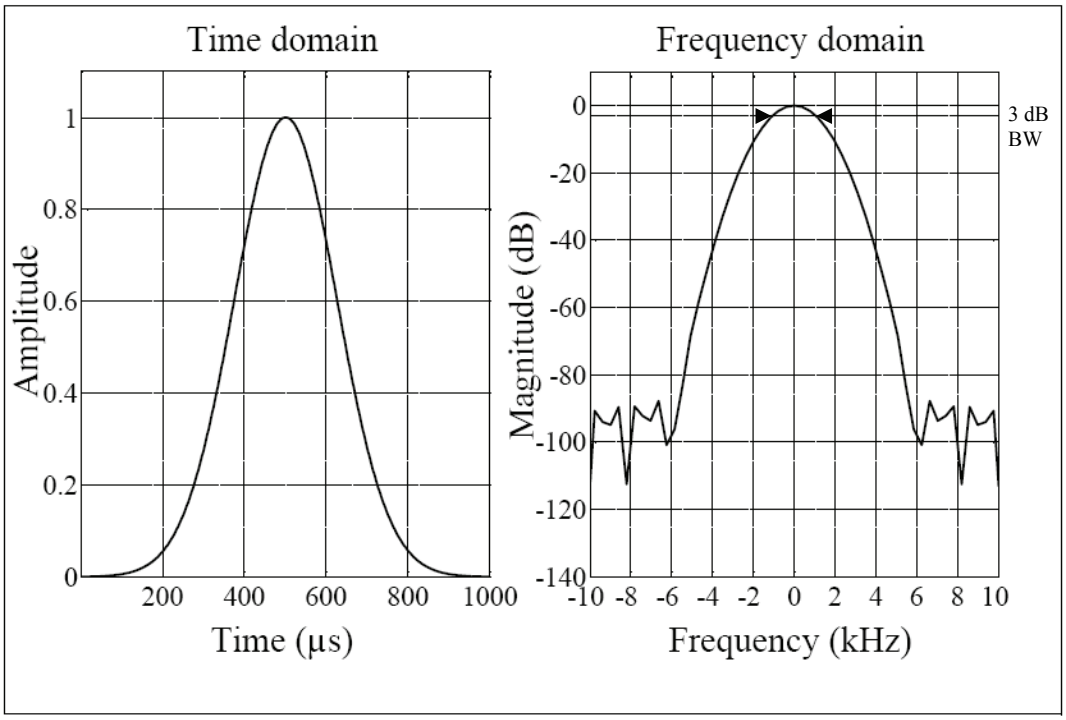

Frequency Range	3 dB Bandwidth (kHz)	Coherent Gain
10 kHz – 150 kHz	2.051	0.313
150 kHz – 10 MHz	20.752	0.313

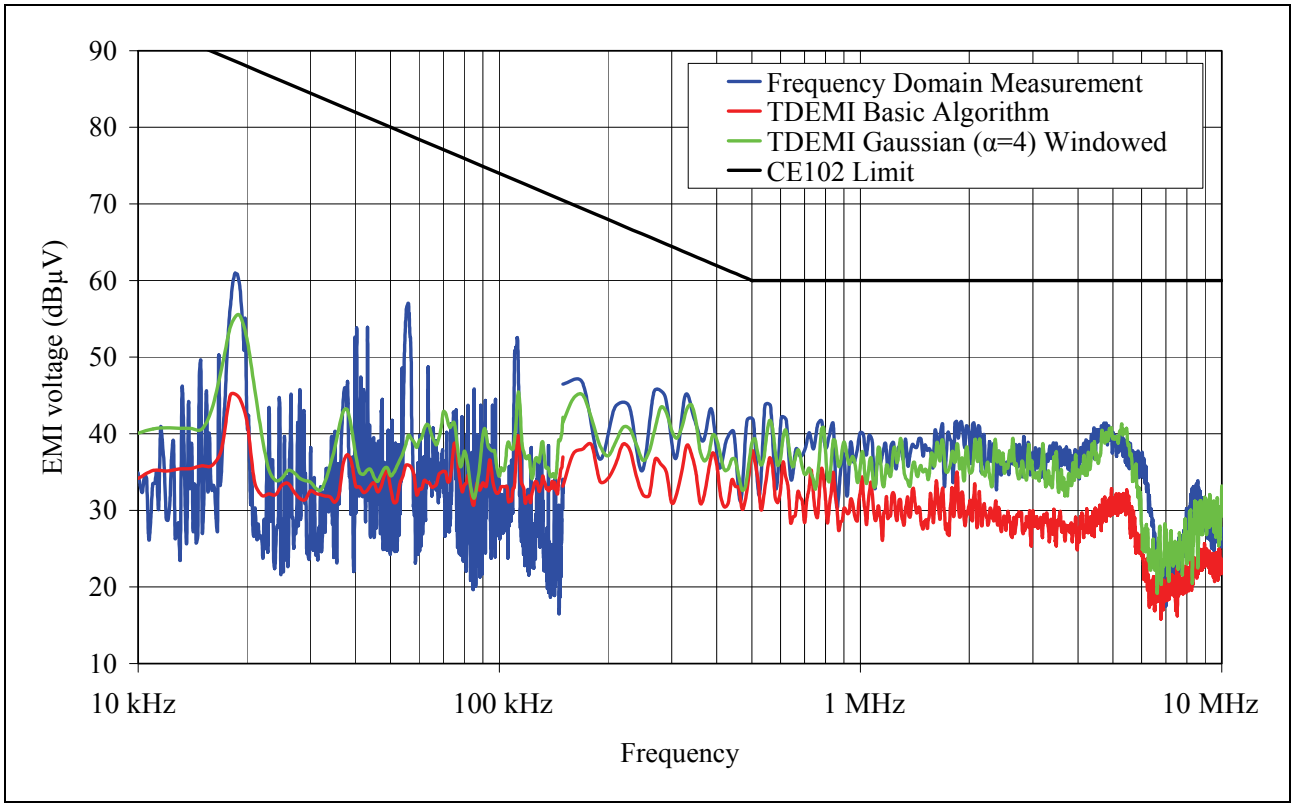

GAUSSIAN WINDOW (α = 5)

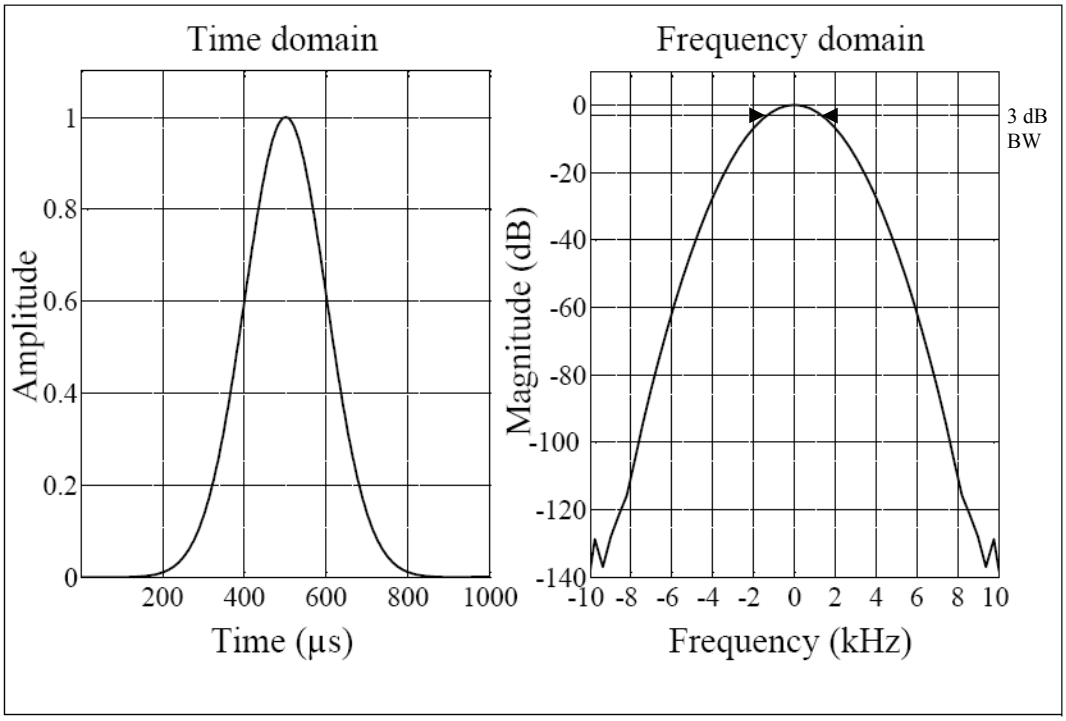

Frequency Range	3 dB Bandwidth (kHz)	Coherent Gain
10 kHz – 150 kHz	2.637	0.251
150 kHz – 10 MHz	25.635	0.251

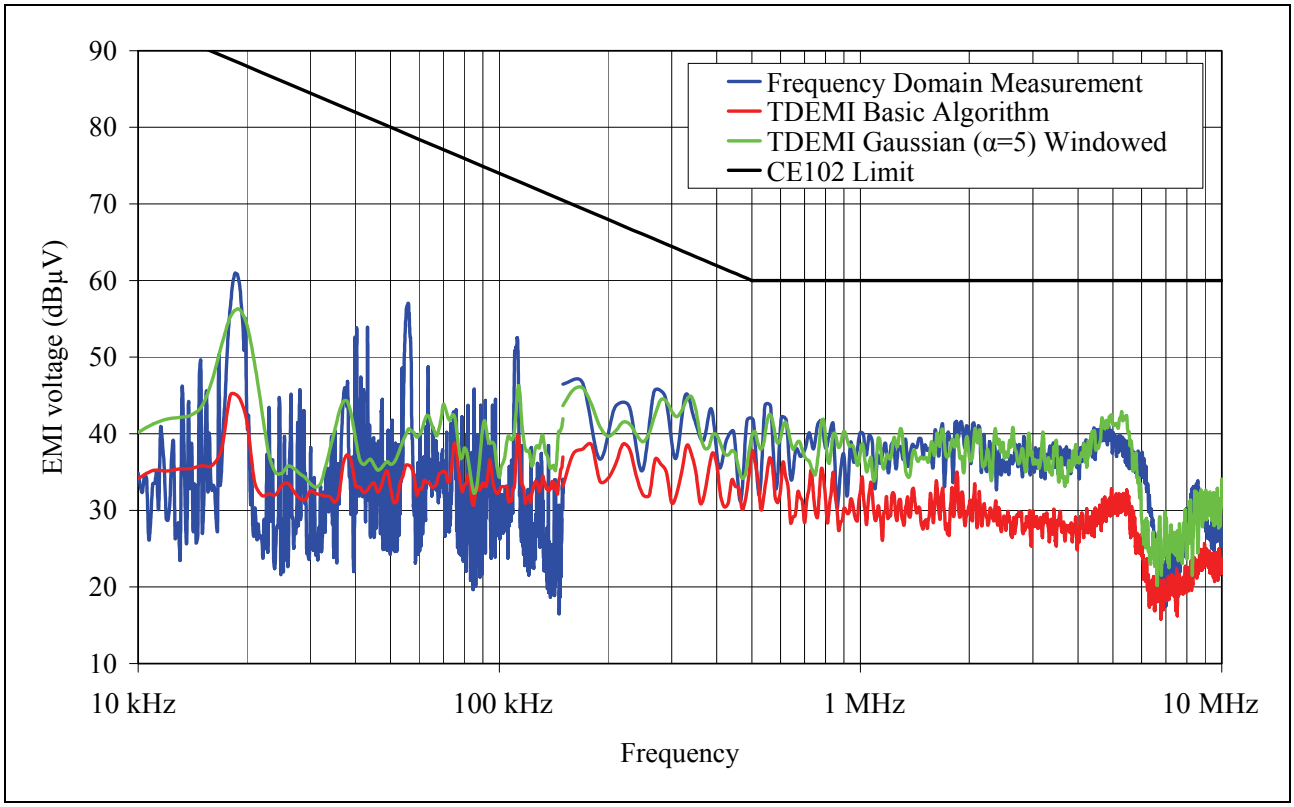

GAUSSIAN WINDOW (α = 6)

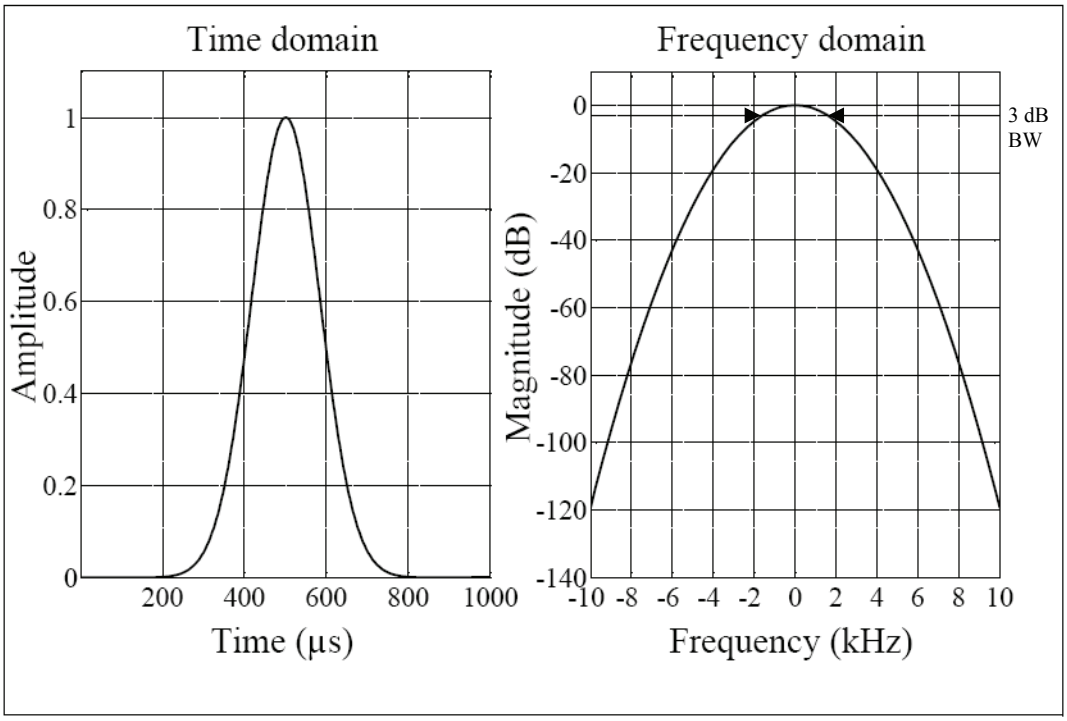

Frequency Range	3 dB Bandwidth (kHz)	Coherent Gain
10 kHz – 150 kHz	3.125	0.209
150 kHz – 10 MHz	31.738	0.209

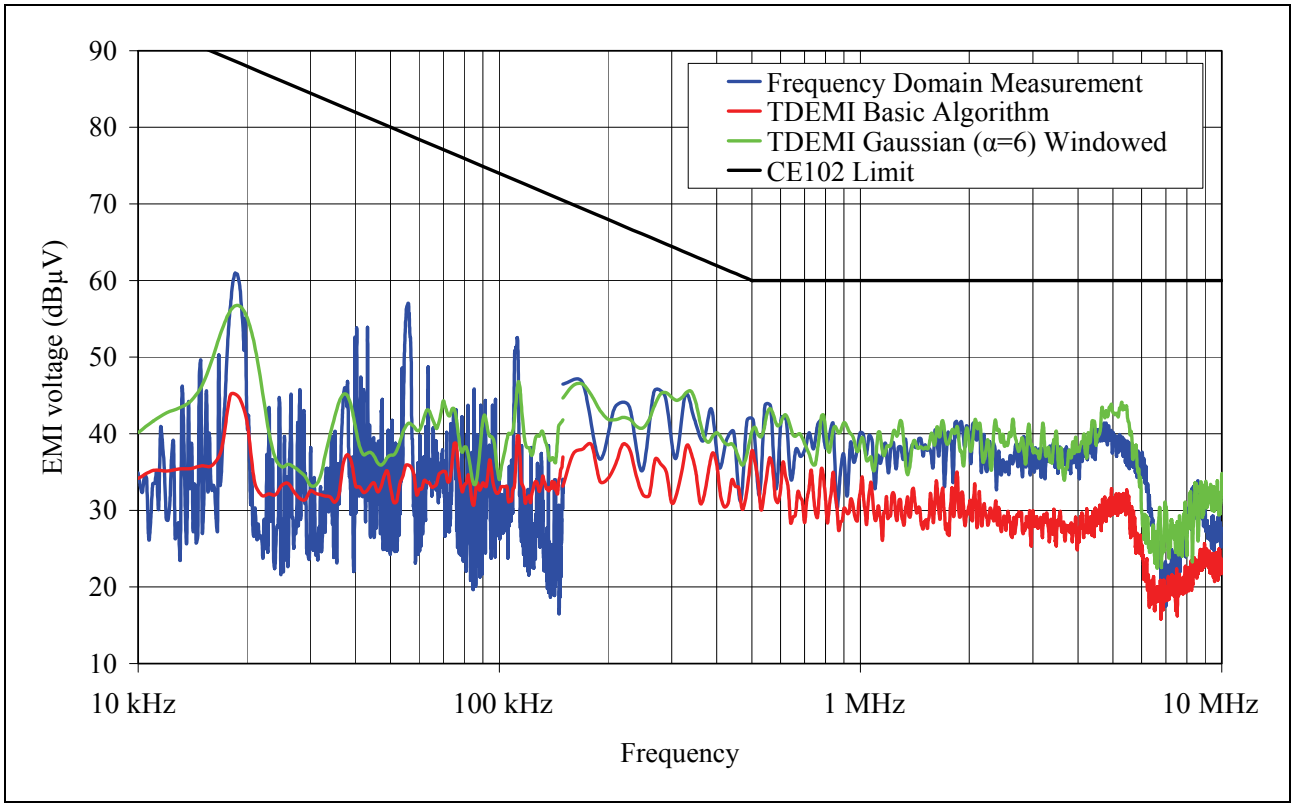

NUTTALL WINDOW

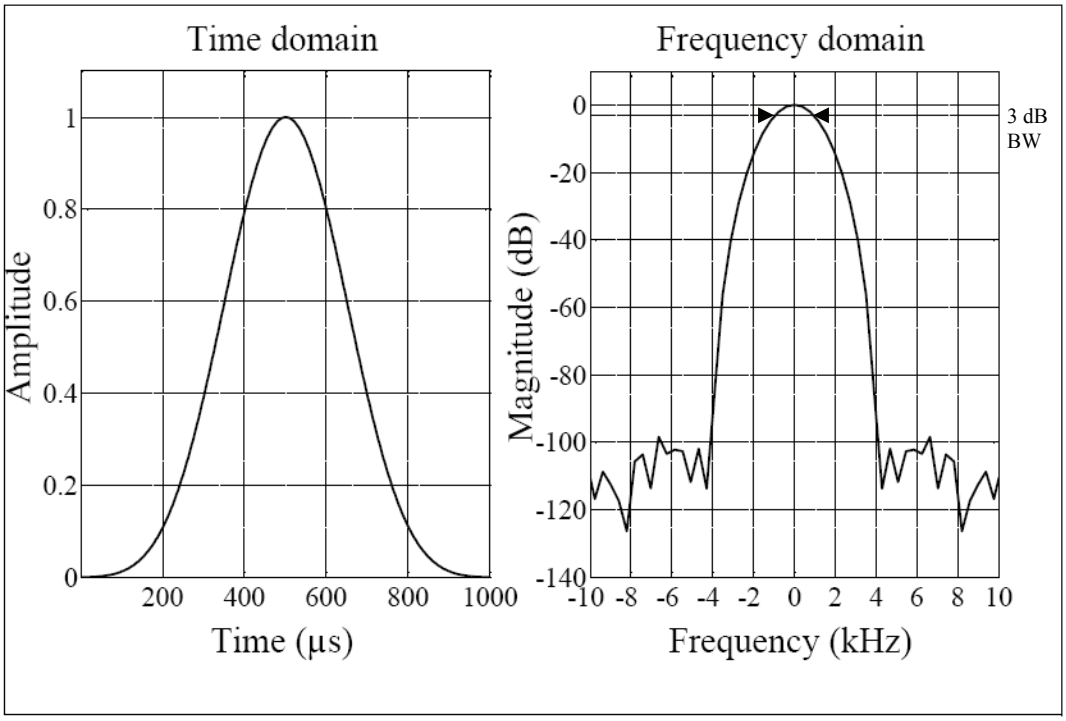

Frequency Range	3 dB Bandwidth (kHz)	Coherent Gain
10 kHz – 150 kHz	1.855	0.363
150 kHz – 10 MHz	18.311	0.363

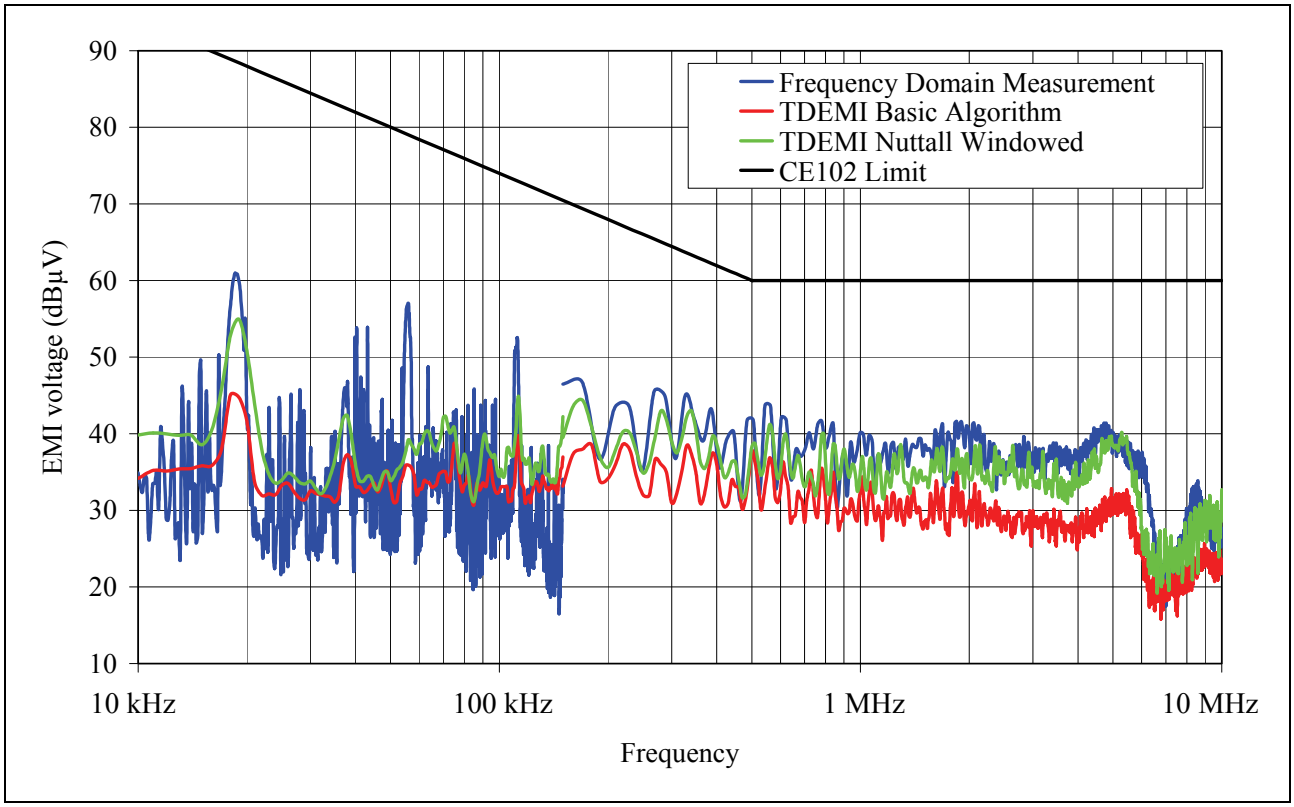

BOHMAN WINDOW

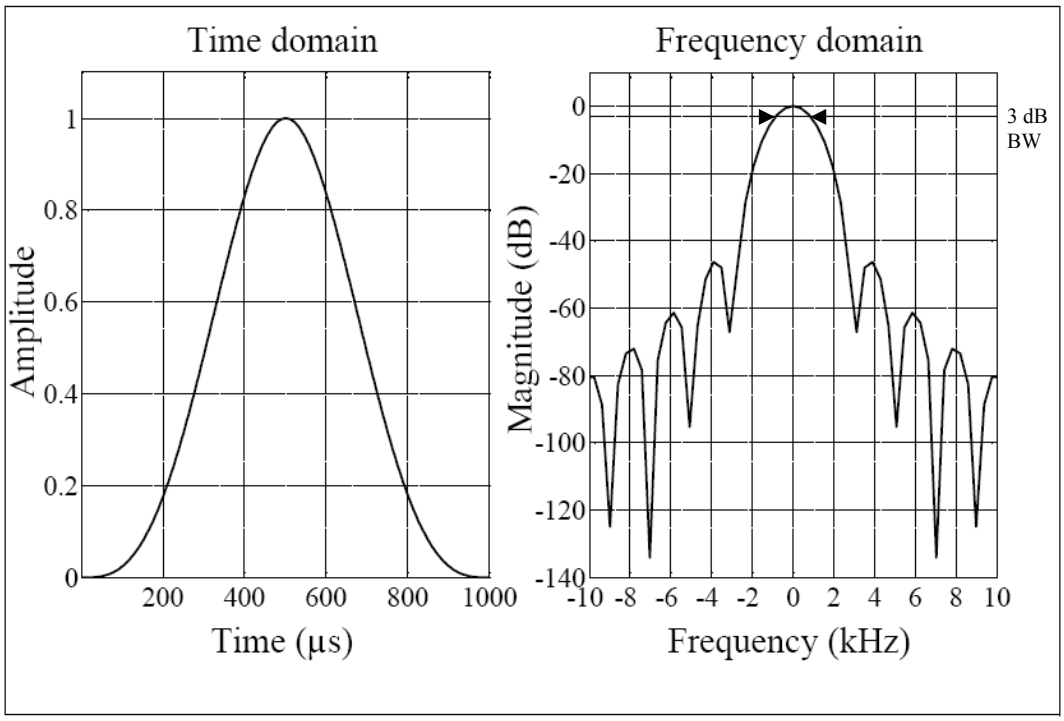

Frequency Range	3 dB Bandwidth (kHz)	Coherent Gain
10 kHz – 150 kHz	1.660	0.404
150 kHz – 10 MHz	15.896	0.405

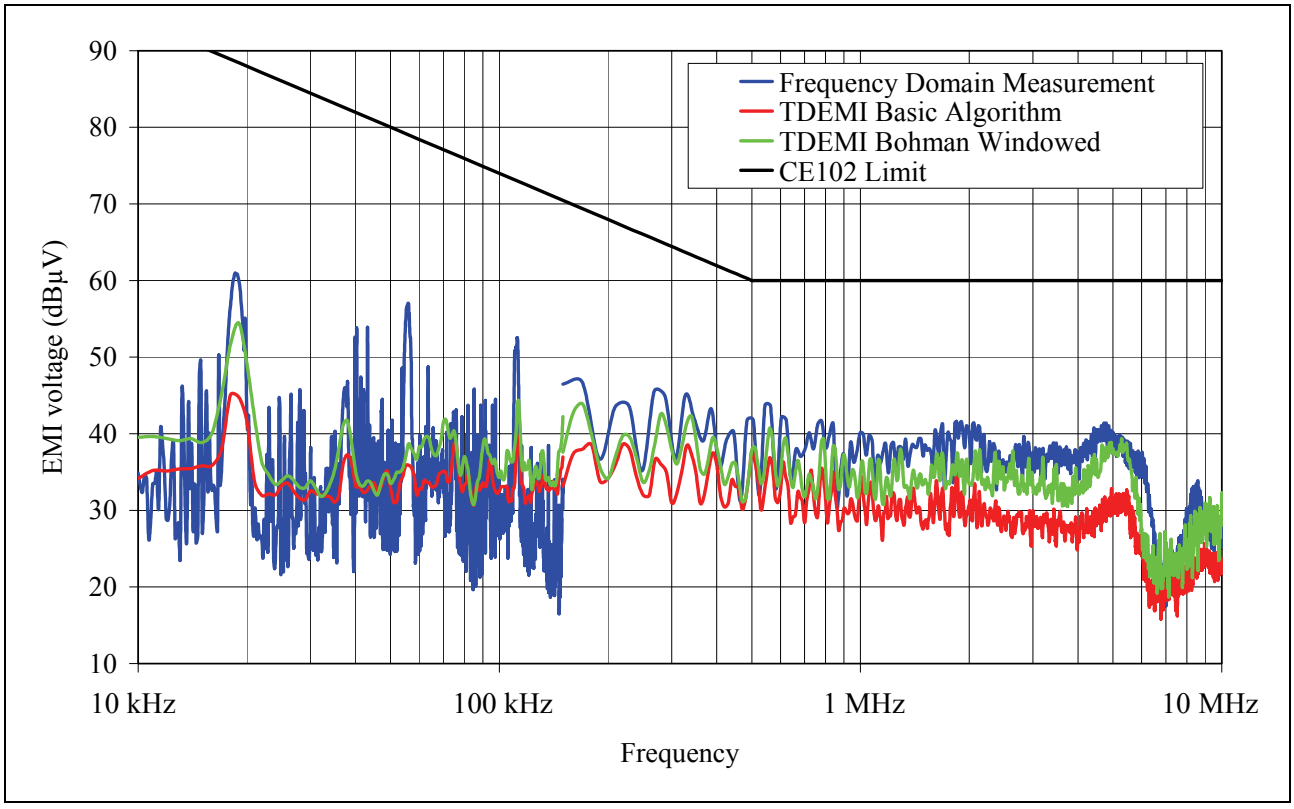

PARZEN WINDOW

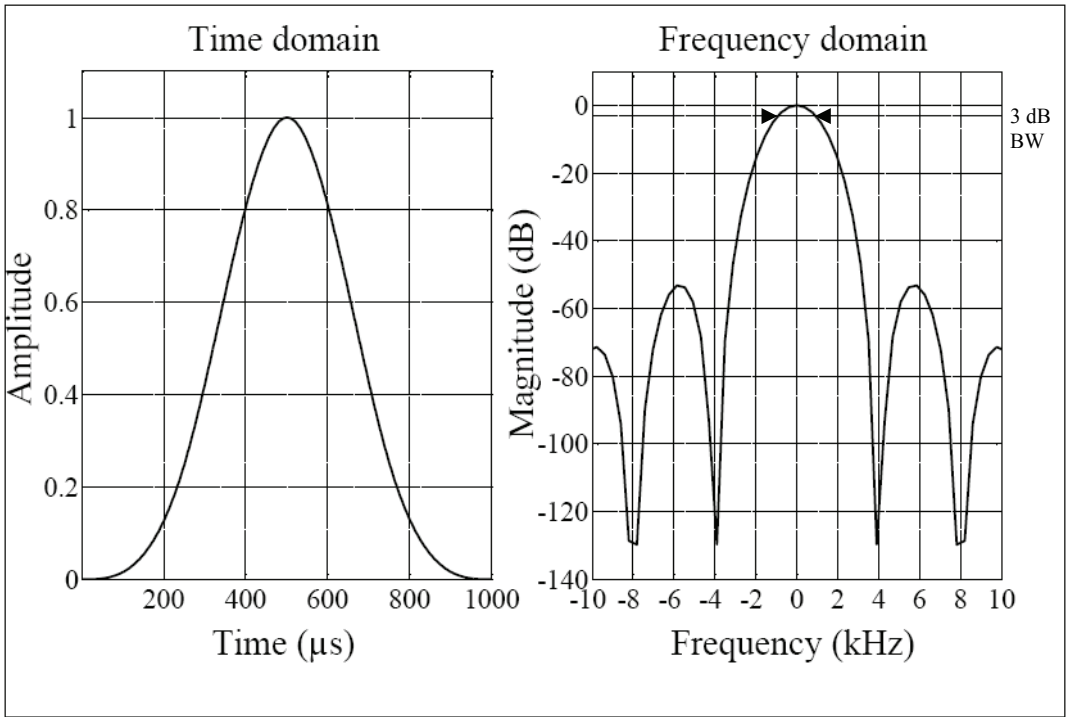

Frequency Range	3 dB Bandwidth (kHz)	Coherent Gain
10 kHz – 150 kHz	1.758	0.375
150 kHz – 10 MHz	17.090	0.375

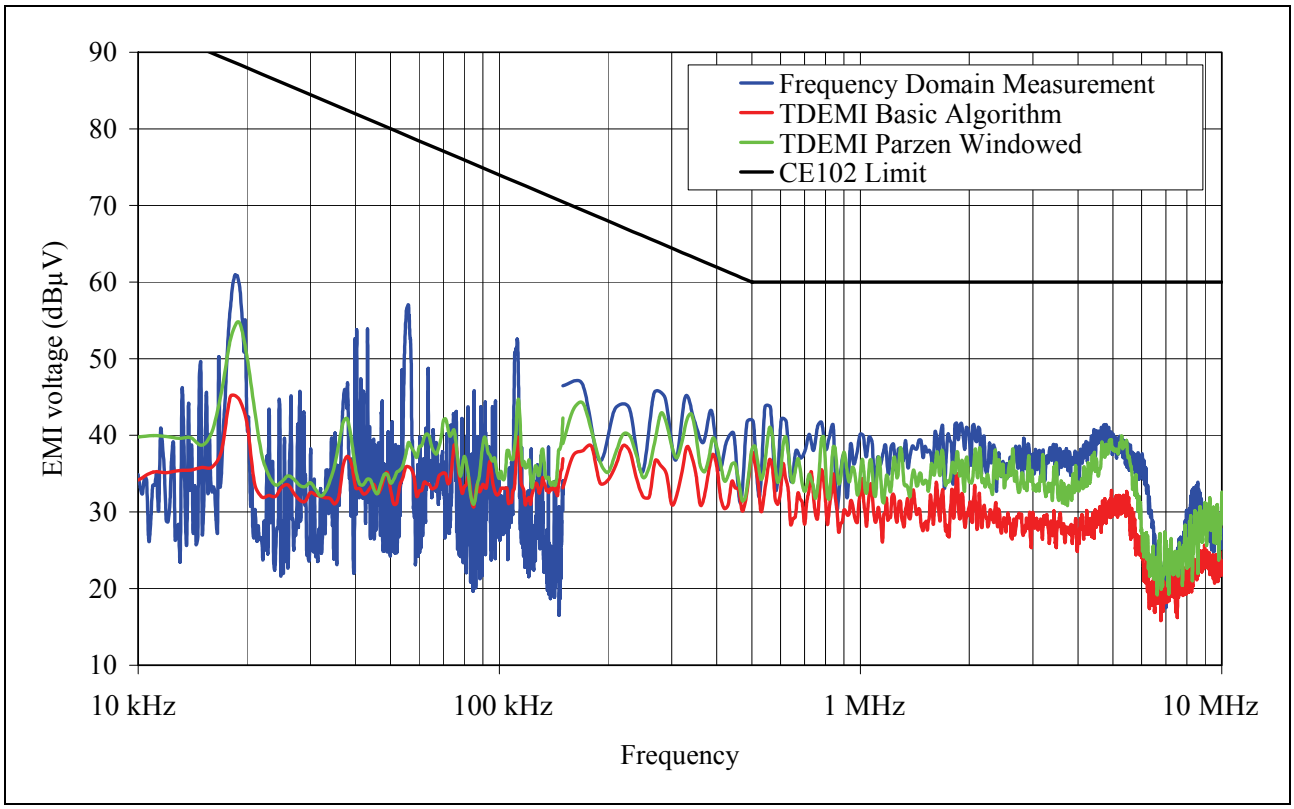

TUKEY WINDOW (α = 1)

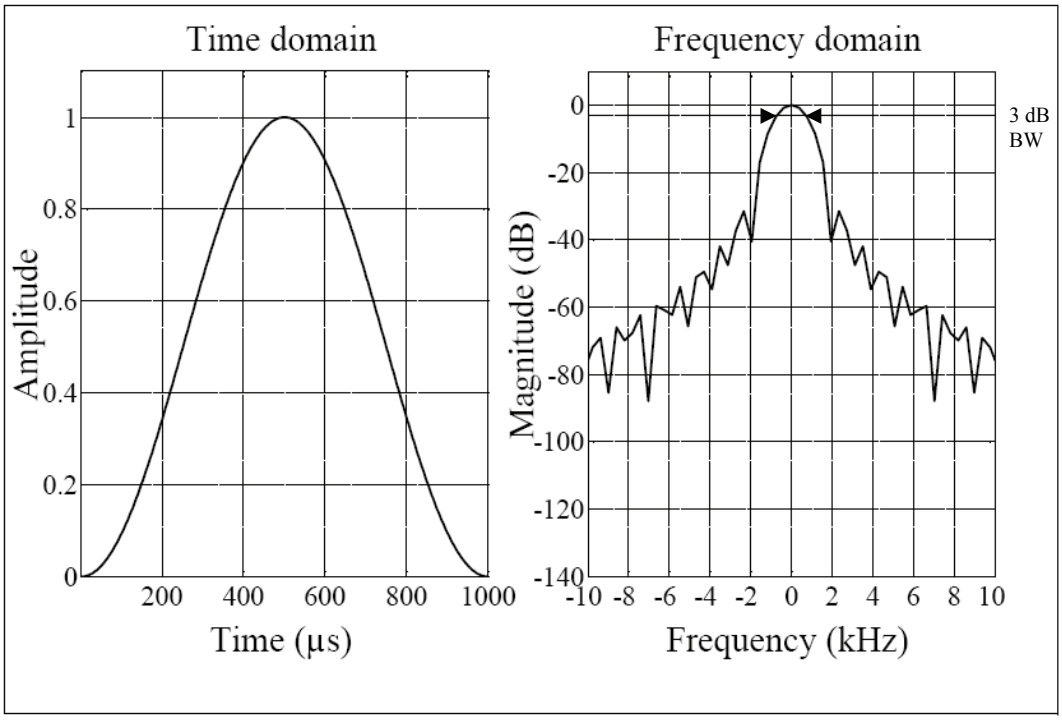

Frequency Range	3 dB Bandwidth (kHz)	Coherent Gain
10 kHz – 150 kHz	1.367	0.499
150 kHz – 10 MHz	13.428	0.500

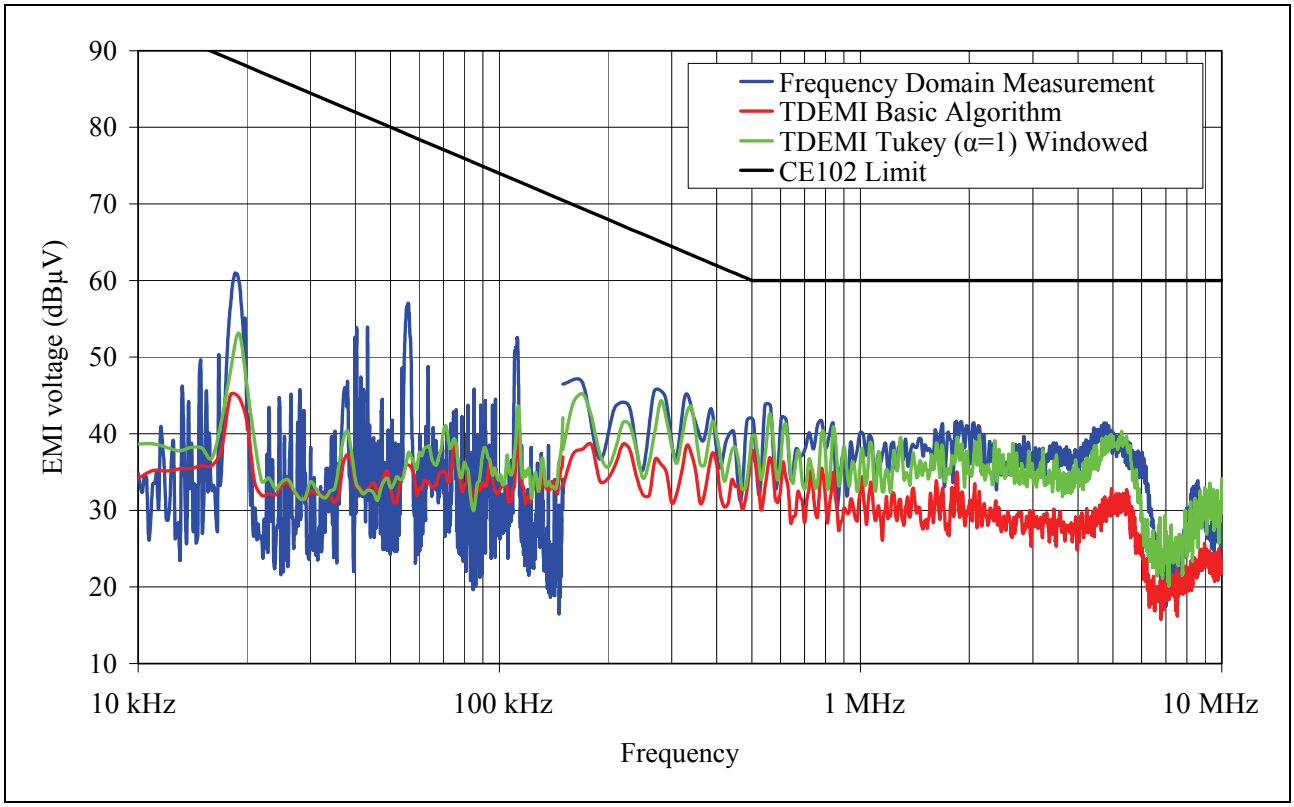

TRIANGULAR WINDOW

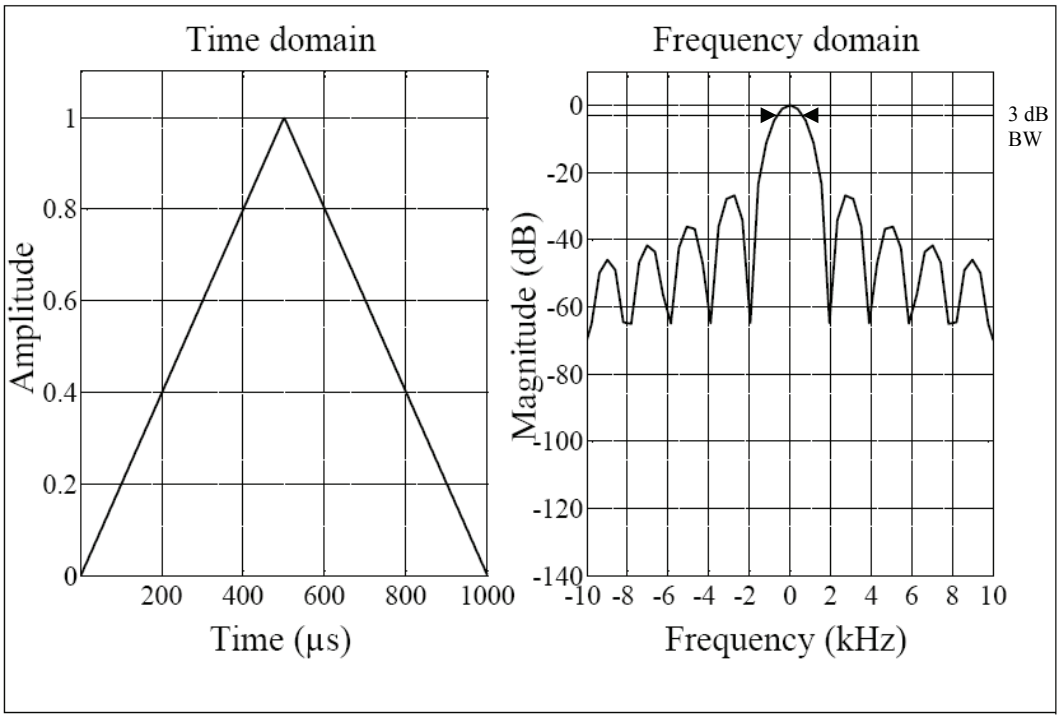

Frequency Range	3 dB Bandwidth (kHz)	Coherent Gain
10 kHz – 150 kHz	1.270	0.500
150 kHz – 10 MHz	12.207	0.500